

ABSTRACT

Title of Dissertation: VIRAL IMMUNE EVASION OF FCRN FUNCTIONS

Xiaoyang Liu, Doctor of Philosophy, 2018

Dissertation directed by: Professor, Xiaoping Zhu, Department of Veterinary Medicine

Human Cytomegalovirus (HCMV) is known to evade host immunity, allowing it to persistently infect humans. Although the strategies of HCMV to evade cellular immunity is well studied, there is limited understanding on how HCMV antagonizes humoral immunity. The neonatal Fc receptor (FcRn), an MHC class I-related Fc γ R, plays a critical role in IgG-mediated humoral immunity. Through screening the HCMV proteome, we discovered that US11 specifically captured FcRn in both virally-infected and US11-expressing cells. US11 selectively inhibited the assembly of FcRn with β_2m , impaired FcRn IgG binding capacity and blocked FcRn trafficking to the endosome by retention of FcRn in ER. Furthermore, US11 recruited Derlin-1 and E3 ubiquitin ligase TMEM129, to induce degradation of FcRn in US11⁺ or HCMV-infected cells. This complex led to the dislocation of FcRn from the ER to the cytosol and facilitated its degradation in an ubiquitination and proteasome-dependent manner. The cytosolic interaction between FcRn and Derlin-1 was shown necessary for degrading FcRn. FcRn is widely expressed in most cell susceptible to

HCMV infection, including epithelial, endothelial and macrophage. Our data showed that either HCMV infection or recombinant US11 expression significantly inhibited human IgG transcytosis across polarized human primary intestinal epithelial Caco-2 cells, vascular endothelial HMEC-1 cells and placental trophoblast BeWo cells, and facilitated considerable IgG degradation inside endothelial HMEC-1 cells. Hence, our results show that HCMV exploits the Derlin-1/TMEM129 pathway through US11 to disable FcRn, revealing a novel strategy for viral evasion from antibody mediated-immunity.

We also studied whether HCMV viral FcγRs (gp34 and gp68) and US11 work together to facilitate IgG degradation. HCMV vFcγRs has been reported to internalize IgG via endocytosis. Interestingly, we found that in acidic pH (6.0) condition, the IgG binding capacity of gp34 was largely impaired while the IgG binding capacity of gp68 had minimal change. Consequently, in the presence of FcRn, gp34 did not enhance IgG degradation whereas gp68 significantly promoted the IgG degradation. Furthermore, the presence of US11 induced more gp34 and gp68-mediated IgG degradation in FcRn⁺ cells.

VIRAL IMMUNE EVASION OF FCRN FUNCTIONS

By

Xiaoyang Liu

Dissertation submitted to the Faculty of the Graduate School of the
University of Maryland, College Park, in partial fulfillment
of the requirements for the degree of
Doctor of Philosophy
2018

Advisory Committee:
Professor, Xiaoping Zhu, Chair
Associate Professor, Georgiy A. Belov
Professor, David M. Mosser
Professor, Siba K. Samal
Associate Professor, Yanjin Zhang

© Copyright by
Xiaoyang Liu
2018

Dedication

This dissertation is dedicated to my parents and my wife. I couldn't have done this without their support and patience. I appreciate them so much for everything they've given me. I love them all very much!

Acknowledgements

First, I thank my advisor, Dr. Xiaoping Zhu. Thanks for recruiting me to the University of Maryland. His true passion for science has impressed and inspired me. His excellent knowledge and professional mentorship lead me to the field of mucosal immunology. What he has done sets up the great model for my future endeavors. Also, I would like to thank all the members of my dissertation committee: David Mosser, Siba Samal, Yanjin Zhang and Georgiy Belov. I sincerely appreciate all of their valuable supports, suggestions and encouragements throughout my graduate study. I thank all of members of the Dr. Zhu's group. In particular, I am grateful to Senthil Kumar. He taught me a few lab techniques with patience, especially the technique IgG transcytosis. I also thank Dr. Weizhong Li, Dr. Susan Park, Dr. Jin Tang, Dr. Song Hui, Dr. Xiaoling Wu, Dr. Chunyan Ma and Arunraj Rajendrakumar who shared a wonderful time with me during my PhD study. Their knowledge and techniques benefit me a lot. Furthermore, I thank Iowis Zhu who carefully helps improving my manuscript writing. My sincere appreciation goes to Dr. Jeffrey Cohen for his kind support to my research. I thank all the faculties and staff in the department. Thanks for all the help and support. Finally, I thank my family. I don't know where I'd be without the love and support they have given me all these years. I am especially grateful to my wife, Danmin Zhao, for her patience and support during the past three years.

Table of Contents

Dedication	ii
Acknowledgements	iii
Table of Contents	iv
List of Figures	vii
List of Abbreviations	ix
Chapter 1: Introduction	1
The Neonatal Fc Receptor (FcRn)	1
Overview	1
FcRn belongs to the MHC- I family	2
The interaction of FcRn with IgG	4
FcRn-mediated IgG transport across polarized epithelial barriers	5
FcRn-mediated IgG protection from catabolism	7
FcRn involvement in Antigen presentation	8
FcRn distribution to endosomes is critical for FcRn functions	9
FcRn-based therapeutic strategies	11
Human Cytomegalovirus (HCMV)	13
Overview	13
The life cycle of HCMV	14
HCMV cell tropism	16
Diseases associated with HCMV infection	17
Therapeutic strategies for HCMV infection	19
Human Cytomegalovirus Immune Evasion	20
Innate immunity evasion	20
Interference with antigen presentation	22
Escape from natural killer cell response	27
Antibody immunity evasion	29
ER-associated degradation (ERAD) Pathway	30
Overview	30
Physiological ERAD pathway	32
Pathogen hijacked-ERAD	35
Questions to be addressed in my project	37
Chapter 2: Human cytomegalovirus evades IgG antibody-mediated immunity through the endoplasmic reticulum-associated degradation of the neonatal Fc receptor (FcRn) for IgG	40
Abstract	40
Introduction	41
Materials and Methods	44
Cell lines, Antibodies and virus	44
Construction of protein expressing vectors	46
Production of affinity-purified US11-specific Abs	49
Transfection and proteins expression	49
SiRNA interference	49

IgG binding Assay	50
Gel electrophoresis, Western blotting, immunoprecipitation	50
Analysis of N-linked glycosylation	51
Confocal immunofluorescence	51
Flowcytometry analysis	52
Quantitative Cycloheximide (CHX) chase assay.....	53
Detection of protein ubiquitination in cultured cells	53
Cell fraction	53
Enzyme-linked immunosorbent assay (ELISA)	54
In vitro human IgG transcytosis.....	54
In vitro human IgG protection	55
Statistic.....	56
Results.....	56
HCMV glycoprotein US11 interacts with FcRn.....	56
US11 interacts with FcRn in HCMV-infected cells	59
US11 expression inhibits FcRn trafficking to early endosomal compartments..	62
US11 blocks FcRn assembly with β_2m and retains FcRn in ER.....	63
HCMV US11 is required for FcRn protein degradation.....	66
US11 recruits Derlin-1 and TMEM-129 to engage FcRn for degradation	70
FcRn HC cytoplasmic tail is required for US11-mediated degradation	74
US11/Derlin-1/TMEM129/Ube2J2 protein complex induces FcRn dislocation, ubiquitylation, and degradation	77
US11 impairs FcRn IgG binding capacity	82
HCMV infection or US11 expression reduced IgG transcytosis in the polarized human epithelial monolayers	84
HCMV infection or US11 expression facilitates IgG degradation	86
Discussion	89
Chapter 3: HCMV Fc γ R cooperates with HCMV FcRn-targeting viral protein in facilitating host IgG degradation	98
Abstract.....	98
Introduction.....	98
Materials and Methods.....	101
Plasmids, cell lines and antibodies.....	101
Transfection and protein expression	103
Confocal immunofluorescence	103
Gel electrophoresis and Western blotting	104
IgG binding Assay	105
In vitro human IgG protection	105
Enzyme-linked immunosorbent assay (ELISA)	105
Results.....	106
HCMV vFcR γ s gp34 and gp68 colocalization with FcRn in the endosomes...	106
The human IgG binding capacity of gp34 but not gp68 significantly decreases in acidic pH condition	108
HCMV gp34 and gp68 enhance IgG degradation when FcRn is blocked by US11 expression	109
Discussion.....	112

Chapter 4: Conclusion and Perspective	115
Bibliography	120

List of Figures

1. Figure 1.1 The structural comparison of FcRn and MHC class I.....	3
2. Figure 1.2 FcRn-mediated recycling and transcytosis of IgG.....	10
3. Figure 1.3 Overview of the human cytomegalovirus life cycle.....	16
4. Figure 2.1 FcRn interacts with the HCMV US11.....	56
5. Figure 2.2 US11 interacts with FcRn in HCMV-infected cells.....	59
6. Figure 2.3 US11 expression inhibits FcRn trafficking to the early endosomal compartment.....	62
7. Figure 2.4 US11 blocks FcRn assembly with β_2m and retains FcRn in ER.....	64
8. Figure 2.5 US11 protein induces FcRn degradation.....	66
9. Figure 2.6 US11 recruits FcRn to Derlin-1 and TMEM129 protein complex.....	71
10. Figure 2.7 FcRn cytoplasmic tail is necessary for US11-mediated FcRn degradation.....	75
11. Figure 2.8 US11/Derlin-1/TMEM129/Ube2J2 protein complex induces FcRn dislocation, ubiquitylation, and degradation.....	79
12. Figure 2.9 US11 impairs FcRn IgG binding capacity.....	82
13. Figure 2.10 HCMV infection or US11 expression reduced IgG transcytosis in the polarized human epithelial monolayers.....	84
14. Figure 2.11 HCMV infection increased IgG catabolism in human endothelial cell.....	87
15. Figure 2.12 Proposed model for US11 interacting with FcRn.....	96
16. Figure 3.1 Intracellular staining pattern of gp68 and gp34.....	106
17. Figure 3.2 The human IgG binding capacity for gp34 but not gp68, significantly decreased in acidic pH condition.....	107
18. Figure 3.3 HCMV gp34 and gp68 enhance IgG degradation when FcRn is blocked by US11 expression.....	110
19. Figure 3.4 Proposed role of HCMV Fc γ R _s in IgG evasion in cooperation of HCMV FcRn-targeting viral proteins.....	112

List of Tables

Table I. I HCMV immune evasion on classical and non-classical MHC I molecules.....	26
Table II. I PCR primers in this study.....	47

List of Abbreviations

acquired immunodeficiency syndrome	AIDS
adaptor protein	AP
antibody dependent cell mediated cytotoxicity	ADCC
antigen presenting cell	APC
β_2 -microglobulin	β_2m
calreticulin	CRT
calnexin	CNX
cycloheximide	CHX
cyclic GMP/AMP synthase	cGAS
cytotoxic T lymphocyte	CTL
delayed early genes	DE
dendritic cell	DC
4', 6'-Diamidino-2-Phenylindole, Dihydrochloride	DAPI
dulbecco's modification of eagle's medium	DMEM
early endosomal Ag-1	EEA1
endo- <i>N</i> -acetylglucosaminidase	Endo H
endoplasmic reticulum	ER
endoplasmic reticulum-associated degradation	ERAD
ER quality control system	ERQC
DNA-dependent activator of IRFs	DAI
epidermal growth factor receptor	EGFR
enzyme Linked Immunosorbent Assay	ELISA

Fc gamma receptor	FcγR
fluorescein isothiocyanate	FITC
heavy chain	HC
heparan sulfate proteoglycan	HSPG
horseradish peroxidase	HRP
human cytomegalovirus	HCMV
Human hemochromatosis protein	HFE
Human herpesvirus 5	HHV-5
human immunodeficiency virus	HIV
human leukocyte antigen	HLA
idiopathic thrombocytopenic purpura	ITP
immune complex	IC
immunoglobulin G	IgG
immunoreceptor tyrosine-based activation motif	ITAM
immunoreceptor tyrosine-based inhibitory activation motif	ITIM
immediate early genes	IE
intestinal epithelial cell	IEC
interferon-inducible protein 16	IFI16
interferon regulatory factor 3	IRF3
intravenous immunoglobulin	IVIG
Janus tyrosine kinase	JAK
Leukocyte Ig-like receptor	LIR
lysosome-associated membrane glycoprotein-1	LAMP-1

lysosome membrane protein II	LIMP II
macrophages	M ϕ
major histocompatibility complex	MHC
major immediate early promoter	MIEP
mannose-6- phosphate receptor	MPR
MHC class I polypeptide-related sequence A	MICA
nature kill cell	NK
natural-killer group 2D receptor	NKG2D
neonatal Fc receptor	FcRn
normal goat serum	NGS
nuclear factor-kappa B	NF κ B
oligoadenylate synthetase	OAS
peptide -N-Glycosidase F	PNGase F
reverse transcription-PCR	RT-PCR
simian immunodeficiency virus	SHIV
signal transducers and activators of transcription	STAT
small interfering RNAs	siRNAs
stimulator of interferon genes	STING
systemic lupus erythematosus	SLE
T cell receptor	TCR
TNF-related apoptosis-inducing ligand	TRAIL
toll-like receptor	TLR
trans-golgi-networks	TGN

transepithelial electrical resistance	TER
transmembrane protein 129	TMEM129
transmembrane segment	TMS
transporter of antigen processing	TAP
tumor necrosis factor	TNF
UDP-glucose/glycoprotein glucosyl transferase	UGGT
UL16 binding protein	ULBP
valosin-containing protein	VCP
viral Fc gamma receptor	vFc γ R

Chapter 1: Introduction

The Neonatal Fc Receptor (FcRn)

Overview

It has been known for decades that the maternal Abs can be transferred to offspring and protect them from infection in their early life. In the 1950s and 1960s, Brambell and his colleagues investigated the phenomenon that γ -globulins were particularly selected for transmission from maternal circulation in contrast to most other circulated proteins, recognizing that this transfer was completely dependent on the Fc region of IgG (2). They also discovered that IgG had a longer persistence in circulation than most other plasma proteins, and this long half-life required its Fc region and a saturable rescue process (3, 4). Based on these studies, Brambell postulated a receptor that controlled both the transport of IgG during early life and the protection of IgG from catabolism later in life.

Brambell's hypothesis has finally been confirmed since the cloning of FcRn was firstly achieved from neonate Rat by Simister and Mostov in 1989 (5). Rat FcRn was a heterodimer, comprised of β 2-microglobulin and a 45-53kDa glycosylated heavy chain, associating with each other noncovalently. Then Human FcRn was also cloned from human syncytiotrophoblast (6), and the gene encoding FcRn heavy chain (*FCGRT*) was mapped to the chromosome 19q13 (7). The *FCGRT* gene products are relatively conserved among mammalian species, with the human *FCGRT* encoded receptor sharing overall 66% homology with mouse FcRn (8).

Over the last two decades, following the discovery of FcRn wide distribution in diverse cell types and tissues, a variety of roles for FcRn have been elucidated. The expression of FcRn in the polarized epithelial cells, such as syncytiotrophoblast (6), enterocytes (9) and bronchial epithelial cells (10), is consistent with its function in the IgG transport across the epithelial barriers. Furthermore, FcRn is also identified to be highly expressed in a variety of endothelial cells (11), which contributes to the protection of IgG from lysosome degradation. Furthermore, FcRn is expressed by human myeloid-derived antigen-presenting cells (APCs), such as macrophages, monocytes, B cells and dendritic cells (12), suggesting an additional role of FcRn in antigen processing and presentation.

FcRn belongs to the MHC- I family

FcRn heavy chain is a type I glycoprotein consisting of $\alpha 1$, $\alpha 2$, $\alpha 3$ extracellular domains, a transmembrane region, and a short cytoplasmic tail. The association with β_2 -microglobulin suggests that FcRn heavy chain may be a major histocompatibility complex (MHC) class I-related molecule as it is a mutual feature of the MHC class I family. Indeed, sequencing analysis unveiled that all three extracellular domains of FcRn heavy chain shared homology with the corresponding regions of MHC class I molecules (13). Despite the similarity between the extracellular domain of FcRn α -chain and other MHC class I molecules, their cytoplasmic domains share much less homology, distinguishing the functional activities of FcRn from that of other MHC class I family members (14).

The X-ray crystallographic structure revealed by Bjorkman et al further confirmed the similarity between the overall three-dimensional structure of FcRn and that of the MHC class I family molecules (Figure 1.1) (15). However, the groove located between the $\alpha 1$ and $\alpha 2$ -helices in the MHC class I for peptide or glycolipid ligands binding is occluded in FcRn.

This occlusion is primarily caused by a proline substitution of the conserved valine at position 165 of the $\alpha 2$ domain helix, resulting in a kink that close the potential peptide binding cleft (16). This nonfunctional version of the MHC peptide-binding groove has allowed FcRn to evolve to new functions as binding IgG and albumin (17). Similar with MHC-I, FcRn has been found to associate with calnexin and ERp57 in ER, which promote the folding and assembly of FcRn HC- β_2m complex. However, unlike MHC-I, FcRn assembly does not require the peptide-loading complex TAP and tapasin, consistent with the absence of the peptide-binding groove in FcRn (294).

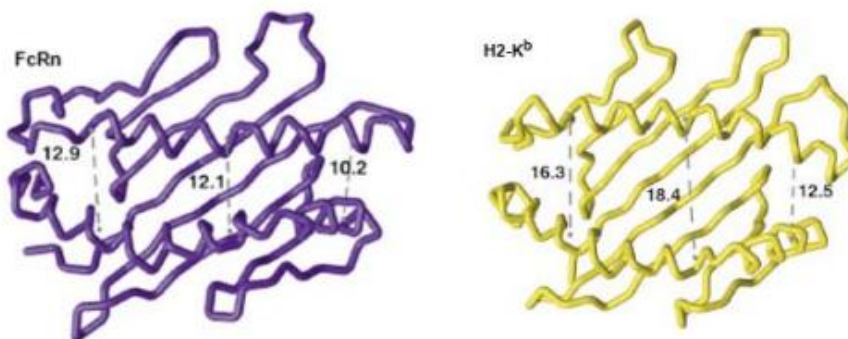
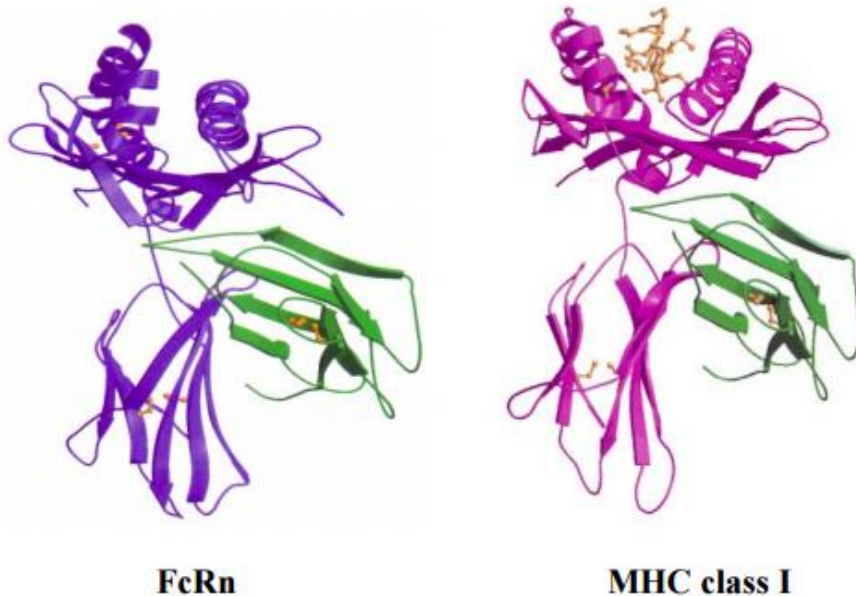


Figure 1.1 The structural comparison of FcRn and MHC class I. A. The crystallographic structure of FcRn and MHC I (18); B. the α 1- α 2 domain of FcRn and MHC I (19).

The interaction of FcRn with IgG

The ability of FcRn to bind IgG lays the foundation for its diverse functions in antibody-mediated immunity, thereby having triggered intensive studies on the mechanisms of FcRn-IgG interaction. The binding affinity of human FcRn to the four IgG subclasses in human (IgG1, IgG2, IgG3, and IgG4) ranges from 20 nM (IgG1) to 80 nM (IgG4) (20). FcRn-IgG co-crystal structure revealed that FcRn binds to the CH₂-CH₃ hinge region of IgG, which overlapped the binding site of IgG with staphylococcal protein A (21). Site-directed mutagenesis analysis disclosed that the Ile253, His310 in CH2 domain and the His435 in CH3 of domain IgG are the key amino acids that mediate in the interaction of IgG with FcRn (22, 23). On the FcRn part, the acidic residues Glu117, Glu132 and Asp 137 on the C-terminal portion of the heavy chain α ₂ domain and the amino acid Ile1 on the β 2m subunit play an essential role in FcRn-IgG binding (24).

Different from other Fc γ Rs, FcRn binding to the Fc region of IgG manifests a strictly pH-dependent manner (25, 26). At physiological pH7.4, FcRn cannot interact with IgG at detectable levels, while at acidic pH condition (pH6.0-6.5), FcRn binds to IgG with high affinity. Biochemical and crystallographic data reveal that, after binding at pH 6, neither FcRn nor IgG undergoes major conformational changes. Instead, it is the protonation of histidine residues (H310, H435, H436) in the CH₂-CH₃ hinge region of IgG1 that enables the formation of salt bridges at the FcRn-Fc interface with the acidic residues (E117, E132, and D137) on the α 2 domain of FcRn, leading to the establishment a hydrophobic interaction between FcRn and the Fc portion of IgG (28).

FcRn-mediated IgG transport across polarized epithelial barriers

FcRn was initially found in the transfer of maternal IgG to offspring in different animals. In the gut of rodents, the expression of FcRn in rodent is mostly on the epithelial cells at the proximal small intestine and then decline rapidly after weaning (29). After the maternal IgG from ingested milk passes through the stomach into the duodenum, the acid pH at the proximal duodenum facilitates the binding of IgG to FcRn on the apical surface of the epithelial cells (30). Then FcRn-IgG complexes are internalized by receptor-mediated-endocytosis and transcytosed across the epithelial cellular plasma, eventually releasing the IgG at the basolateral surface of the cell, due to an increase to physiological pH (28). No maternal IgG was transported in β_2 -microglobulin^{-/-} or FcRn ^{-/-} mice (31), confirming the role of FcRn in the transport of IgG from mother's milk to newborns. Nevertheless, in human, transporting across the placenta is the major route of maternal IgG delivery to the fetus. FcRn is highly expressed on the syncytiotrophoblasts epithelial monolayer, which transports IgG from maternal circulation to the placental villi capillaries of the fetus (32). The maternal IgG uptaken via the fluid-phase pinocytosis accumulates in endosome vesicles, where the gradual acidification makes possible the tight binding of IgG to the FcRn present in this compartment (33, 34). The vesicle then fuses with the membrane on the fetal side of the syncytiotrophoblast monolayer, where the physiological pH promotes the dissociation of IgG from FcRn (35, 36). FcRn is also present in human fetal intestine epithelial cells, where it may play an additional role in the uptake of IgG from ingested amniotic fluid to the fetal circulation (37).

As a bi-directional IgG transporting receptor, FcRn can also mediated the transport of IgG from basolateral to apical direction (38). This leads to the considerations that FcRn may transport the pathogen-specific IgG from the circulation or lamina propria to the mucosal

surface to protect host from mucosal infection. Mucosal secretions of the human gastrointestinal, respiratory, and genital tracts contain both the IgG and secretory IgA (sIgA), which are equally effective against mucosal infection (39). Actually in humans, IgG concentrations predominate over sIgA in the lumen of the lower respiratory and female genital tracts (40, 41). Previous studies showed that systemically administered IgG provided protection against infection by respiratory syncytial virus in the human lung (42) and HIV in the monkey intestine and vagina (43). Given that FcRn is the sole transporter for IgG across the mucosal epithelial barrier, the secretions of protective IgG to the mucosal surface, mainly depend on this receptor. At the basolateral side of mucosal barrier, circulating IgG is likely internalized into polarized epithelial cells via fluid-phase pinocytosis and captured by FcRn in acidified endosome compartments (50). Subsequently, FcRn can recycle the internalized IgG away from lysosome and to the cell surface at the lumen side of mucosal barrier, where the IgG is released into the extracellular milieu as a result of the neutral pH. Indeed, several studies have demonstrated the importance of FcRn in the prevention or clearance of mucosal surface infection. Systemically administered pathogen-specific IgG reduced mucosal diseases severity only in FcRn-competent mice upon challenge with pathogens such as *Helicobacter pylori* in gastric surface (44) and *Chlamydia muridarum* in genital tract (45). Moreover, passive transfer of neutralizing antibodies efficiently protected the mice from infection after genital challenge with SHIV in an FcRn-dependent manner (46), although it also relied on the antibody-neutralizing capacity and the non-neutralizing antibodies actually facilitated infection.

Moreover, the capacity of bi-directionally transporting enables FcRn to serve more complex functions in immune surveillance, which are to secrete IgG to mucosal surface for capturing luminal antigens and to retrieve the IgG/antigen complex to the lamina propria for recognition by immune system. In contrast to the rapid decline in rodent gut after weaning,

the expression FcRn in human gut is constitutive throughout the entire life, suggesting an additional role of FcRn in human intestine besides maternal IgG transfer. By using a human FcRn transgenic mice, Blumberg and his colleagues showed that systemically injected antigen-specific IgG was secreted across intestinal epithelial barrier into the lumen, where it can bind the orally-administrated antigen. Then FcRn was able to recycle the IgG-antigen complex back across the intestinal barrier into the lamina propria for processing by dendritic cells and presentation to CD4⁺ T cells in in the draining lymph node (47). Later, in a murine model of intestinal infection with *Citrobacter rodentium*, FcRn was shown to be essential in directing the bacteria-associated antigens from the intestinal epithelium to regional lymph nodes for initiation of an adaptive immune response (48). Beyond the intestinal, evidence also demonstrated that FcRn expressed in lung epithelial cells can scavenge luminal antigens across mucosal barrier and permit their efficient delivery to the immune system (10).

FcRn-mediated IgG protection from catabolism

In circulation, IgG has a longer half-life (6-8 days in mice and 21 days in human) than other serum proteins (1 day) that are not freely filtered by the kidneys (28). Evidence from the FcRn or β 2-microglobulin knockout mice have demonstrated the important role of FcRn in maintaining the IgG homeostasis. In FcRn-deficient mice, the IgG half-life in circulation is significantly reduced from 6-8 days to 1 day (49), with the serum IgG level dramatic decreasing to 20–30% of wild-type animals (50, 51). The mechanism for FcRn-mediated IgG protection is likely through the salvage of the internalized IgG in FcRn-expressing cells. Following the entry into endosomes via fluid-phase pinocytosis, serum IgG is captured by FcRn present in these acidic cellular compartments. Subsequently, FcRn-bound IgG will be recycled away from the downstream lysosome vesicles and back to the cell surface, while the unbound IgG will be destined to degradation in lysosome (28). This hypothesis has been confirmed by several studies: (1). FcRn mainly resides in early endosomes, rather than at cell

surface (52, 12); (2). Recombinant IgG with FcRn binding site mutations was found mostly located and eventually degraded in lysosome as revealed by confocal microscopy analysis (53, 54); (3). Live images have successfully elucidated the IgG intracellular recycling pathways (55, 56).

Besides the mechanism, the exact tissue and cell type for the FcRn-mediated IgG protection also need further investigation. In fact, the relative contribution of different cell types to IgG recycling depends on many factors, such as FcRn expression level, the rate of pinocytotic/phagocytotic activity and the concentration of IgG in the microenvironment. The conditional deletion of FcRn in the vascular endothelium of mice by using the Tie-2-driven Cre promoter revealed that the primary sites for the maintenance of endogenous IgG in mice are endothelial cells (57). Furthermore, a study using the bone marrow chimeric mice proved that myeloid-driven APCs such as monocytes, macrophages and dendritic cells also involved in the homeostasis of serum IgG in a FcRn-dependent manner (58).

FcRn involvement in Antigen presentation

Expression of FcRn has been demonstrated on both mouse and human hematopoietic cells, including APCs such as all subsets of DCs, macrophages, and monocytes and B cells (12, 58). This suggests that, in addition to the salvage of monomeric IgG, FcRn may also play an important role in antigen presentation via binding the IgG/antigen immune complex (IgG-IC). Indeed, several reports have provided evidence that FcRn expression by DCs can promote the antigen presentation by MHC class II molecules to CD4⁺ T cells (59) and the cross presentation by MHC class I molecules to CD8⁺ T cells (60, 61). DCs exposed to IgG-ICs, but not to the FcRn nonbinding IgG_{IHH}-ICs (an IgG Fc mutant with I253A, H310A, and H435A mutations), induce significant CD4⁺ T cell proliferation both in vitro and in vivo in WT mice, while the capacity of DCs to present IgG-ICs is largely impaired in FcRn-

deficient mice (59). The mechanism for FcRn involvement in this presentation process is proposed that Fc γ Rs expressed on the surface of APCs cooperate with FcRn in the processes of antigen presentation, with Fc γ Rs binding IgG-ICs on the cell surface at neutral pH and handing off them to FcRn in the acidified endosomes (58). The reason why the FcRn in DCs facilitates IgG-ICs degradation for antigen processing rather than protection and recycle of them is that the physical properties of the IgG-IC complex determine where it will be delivered by FcRn. Multivalent IgG-ICs are more likely to be diverted to the lysosome, in contrast, monomeric IgG is sorting into recycling endosomes and away from lysosomes (62). It was proved that the cross-linking of FcRn upon multivalent ligands binding diverts this receptor and its cargo to lysosomes (62), although the general mechanism for this sorting pathway is not clear. Furthermore, the invariant chain (Ii), which expresses in APCs and stabilizes the MHC class II, can also interact with FcRn and enhance FcRn distribution to late endosome /lysosome (63).

FcRn distribution to endosomes is critical for FcRn functions

In epithelial and endothelial cells, two major cell types where FcRn is highly expressed and governing the IgG transcytosis and homeostasis, FcRn displays a preferential intracellular distribution to an acidic compartment - endosome (12, 28 and 52). This is consistent with an important feature of FcRn that its binding to IgG exclusively occurs at acidic pH condition (25, 26). Thus, it is reasonable to conclude that it is indispensable for FcRn to enter into endosomes either directly from trans-Golgi-networks (TGN) or endocytosed from the cell membrane, in order to perform its major functions such as transporting IgG across mucosal epithelial barriers and maintaining IgG homeostasis in circulation (Fig 1.2). However, the mechanisms for the regulation of FcRn distribution into endosome pathway are not fully elucidated.

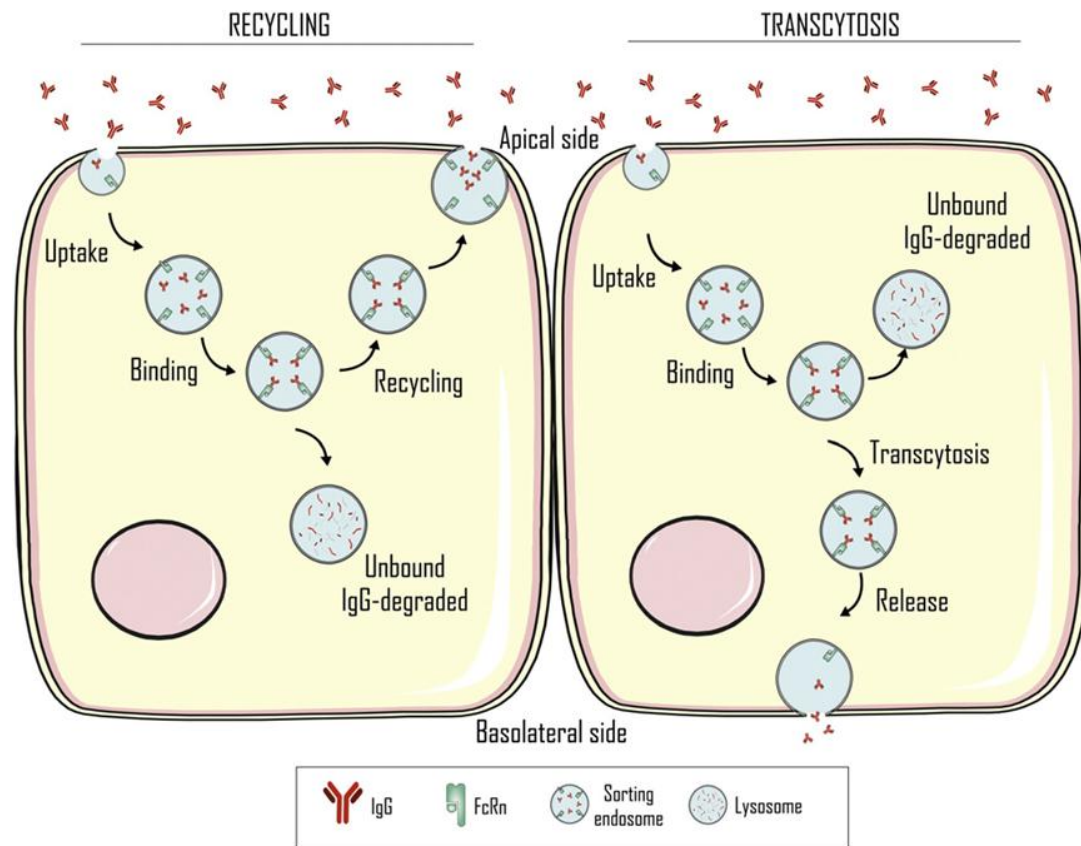


Fig 1.2. FcRn-mediated recycling and transcytosis of IgG. From Martins et al., *s Pharmacology & Therapeutics* 161 (2016) 22–39.

The sorting signals on the cytosolic tail of transmembrane proteins determine their trafficking pathway to endosomes (64, 65). These signals are consensus motifs, with a short and linear sequence of amino acids, including the tyrosine-based NPXY or YXX ϕ motifs (66, 67) and the dileucine-based [DE]XXXL[LI] or DXXLL motifs (67, 68). The LDL receptor and insulin receptor contain NPXY-type sorting signals, whereas LAMP1, CD3, Polymeric Ig receptor and Transferrin receptor possess YXX ϕ -type signals (68, 65). Another large group of endosomal proteins contain dileucine-based motifs sorting signals, such as LIMP II, Invariant chain, CI-MPR and CD-MPR (65, 69). Both of the tyrosine-based and the dileucine-based motifs recruit the adaptor protein AP2 and induce the clathrin-mediated

endocytosis (70, 71). It should be emphasized that the later is also recognized by adaptor protein GGAs (Golgi-localizing, gamma-adaptor homology domain, ARF-binding protein), which involve in protein trafficking from the Golgi to the endosome (72).

The cytoplasmic tail of all species of FcRn contains the endosome sorting signals: the DDXXXLL motif and the WXX ϕ motif, a variant of the canonical YXX ϕ motif (73). By using the FcRn mutations with alanine replacing the key residues in these two motifs, Zhen Wu and Neil E. Simister demonstrated that both dileucine-based and tryptophan-based motifs were responsible for the endocytosis of FcRn and its ligand IgG-Fc, yet showing no evidence that such signals were also responsible for the sorting of FcRn from TGN (Trans Golgi) to the endosomes (74). Furthermore, the identification of calmodulin-binding motif in the cytoplasmic tail of FcRn solved the question why FcRn, after trafficking to endosome, was not further delivered to its downstream vesicle – lysosome. It was reported that calmodulin can bind directly to the FcRn cytoplasmic domain and sort FcRn and its cargo away from the lysosome degradation pathway and into a bidirectional transcytosis or recycle route (75).

FcRn-based therapeutic strategies

As FcRn prolongs the half-life of IgG, it is reasonable to think that therapeutic antibodies engineered with higher FcRn-binding affinity would have improved efficacy due to longer persistence in circulation. Subsequently, exploitation of the IgG–FcRn interaction has continued in non-human primates. It was reported that mutations (M252Y/S254T/T256E) in the anti-respiratory syncytial virus human IgG1 exhibited 10-fold increase in the affinity for FcRn, and a 4-fold increase in the half-life in monkeys, as compared to WT human IgG1 (76). Moreover, antibodies with T250Q/M428L mutations exhibited a 29-fold increase in FcRn binding and a 2.5-fold increase in serum half-life in monkeys without alterations in antigen binding functions (77). In fact, the fusion of IgG-Fc portion to target proteins

constitutes a novel strategy for the half-life extension of all protein-based agents in the serum. Currently, 11 Fc-fusion proteins of various types had been approved by FDA (78), in some cases, with the half-life increasing up to 13 days in humans.

Based on FcRn's capability to transfer IgG across the polarized epithelial barrier, numerous strategies are proposed and applied in passive or maternal immunity that can give protection against pathogenic infection at the mucosal sites or in the fetus. Several studies demonstrated that FcRn mediated the transport of systemically administered, pathogen-specific, neutralizing antibodies to the gastrointestinal or genital tract mucosal sites to defend against pathogen infections at the site of their entry (79, 80 and 81). And FcRn-mediated IgG across the syncytiotrophoblasts barrier was also employed in maternal immunity, as the treatment of mothers with human cytomegalovirus (HCMV) neutralizing antibodies protected fetus from congenital infection (82, 83). The abilities of FcRn to sample and process the IgG-bounded antigens from the mucosal site are also explored to produce mucosal vaccines that can induce protections at the sites of the pathogen entry. Most commercially available vaccines administered by subcutaneous or intravenous injections can provide only minimal protection at sites of infection due to suboptimal activation of the mucosal immune system. Ye and his colleagues constructed a novel mucosal vaccine by fusing the HSV-2 glycoprotein gD antigen to the IgG-Fc portion and they found this gD-Fc fusion protein can be transferred by FcRn across the mucosal barrier to the lamina propria, thus inducing efficient immune responses both at mucosal and systemic levels (84).

On the contrary, there are also attempts to interfere with the IgG-FcRn interaction so as to modulate the serum antibody level. These strategies are mainly applied in the treatment of autoimmune diseases, such as the myasthenia gravis, idiopathic thrombocytopenic purpura (ITP), rheumatoid arthritis and systemic lupus erythematosus (SLE). These diseases are

caused by excessive self-recognizing antibodies (85), which can be decreased by several FcRn-based therapeutic methods. In humans, high dosage of intravenous immunoglobulin (IVIG) has been approved for clinical treatment of autoimmunity, as it can reduce the endogenous pathogenic antibodies by saturating the IgG salvage pathway (86). Alternatively, administration of engineered IgG Fc mutants with unusually high affinity to FcRn results in rapid degradation of endogenous antibodies and attenuation of arthritic lesions (87). Blocking FcRn-IgG interaction by employing FcRn specific antibody is another approach to reduce pathogenic IgG. It has been reported that anti-FcRn monoclonal antibody alleviates the disease morbidity in rats with experimentally induced myasthenia gravis but not other immune diseases (88).

Human Cytomegalovirus (HCMV)

Overview

Human cytomegalovirus, also known as Human herpes virus-5 (HHV-5), is a member of the pathogenic human β -herpesvirus subfamily of *Herpesviridae*. It has the largest genome of the characterized human herpesviruses, nearly 235 kb, containing approximately 192 open reading frames (ORFs) with the capacity to encode functional proteins (89). The double-stranded genome DNA of HCMV is comprised of two domains, the unique long region (UL) and the unique short (US) region, separated by an internal repeat segment (IR). The UL region encodes 151 proteins from UL1 to UL151, while the US region encodes 34 proteins from US1 to US34 (90). In mature virions, the HCMV genome is housed in an icosahedral protein capsid that is surrounded by a layer of proteins called the tegument. The tegumented capsid is in turn enclosed within a lipid membrane envelope, which contains glycoproteins that mediate the viral entry into a host cell (91). Beyond the proteins necessary for the viral replication and structure, the large DNA genome enables HCMV to encode numerous

products for the host interaction, including: manipulation of cell cycle progress, modulation of the cellular stress response, apoptosis control and immune evasion (92). HCMV can infect and replicate in a wide variety of human cells, including epithelial cells of the gland and mucosal tissue, smooth muscle cells, fibroblasts, hepatocytes, vascular endothelial cells, macrophages and dendritic cells (93). This broad cell tropism facilitates the viral systemic spread in the individual human body and across the population. Moreover, HCMV establishes latency in myeloid cells of the bone marrow, leading to a life-long infection with sporadic reactivation (94). HCMV infection is typically asymptomatic and unnoticed in healthy people.

In worldwide, HCMV infection is found in approximately 60% of adults in developed countries and almost 100% in developing countries (95). Although seemingly innocuous in healthy people, HCMV infection poses a life-threatening risk to immune compromised individuals. It is a common opportunistic infection in fetus, allograft recipients, bone marrow transplant patients and AIDS patients, causing significant increase in their morbidity and mortality (92, 96). Notably, HCMV is recognized as the leading infectious cause of congenital neurological disease via transmission through the placenta from the mother to the fetus (97). The social burden caused by HCMV has motivated the development of treatments and vaccines. However, so far, there is no HCMV vaccine approaching imminent licensure. And drugs, such as ganciclovir or cidofovir, which can inhibit HCMV replication, are far from ideal due to high toxicity, low bioavailability, and the development of drug-resistant virus strains (98).

The life cycle of HCMV

The first step of HCMV life cycle is the viral entry (Fig 1. 3. A) , during which viral envelope glycoproteins gB (UL55), gM/gN (UL100/UL73), and gH/gL (UL75/UL115), interact with host receptors HSPG, EGFR and integrins to mediate fusion or endocytosis of

the virion into the cell (99). Then viral capsid and tegument proteins are delivered to the cytosol. Capsid-bound tegument proteins UL47/UL48 interact with the host microtubule machinery to transport viral capsids to the nuclear envelope (Fig 1. 3. B), with the subsequent release of the viral DNA into the nucleus (100). Other tegument proteins are delivered to different subcellular locations to inhibit the initial steps of immune response (UL83) (101), control cellular apoptosis (UL38) (102) and trigger the viral gene expression (UL82) (103). Tegument proteins induce a temporally regulated cascade of the expression of viral immediate early (IE) genes, followed by delayed early (DE) genes, which initiate viral genome replication, and late (L) genes, which constitute the viral structure (91, 102, 104). Four HCMV L gene products (pUL46, pUL80, pUL85, pUL104) assemble the viral capsid in the nucleus and egress through the nuclear membrane by disruption of the nuclear lamina (Fig 1. 3. C) (105, 106). After the capsids enter the cytoplasm, the cellular secretory machinery, including the endoplasmic reticulum (ER), Golgi apparatus, and endosome, is hijacked to form a cytoplasmic viral assembly complex (AC), where capsids acquire their tegument layer and envelope by budding into intracellular vesicles (Fig 1. 3. D) (107, 108, 109). Finally, the enveloped virion particles are released into the extracellular space.

Like other herpesviruses, HCMV has two life cycle phases: a productive phase, where new virions are produced and a latent phase where gene transcription is restricted and no new virion produced. It is now well known that the site of HCMV latency is in myeloid lineage cells, including CD14⁺ monocytes and their CD34⁺ progenitor (110, 111). In these cells, a combination of lacking viral activators (112) and the presence of latency-associated repressors (110) on the major immediate early promoter (MIEP), suppresses lytic transcription and maintains latent state (113, 114). Upon terminal differentiation of these cells to mature macrophage or dendritic cells, however, changes in the nuclear environment trigger the activation of the viral MIEP and reactivation of lytic replication (113, 114).

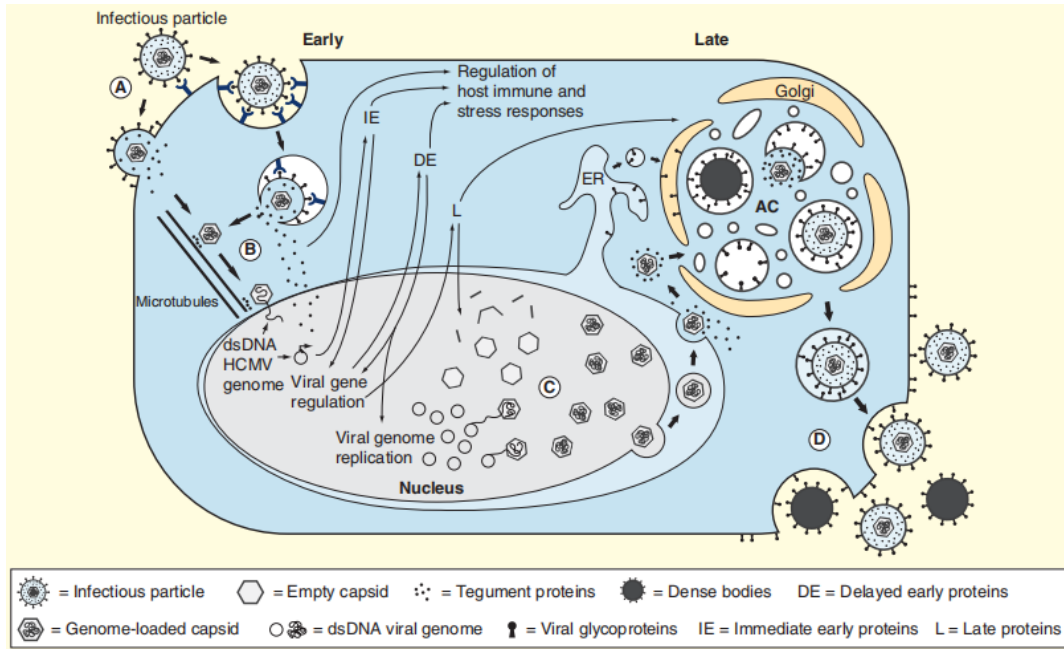


Fig 1. 3. Overview of the human cytomegalovirus life cycle (92).

HCMV cell tropism

HCMV has a broad cell tropism, which has great influence on the pathogenesis of acute HCMV infections. Mucosal epithelial cells, vascular endothelial cells, smooth muscle cells, fibroblasts, monocytes and dendritic cells, are the predominant targets for viral replication (93). Infection of epithelial cells presumably contributes to inter-host transmission. For example, the infants' gastrointestinal tract epithelial cells are exposed during breast feeding, through which HCMV can be transmitted from the breast milk of a seropositive mother (115). On the other hand, infection of endothelial cells facilitates systemic spread within the host. These cells support productive lytic infection and thus promote dissemination of HCMV from the circulating blood into organ tissues (116). As for the smooth muscle cells and fibroblasts, their ubiquitous distribution throughout the human body and high titers of viral release imply that they are the ideal platform for efficient proliferation of the HCMV (116, 117). In addition, as mentioned above, the myeloid lineage monocytes and dendritic

cells provide the shelter where HCMV can establish a latent infection to evade immune surveillance.

In cell culture studies, a variety of primary cells cultures including retinal pigment epithelial cells, placental trophoblast cells, hepatocytes, neuronal and glial brain cells, kidney epithelial cells, vascular endothelial cells, monocyte-derived macrophages and dendritic cells, support the complete viral replication cycle (118,119). And skin or lung fibroblasts have become the standard cell type for isolation and propagation of HCMV from patient samples (91). However, the extensive propagation in fibroblasts results in the loss of broad cell tropism in the popular laboratory HCMV strains, such as AD169 and Towne. They have very low efficiency in infecting the epithelial and endothelial cells, while their parental clinical isolated strains such as TR and FIX maintained their epithelial and endothelial cell tropism. It was found later that the loss of broad cell tropism in laboratory strains is mainly because of the failure in viral entry stage (120). The introduction of bacterial artificial chromosome (BAC) technology and subsequent site-directed mutagenesis enables the scientists to identify that UL131–128 genes, absent in laboratory-adapted strains, are indispensable for the broad cell tropism (121). Their gene products, UL128, UL130 and UL131, associate with the viral envelope glycoproteins gH and gL to form a complex that plays a crucial role in viral entry into epithelial and endothelial cells (122).

Diseases associated with HCMV infection

With a widespread infection among the world population, HCMV has been associated with severe diseases in three groups of immunocompromised hosts: (a) fetuses presumably due to immunological immaturity, (b) allograft recipients due to cytotoxic anti-rejection agents and in some cases graft-vs-host reaction, and (c) HIV infection with loss of CD4⁺

lymphocytes and the consequent loss of adaptive immune responses (92). Diseases in these patients range from pneumonia, hepatitis, retinitis, enteritis to hearing loss and neurological damage (96).

HCMV can be transmitted through the placenta from the mother to the fetus, resulting in spontaneous abortion, premature delivery and birth defects. Actually, it is believed as the leading infectious cause of congenital neurological disease (97). Approximately 2% women have their primary infection by HCMV during pregnancy (123). Among them, 32% transmit virus across the placenta to cause intrauterine infection (96). The fetus can also be infected by reactivation of latent maternal infection or by maternal reinfection with a new strain (124). Approximately 1% of women who are seropositive prior to pregnancy deliver babies with congenital HCMV infection (125). Considering the large abundance of seropositive women in the antenatal population, the number of consequent HCMV-infected newborns is substantial. Hearing loss and mental retard are the two major long-lasting sequelae, which occurs at a frequency of up to 5%-20% among infants with congenital HCMV infection (126, 127). Brain neurological damage by intrauterine HCMV infection mainly results from the loss of normal cortical architecture and intracranial calcium deposits, followed by the loss of the integrity of the endothelium and loss of cognitive function (128). Children with the neurodevelopmental disability caused by congenital HCMV infection often require long-term custodial care and extensive medical interventions, leading to a huge burden on the social healthcare system.

Another type of immunocompromised people, allograft recipients, and bone marrow transplant patients also suffer from diseases by HCMV infection, causing end-organ severe diseases such as gastrointestinal ulceration, hepatitis, pneumonia or retinitis, and aggregating the graft rejection and dysfunction (91). The HCMV infection in these patients is mainly due

to infection in the transplanted organs or reactivation of host latent infection in the context of immune suppression. During solid organ transplantation, seropositive donors transmit HCMV to seronegative recipients at a frequency of 70% (129). Approximately 40% of seropositive recipients reactivate latent HCMV when given immunosuppressive drugs (130). Although many recipients receive antiviral prophylaxis treatment up to 100 days after transplantation, late infections still occur in approximately 20-30% of patients, and up to 50% of these infections are severe, suggesting that antiviral prophylaxis does not eliminate the clinical impact of HCMV in allograft recipients (131). As for the hematopoietic allograft recipients, the most severe disease is associated with pulmonary infection, a site rarely observed in solid organ allograft recipients, presumably due to the concomitant graft-versus-host reaction. Early reports showed a mortality rate of 70%-95% in patients with HCMV pneumonia in bone marrow allograft recipients (132).

HCMV was one of the first opportunistic pathogens identified in the acquired immunodeficiency syndrome (AIDS) patients (133). The unique feature associated with HCMV infection in these patients is the end-organ disease in two organ systems, the gastrointestinal tract and the eye. The pathogenesis of disease in the gastrointestinal tract includes focal colitis and chronic dysfunction of the absorptive functions (134,135). A second unique manifestation of HCMV infection in AIDS patients is retinitis. In some reported studies, it led to vision loss as many as 25% of patients with AIDS (136).

Therapeutic strategies for HCMV infection

For the past several decades, the major drugs for preventing or treating HCMV infection are cidofovir and ganciclovir. Cidofovir showed activity against HCMV, but its renal toxicity precludes its application in routine clinical practice (92). Ganciclovir is used for preemptive therapy or prophylaxis in allograft recipients and also in AIDS patients to treat

with HCMV associated end-organ disease. However, its use in neonates to treat with congenital infection needs more cautious evaluation. A phase III clinical trial, where the neonates with CNS symptoms were randomized to receive ganciclovir or placebo treatment (137), showed that ganciclovir treatment reduced the cases of hearing loss and miss of developmental milestones. But it also showed that, at some doses level, this drug produced clinically significant neutropenia (138).

So far, no HCMV vaccine appears to be approaching the imminent licensure (91). Yet, several potential live attenuated or subunit vaccines are actively testing in clinical trials. Among them, recombinant vaccines based on HCMV envelope glycoprotein gB is the most promising candidate, since up to 70% of the neutralizing antibody response to HCMV is gB-specific (139). A double-blinded, placebo-controlled phase II study of gB/MF59 vaccine revealed 50% protective efficacy of this vaccine in young women (140). For the protection of the fetus against the congenital infection, the optimal method is through the maternal immunity. The HCMV-specific neutralizing antibody produced in immunized mothers can be passively transferred through the placenta to the fetus. Although previous non-randomized studies with maternal HCMV-specific antibodies therapy manifested reduced intrauterine transmission of HCMV (141, 142), a randomized, placebo-controlled trial of the same preparation failed to repeat the initial observations(143). Thus, the application of maternal immunization in the prevention of neonatal HCMV infection still needs further evaluation.

Human Cytomegalovirus Immune Evasion

Innate immunity evasion

During the viral entry into a host cell, HCMV envelope glycoproteins gB and gH activate the innate immunity receptor TLR2 through a physical interaction and initiate the

activation of cellular transcription factors NF κ B (144). In most cases, the activation of canonic NF κ B pathway will lead to the induction of a variety of inflammatory cytokines, including TNF- α , IL-1, IL-6, IL-8, IL-12, and IL-18 that are critical for the recruitment and activation of phagocytic leukocytes to the sites of infection (145). However, in HCMV infection, it was proved that the immediate early 86 kDa protein (IE2) can block the binding of NF κ B to the target DNA, thus inhibiting the transcription of downstream inflammatory cytokines. (146, 147).

Another innate immune response triggered by HCMV infection is the activation of the regulatory transcription factor IRF3 and the subsequent induction of Type I interferons, which establish an antiviral state in the infected and surrounding cells. It was proved that viral envelope gB was not involved in triggering the IRF3 pathway (148). Instead, the intracellular DNA sensor DNA-dependent activator of IRFs (DAI) was proved essential in activating the IRF3 in fibroblast cells (149). Recently a report shows that, in monocyte--derived DC and macrophages, cyclic GMP/AMP synthase (cGAS) which senses viral cytosolic DNA and catalyzes the formation of the cyclic dinucleotide cGAMP, induces robust type I interferon responses to HCMV infection through the STING-TBK1-IRF3 signaling pathway (150). HCMV tegument protein pUL83 was found to counteract nuclear DNA sensor interferon-inducible protein IFI16 by interacting with its pyrin domain and blocking its oligomerization upon DNA sensing (151).

Although interferon IFN production can be recognized by DNA sensors, HCMV can still block its downstream JAK/STAT signaling pathway. After the binding IFN- α or β to the type I IFN receptor, the phosphorylation of tyrosine kinase 2 (Tyk2) and Janus kinase 1 (JAK1) phosphorylates STAT1 and 2, which will form a heterodimer and induce the upregulation of IFN-stimulated genes ISGs (152). A previous study uncovered that HCMV IE

72 kDa protein (IE1) associated with STAT2 to prevent its DNA binding and subsequent ISG induction (153). HCMV can even survive in the ultimate stage of IFN-immunity, by compromising the function of ISGs products. IFN-induced protein kinase R (PKR) and 2'-5' oligoadenylate synthetase (OAS)/RNaseL can shut off protein synthesis during viral infection. HCMV proteins pTRS1 and pIRS1 have been identified to block OAS-mediated eIF2 α phosphorylation and to reduce RNA degradation by RNase L (154).

Interference with antigen presentation

Antigen presentation is the key step to initiate the host adaptive immune response against the invading pathogens. Classical MHC-I molecules can present the endogenous antigens to the TCR complex of the CD8⁺ T cells and activate the CD8⁺ T cells, which plays the crucial role in eliminating the intracellular pathogens, such as virus and mycobacteria (155). Classical MHC I molecules consist of α heavy chain, heterodimerized with the β_2m subunit in the lumen of the endoplasmic reticulum (ER). The peptide loading complex (PLC), comprising of TAP1 and TAP2 subunits, is recruited to the MHC-I and translocates the cytosolic antigen peptides to the ER lumen (156), where these peptides are trimmed by ER aminopeptidases to obtain a length fitting the MHC I peptide binding groove (157). The MHC I-peptide complex is then transported to the cell surface for antigen presentation. The HCMV US6 gene family products, include US2, US3, US6, US10 and US11, induce strong downregulation of the MHC-I molecules from the cell surface (as summarized in Table I. I), thus evading the CD8⁺ T mediated cytotoxicity.

Expressed as an immediate early protein only a few hours after infection, US3 interacts with MHC-I and retain MHC-I in ER lumen, consequently impairing its trafficking to cell surface (158). By using site-directed mutagenesis, Lee and his colleagues identified

three residues (Ser 58, Glu 63 and Lys 64) in the ectodomain of US3 are essential for US3 retention, with a single mutation of any of the three residues interrupting its ER localization and MHC I retention ability (159). However, these three residues are not responsible for interaction of US3 with MHC I. Although the exact residues responsible for the interaction between US3 and MHC I remains unidentified, both of the ectodomain and the transmembrane segment (TMS) of US3 were reported necessary to maintain this interaction (160).

After retained in the ER, MHC-I molecules can be dislocated by HCMV early protein US2 from ER lumen to the cytosol for proteasome degradation (161). The luminal domain of US2 is responsible for the recognition of MHC-I molecules (162). Although its transmembrane (TMS) and cytosolic tail are dispensable for MHC-I contact, they are necessary to complete subsequent steps of the interaction, such as forwarding MHC I for proteasomal degradation (163). On the MHC I part, the residues interacting with US2 are located in a region between the C-terminus of the $\alpha 2$ domain and the $\alpha 3$ domain (164). US2-mediated MHC-I dislocation and degradation are through the hijacking of host ER-associated degradation (ERAD) (165). As revealed in an analysis of a lysine-free HLA-A allele, ubiquitination of the target MHC-I molecule is a prerequisite for US2-mediated MHC-I dislocation and degradation (166). Through a functional siRNA library screening, a multimembrane-spanning, ER-resident protein TRC8 was identified to be the E3 ligase utilized by US2, as the TRC8 depletion prevented the US2-induced ubiquitination and dislocation of MHC I and rescued MHC I from US2-mediated degradation (167). It was suggested that US2 interacts with the E3 ligase TRC8 via its TMS. US2 shows a broad substrate specificity beyond the classical MHC I molecules. A variety of reports uncovered that US2 can degrade non-classical MHC I molecules HLA-G (168), HFE (169,170) and CD1d (171), and the MHC class II α chains DR and DM (172). A recent study employing

plasma membrane profiling further expand the US2 targets to several surfacing receptors, including the NK cell ligand CD112, the anticoagulation factor thrombomodulin, IL12 receptor β 1 subunit and integrin family members α 1, α 2, α 4, β 1 (173). Consistent with previous discovery, US2 was proved to mediate their degradation in a TRC8-dependent manner (173).

HCMV US11 is another protein that manipulates the host ERAD pathway to degrade the MHC-I molecules (174). The ectodomain of US11 interacts with the α 2 domain and the α 3 domain of the MHC I, but the TMS of US11 and the cytosolic tail of the MHC-I molecules are crucial in determining the MHC I degradation efficiency (175, 176). Later it was found that US11 is associated through its TMS with an ER transmembrane protein Derlin-1, which is required for the US11 mediated MHC I degradation (177). A single amino acid mutation (Q192L) in the US11 TMS disrupted its interaction with Derlin-1 and abolished the dislocation of MHC-I by US11 (178). Furthermore, the C-terminal amino acid of the MHC I determines the recruitment of Derlin-1 to MHC I by US11 (179). MHC-I molecules with the C-terminal amino acid being valine or alanine, such as HLA-A, B or C, will be degraded by US11, whereas other MHC-I molecules like HLA-G with other the C-terminal residues are not affected. Taking advantage of the temperature sensitive E1 ubiquitin enzyme cell line, the requirement of ubiquitin is proved necessary for US11 activity (180). Further study showed that US11-mediated the degradation of a lysine-less MHC-I molecule (181), presumably through the ubiquitination of the nonlysine residues, including serine/threonine and cysteine (182). To uncover the E3 ligase utilized by US11, two independent groups used two different genetic screening approaches, the genome retroviral mutagenesis and shRNA screening (183,184). They revealed that the ER-resident membrane protein TMEM129 is the E3 ligase required for the US11-induced ubiquitination of MHC I and its subsequent retrotranslocation and proteasomal degradation. Both the studies

demonstrated the role of Derlin-1 is to bridge the US11 to TMEM129 through its TMS domain (183, 184). Ube2j2 was identified to be the E2 enzyme required by US11-mediated ERAD pathway. Interestingly, unlike the US2 proteins that will release the MHC I to the cell surface upon the depletion of its E3 ligase TRC8, US11 can still retain the MHC-I in the ER in the absence of TMEM129 (184). Therefore, US11 not only serves as a degradation factor but also as an ER retention factor, as previously observed with the US11 Q192L mutant (178).

The HCMV late protein US6 does not interact directly with MHC I molecules, but blocks peptide loading by the peptide transporter TAP, leading to the efficient downregulation of all peptide-dependent classical and non-classical MHC I molecules (185, 186). Like other US6 gene family members, US6 is a glycosylated type I transmembrane protein and blocks TAP through its ectodomain, with a core domain (aa 89–108) indispensable for TAP inhibition but not for binding and a site proximal to the ER membrane (aa 116–125) that confers TAP interaction capability (187). After binding to TAP, US6 inhibits crosstalk between the TMS domain and the cytosolic tail of both TAP subunits, thus blocking the binding of ATP to TAP, which is necessary for peptide translocation (188).

The HCMV protein US10 was also proved to interact with MHC-I molecules (189). Further study revealed that this protein is able to degrade the HLA-G, which is a non-classical MHC-I molecule mainly expressed in trophoblasts (190). The C-terminal cytosolic tail of HLA-G was important for this function, as the substitution with HLA-A2 cytosolic tail blocked US10-mediated degradation (190). A tri-leucine motif in the cytoplasmic tail of US10 was found to be crucial for HLA-G degradation (190). However, the degradation pathway utilized by US10 remains enigmatic and is believed to be different from that used by US2 or US11.

Table I. I HCMV immune evasion on classical and non-classical MHC-I molecules (155).

MHC-I	Immune function	ligand binding between the $\alpha 1$, $\alpha 2$ domains	TCR binding	NKR binding	$\beta 2m$-association	Interfering HCMV genes
<i>Classical/MHC-I molecules</i>						
HLA-A	Yes	Peptide	Yes	LIR, KIR	Yes	US2, US3, US6, US11
HLA-B	Yes	Peptide	Yes	LIR, KIR	Yes	US2, US3, US6, US12
HLA-C	Yes	Peptide	Yes	LIR, KIR	Yes	US3, US6
<i>Non-classical/MHC-I molecules</i>						
HLA-E	Yes	Peptide	Yes	CD94/NKG2A/C, LIR	Yes	US6, UL40
HLA-G	Yes	Peptide	Yes	LIR, KIR2DL4	Yes	US10, US2
HLA-F	Yes	No	Yes	LIR	Yes	
CD1	Yes	Lipids	Yes		Yes	cmvIL-10, US2
MICA	Yes	No	Yes ($\gamma\delta$ lineage)	NKG2D	No	UL142, US18, US20
MCB	Yes	No	Yes ($\gamma\delta$ lineage)	NKG2D	No	UL16, UL142, miR-UL112
ULBPs	Yes	No	ULBP4 ($\gamma\delta$ lineage)	NKG2D	No	UL16, UL142
FcRn	Yes	No	No		Yes	
HFE	No	No	No		Yes	US2
MR1	Yes	Vitamin B metabolites	Yes (MAIT cells)		Yes	
ERCP	Yes	Phospholipid	Yes ($\gamma\delta$ lineage)		No	
ZAG	No	Fatty acids	Yes		No	
<i>HCMV-encoded MHC-I like molecules</i>						
UL18	Yes	Peptide	No	LIR	Yes	
UL142	Yes					
UL37						

Escape from natural killer cell response

After using the US2-11 gene products to interfere with MHC-I to compromise CD8⁺ T cell activation, HCMV still needs to face the robust immune response from the natural killer cells (191). The downregulation of MHC-I molecules deprives NK cell inhibitory receptors of their ligands (192) and HCMV infection induces strong expression of ligands for NK cell activating receptors (193,194), rendering the HCMV-infected cells highly susceptible to NK cell recognition. However, HCMV has evolved strategies to evade NK cell immunity by either mimicking the endogenous MHC-I molecules or blocking the surface expression of NK activating ligands in the virally infected cells.

HCMV mainly manipulates two NK cell inhibitory receptors: Leukocyte Ig-like receptor (LIR)-1 and the heterodimeric receptor CD94-NKG2A. LIR-1 is a type I transmembrane protein consisting of four Ig-like domains with a cytosolic tail harboring four ITIM repeats for the inhibitory signaling (195). A broad range of host MHC I molecules was identified as the ligands for LIR-1 to inhibit the NK cell activation (196). After downregulating most MHC-I molecules on the cell surface, HCMV expresses its own MHC-I homolog protein UL18 to engage the LIR-1 (195, 197). UL18 has 1000-fold higher affinity for LIR-1 than the HLA-A2, therefore, it can efficiently preserve the inhibitor signals at a low-level expression (198). The high glycosylation of UL18 enables it to block the interaction with TCR, CD8, US2, US3, US11, thus avoiding the T cell activation and also escaping the viral-induced MHC-I inhibitory effects (195, 199). Another NK inhibitory receptor containing ITIM domain is the dimeric CD94/NKG2A, which engages with the peptide-bound HLA-E (200). Unlike other MHC-I molecules, HLA-E has high stringency for its peptides ligands, only presenting the leader sequences from the classical MHC-I such as

HLA-A, B, C. (201). The inhibition of TAP by HCMV US6 also impairs the peptide loading to the HLA-E (202). However, the signal peptide of HCMV UL40 protein has the identical sequence to the HLA-C leader sequence VMAPRTLIL and can be loaded to the HLA-E in a TAP-independent manner (203). Therefore, HCMV utilizes the UL40 protein to enhance the HLA-E surface expression and compromise the NK activation via CD94/NKG2A (204).

Downregulation of MHC class I proteins on target cells is insufficient to elicit NK cell-mediated cytotoxicity, and the lysis of target cells requires the ligation of specific NK activating receptors. NKG2D is broadly expressed NK cell activating receptor that is capable of recognizing at least 8 distinct ligands, with all of them non-classical MHC-I molecules (as summarized in Table I. I): MICA, MICB and the UL16-binding proteins 1-6 (ULBP1-ULBP6) (205). MICA and MICB are type I transmembrane proteins which preserve the MHC-I like α 1-3 domains but do not associate with the β_2m . The ULBP family are also non-classical MHC-I molecules but lacking the α 3 and TMS domain and attaching to the cell membrane via a glycosyl-phosphatidylinositol (GPI) anchor (206). Cell surface expression of NKG2D ligands can be induced by the cellular stress, including genotoxic damage, growth stimulation or viral infection. Within 24 h post infection, HCMV activates all NKG2D ligands expression (193). HCMV blocks the upregulation of NKG2D ligands through the sequestration of MICB, ULBP1, ULBP2, and ULBP6 in the ER by the UL16 protein (207, 208, 209, 210), the retention of MICA and ULBP3 within the cis-Golgi by the UL142 protein (211, 212), and the silence of MICB transcript by microRNA miRUL112 (213). Recently, HCMV US18 and US20 are identified as novel NK cell evasion proteins capable of promoting MICA degradation in lysosome (214).

HCMV also interferes other NK cell activating receptors such as NKp30 and DNAM-1. The HCMV tegument protein pp65 (UL83) mediates the dissociation of the ζ -chain from

NKp30, consequently diminishing the activating signal (215). HCMV UL141 is capable of suppressing surface expression of the DNAM-1 ligands: the nectin-2 (CD112) and nectin-5 (CD155) (216, 217). Whereas UL141 alone is sufficient to mediate retention of CD155 in the ER, it requires the cooperation of US2 to downregulate the CD112 (216). UL141 has a broad target specificity and can also promote intracellular retention of the TRAIL receptors DRs, which prevents virus infected cells from TRAIL-dependent NK cell-mediated killing (218).

Antibody immunity evasion

Antibody immunity is also critical for controlling the HCMV infection and dissemination, as the viral specific IgG can either directly neutralize the HCMV virion or activate the immune cells, such as Macrophages or NK cells through the surface FcγRs (219, 220). However, even in people with normal humoral immunity, HCMV still frequently reactivates and causes interhost spread to uninfected population (124, 125). Recent clinical trials with the passive transfer of HCMV-neutralizing antibodies to HCMV-infected mothers failed in the control of congenital HCMV transmission to the fetus (143). All those observations mentioned above suggest that HCMV has evolved strategies to resist the host neutralizing antibodies. Unlike HCMV evasion to cell-mediated immunity, the elucidation of the mechanism for HCMV antibody evasion is just starting.

A recent report shows that the glycosylation of HCMV envelope protein gN contributes to resistance of the virus to neutralizing antibodies (221). Another study uncovers that HCMV can incorporate the envelope protein gH-specific antibodies into the assembling virions and utilizes the Fc domain of the incorporated antibody to infect naive cells, thus avoiding the blocking of viral entry by gH antibodies (222). More studies have focused the HCMV-encoded FcγRs such as gp34 and gp68, which are identified to play a crucial role in

interfering with the host antibody response. Through the HCMV deletion mutations, Atalay et al identified that the UL119-UL118 gene encodes the 68 kDa glycoprotein gp68 and the RL11 gene encodes the 34 kDa glycoprotein gp34 (223). Both of those receptors can bind to human IgG through their extracellular domains and mediate the internalization of human IgG through a DxxxLL dileucine consensus motif in their cytoplasmic tail (224, 225). Those two viral FcγRs are believed to interfere with IgG binding to host FcγRs and enhance the IgG degradation through receptor-mediated endocytosis. Later, it was demonstrated they can compete with host FcγRIIIA (CD16) for binding to the viral-specific antibody on the surface of viral-infected cells, thus antagonizing the NK cell activation through antibody-dependent cellular cytotoxicity (ADCC) effect (226). Recent study elucidates two more HCMV vFcγRs: RL12 and RL13 (227). Although only expressed in clinical HCMV strains such as TR and Merlin and not necessary for the HCMV replication in cell culture, they show the efficient binding capacity to human IgG and are indispensable for the viral survive in the host, suggesting their role in the evasion of host antibody response.

ER-associated degradation (ERAD) Pathway

Overview

An estimated one-third of the mammalian genome-encoded proteins are synthesized in the ER. Those proteins fold and assemble into naive structures with the aid of molecular chaperones and acquire posttranslational modifications in the ER before they are destined by the secretory pathway to cell surface membrane or extracellular space. However, proteins may not always fold and assemble into the correct conformation due to spontaneous errors, genetic mutations, toxic compounds and cellular stresses, such as increased temperature and osmotic stress (228). The newly synthesized proteins in ER is monitored by ER quality

control (ERQC) system which is mediated by molecular chaperones that not only help polypeptides folding but also evaluate the conformations of their substrates (229). Misfolded and aberrant proteins failing to pass the ERQC will be degraded via ERAD pathway, a complex process through which folding-defective proteins are recognized, retrotranslocated from ER to the cytosol and ultimately degraded by the ubiquitin-proteasome machinery (230). Canonical ERAD pathway proceeds through four tightly coupled steps involving substrate recognition, retrotranslocation across the ER membrane, covalent conjugation with polyubiquitin, and proteasomal degradation. Each step is mediated by ERAD machinery components that are conservative among the mammalian cells. The inability of the ERAD system to destroy misfolded proteins is related to more than 60 diseases, such as neurological illnesses (Alzheimer's and Parkinson's) and cystic fibrosis (228).

Infectious pathogens exploit various host cell biological processes for their survival and proliferation. Certain types of pathogens, including viruses and bacteria, preferably hijack the ERAD pathway, which can benefit them in two aspects. First, the downregulation of cell surface immune receptors by the ERAD is utilized for pathogens to escape the immune surveillance system. Typical examples are MHC I degradation induced by HCMV US2 and US11, and CD4 elimination mediated by HIV Vpu (231). Second, membrane translocation machinery from the ER into the cytosol is employed for the invasion of pathogenic toxins. The lumen of the ER is connected to the cell surface via vesicular transport, therefore the ERAD retrotranslocation machinery in the ER membrane could provide a channel for the exogenous pathogens to enter into the cytosol from the cell surface. After internalized via endocytosis and further transferred in a retrograde direction via the secretory pathway from endosomes to the ER lumen, the AB toxins from cholera and diphtheria penetrate the ER membrane into the cytosol by utilizing the components from the ERAD machinery (231).

Physiological ERAD pathway

The first step for ERAD pathway is to recognize its target. This is mediated by the ER quality control system which monitors the hydrophobic patches in the misfolded proteins and relies on their N-linked glycans to initiate ERAD. The vast majority of proteins synthesized in the ER are posttranslationally modified by covalent adding a high-mannose glycans chain to Asn residues within a consensus N-glycosylation motif (Asn-X-Ser/Thr) (232). The core structure of N-linked glycans is Glc3-Man9-GlcNAc2 (Glc: glucose, Man: mannose, GlcNAc: N-acetylglucosamine). These glycans are essential for the quality control system to monitor the conformational maturation of nascent glycoproteins. The N-linked glycans of the ER protein will be deglycosylated by glucosidases I and II to Glc1Man9GlcNAc2. The trim of glucose enables nascent glycoproteins to bind to the lectin-like chaperones calnexin (CNX) or calreticulin (CRT), which form a scaffold facilitating the oxidative folding. Further deglycosylation removes the final glucose from the N-glycan, subsequently precluding CNX/CRT binding to the glycoprotein and allowing the protein to egress from the ER (233). Proteins that have not acquired native conformation are captured by UDP-glucose/glycoprotein glucosyl transferase (UGGT) for reglucosylation, thereby returning them to CNX/ CRT to undergo further rounds of oxidative folding (234). Proteins failing in native conformation will be sent to those ER mannosidases ERManI, EDEM1 and EDEM3 for trimming the N-linked glycans to the demannosylated forms (Man5–Man7) (233, 235). This glycan form can not be targeted by UGGT for reglucosylation but will be recognized by ER mannose-specific lectins such as OS-9 and XTP3-B. Both OS-9 and XTP3-B contain the mannose-6-phosphate receptor homology (MRH) domains that bind to the terminal α -1,6 mannosyl linkage exposed by the mannosidases trimming (236, 237).

In the next stage, the misfolded glycoproteins captured by OS-9 and XTP3-B will be linked to the ERAD dislocation machinery on the ER membrane through various adaptors. SEL1L is one of the adaptors that can bind OS-9 and XTP3-B (236, 238) and at the same time also interact with the ER dislocation derlin-1 (238, 239), which in turn recruits the VCP/p97 complexes to drive substrate dislocation across the ER. Derlin-1 is a rhomboid pseudoprotease belonging to the rhomboid family with a compact helical bundle of six transmembrane domains (240). Although lacking the catalytic residues necessary for proteolysis, Derlin-1 preserves the overall rhomboid structure and conserved architectural elements (240). The rhomboid structure has been proposed to cause bilayer thinning, which could contribute to the destabilization of transmembrane domains by exposure of normally buried residues to a more aqueous environment (241). Therefore, when derlin-1 binds to the transmembrane domains of ERAD substrates, it destabilizes the substrate and lowers the energy barrier for extraction by VCP/p97 (230). VCP/p97 is a homo-hexameric enzyme that couples ATP hydrolysis to unfold and reorganize the structure of its substrate proteins, and plays a central role in the extraction of nearly all ERAD substrates out of ER. Its critical role in the ER dislocation is proved by the stabilization of nearly all ERAD substrates by the RNAi-mediated knockdown, expression of dominant-negative, or chemical inhibition of VCP/p97 (242, 243 and 244). However, as a cytoplasmic protein, VCP/p97 can only contact a luminal ERAD substrate after it at least partially passed across the membrane to the cytosol. The mechanism for the initiation of substrate dislocation still needs further elucidation.

The key step in the ERAD process is the ubiquitination of substrate, which determines their further recognition by the 19S proteasome subunits in cytosol. Protein ubiquitylation requires the action of an E1 ubiquitin-activating enzyme, E2 ubiquitin-conjugating enzymes and E3 ubiquitin ligases. In mammals, ERAD-associated ubiquitination is primarily mediated by two RING domain E3 ligases: HRD1 ((Synoviolin) and gp78 (AMFR) (245,

246). Three E2 ubiquitin-conjugating enzymes function in mammalian ERAD are Ube2j1, Ube2j2 and Ube2g2 (247, 248). In a previous study that investigated the ERAD degradation of misfolded MHC I molecules in the absence of β_2m , misfolded MHC I polypeptide forms a complex with SEL1L, HRD1, gp78 and Derlin-1. However, HRD1 is identified as the only E3 ligase responsible for the MHC I ubiquitination and degradation, with Ube2j1 identified as the E2 ubiquitin-conjugating enzyme (245). Besides the HRD1 and gp78, more other ERAD E3 ligases with limited substrate range have been discovered, such as TEB4 (MARCH6) (249), RNF5 (Rma-1) (250), TRC8 (167) and RNF170 (251). The involvement of those E3 ligases in ERAD mainly depends on the adaptors that link them to a specific substrate. The ERAD substrate 3-hydroxy-3-methyl-glutaryl-CoA reductase (HMG-CoAR) is linked to its E3 ligase gp78 through Insig-1 (246), while the inositol 1, 4, 5-triphosphate receptors (IP3R) is linked to the E3 ligase RNF170 via Erlin-1/2 (251). Since most ERAD E3 ligases have their RING domains in the cytosolic side of the ER membrane, it is reasonable to propose that they only ligase the ubiquitin to the cytosolic tail of their substrate. However, this hypothesis is contradictory to a recent report showing that, in the β_2m -depleted cells, misassembled MHC I molecules are preferentially ubiquitinated on ER luminal residues by HRD1 (252). Therefore, the ERAD substrate should be partially dislocated before they are exposed to the ERAD E3 ligase for ubiquitination.

Finally, the ubiquitinated substrate is further extract across ER membrane by the VCP/p97 which forms a complex with the heterodimer nuclear protein localization homolog 4 (Npl4) and ubiquitin fusion degradation 1 (Ufd1) (253). Ufd1 and Npl4 recognize the K48-linked polyubiquitin chains, which have been added by E3 ligase (254). The cytoplasmic deglycosylating enzyme Peptide N-glycanase (pNGase) is recruited to VCP/p97 complex to remove the N-linked glycans from dislocating substrate to facilitate its entry into proteasome (255). After retrotranslocation from ER to the cytosol, the ubiquitinated substrate will be

delivered to the proteasome for degradation. The 19S proteasome resident subunits regulatory particle non-ATPase-13 (Rpn13), Rpn10 and regulatory particle ATPase-5 (Rpt5) are identified as the ubiquitin receptors that bind the ubiquitin chains on the substrate (256). Rpn13 is proved to mediate the high affinity binding, and play a key role during substrate degradation in proteasome Rpn10, while the Rpn10 is thought to drive the substrates into the 19S proteasome core for degradation (256).

Pathogen hijacked-ERAD

HCMV US2 protein can dislocate the ER MHC I molecules for proteasome degradation by taking advantage of the host ERAD machinery. US2 can physically bind to the MHC I heavy chain and link it to several ERAD components: p97 providing the driving force for retrograde transport, the Sec61 serving as the translocon and TRC8 as the ubiquitin E3 ligase (167, 239 and 257). However, other necessary components for endogenous ERAD pathway such as Derlin-1, SEL1L, Ufd1, and Npl4 were not included in the US2 mediated-ERAD pathway (177, 257 and 258). US2 only utilized the minimal components from the host ERAD to degrade MHC I, presumably in order to avoid the competition with other host proteins that also degrade via ERAD pathway. How US2 utilize the p97 without the involvement of Npl4 and Ufd1 is still a mystery. E3 ligase TRC8 binds to the cytosolic tail of US2 to trigger the MHC-I ubiquitination and dislocation. Although US2-induced MHC I ubiquitination is lysine dependent, lysines residues in the cytoplasmic tail of MHC-I are not necessary, indicating TRC8 targets the luminal domain of the MHC-I heavy chain for ubiquitination (259). This is consistent with the ERAD degradation of endogenous MHC I, where partial dislocation is prior to the ubiquitination of the misassembled MHC-I molecules (252).

Compared to US2, HCMV US11 appears to rearrange the endogenous ERAD complex in a less drastic way. US11 directly interacts with MHC class I HC and delivers it to the ERAD pathway in conjugation with common ERAD components, including SEL1L (258), Derlin-1 (177), p97, Ufd1, Npl4 (254). The only difference between the US11-mediated ERAD and the physiological ERAD is that the US11 utilizes a less common ubiquitin E3 ligase TMEM129 instead of the regular ERAD E3 ligase HRD1 (183, 184). US11 itself will not be degraded via by TMEM129-mediated ERAD, due to its short cytosolic tail that precludes its ubiquitination by TMEM129 (184). A cytosolic tail switch between US11 and MHC-I reversed their fate, triggering a rapid degradation of US11 in TMEM129-dependent manner, but leaving MHC-I completely unaffected (184). Thus, the US11 may acts as a pseudosubstrate for the E3 ligase TMEM129, which continually recruits the MHC I to the TMEM129 for ubiquitination. The subsequent degradation of MHC-I makes US11 free and able to bind the next MHC-I molecule and restarts the degradation cycle.

Human immunodeficiency virus can also use its virus protein U (Vpu) to drive CD4 receptor to ERAD pathway for proteasomal degradation. In this way, HIV compromises the activation of helper T cells via MHC II-mediated antigen presentation and TCR recognition. (260). Vpu utilizes the cytosolic SCF-type ubiquitin ligase β -TrCP to ubiquitinate the CD4 receptor, although β -TrCP does not usually contribute to the ERAD pathway (261). Ubiquitination of the non-lysine residues such as serine and threonine is also observed during Vpu-mediated CD4 elimination, although it is uncertain whether β -TrCP is responsible for this kind of ubiquitination (262). It has not been identified whether Vpu collaborates with other ER luminal or membrane-associated ERAD components for the retrotranslocation of CD4, however, Vpu itself contains a transmembrane region that contributes to CD4 degradation (263). The ERAD extraction complex p97, Npl4, and Ufd1 have been reported to

participate in the Vpu-induced elimination of CD4 to provide the driving force for CD4 penetration across the ER membrane to the cytosol (262).

Bacterial toxins that exploit the host ERAD pathway for their invasion include cholera toxin (CTx), *Pseudomonas* exotoxin (PEx), Shiga toxins (STx), pertussis toxin, cytolethal distending toxin (CDT) (264). These toxins have a common complex structure, typically consisting of a single enzymatically active (A) subunit and multiple transmembrane-binding (B) subunits, and therefore called AB toxins. Through binding to specific cell surface glycolipids, glycoproteins, or receptor proteins, those toxins are internalized via endocytosis and transported in a retrograde direction from endosomes to the ER lumen (265). ERAD exploitation by bacterial CTx has been well characterized. CTx utilizes the endogenous ERAD components for its ER penetration such as Derlin-1, SEL1L and E3 ligase HRD1 / gp78 for its membrane penetration (266). A recent study suggests that the ubiquitin ligase activity of HRD1 and gp78 is indispensable for dislocation of the A1 chain, while it remains unclear whether the A1 chain itself is the target of this poly-ubiquitylation activity (267). The usage of p97, which is required as a driving force for extracting the poly-ubiquitylation of A1 chain is undetermined, with evidence both supporting and refuting this (268, 269). A striking feature of ERAD hijacking by toxins is the evasion from proteasomal degradation after dislocation, the mechanism for which remains elusive.

Questions to be addressed in my project

HCMV expresses multiple viral proteins, such as US2 (161), US3 (158), US6 (186), US11 (174) and UL16 (205) to interfere with the expression, assembly and trafficking of classical and non-classical MHC-I molecules. Given that FcRn and MHC I molecules share a similar structure and sequence homology, does HCMV interfere with FcRn within infected

cells, so as to evade FcRn-mediated antibody immunity? First, we need to identify which proteins of HCMV can interact with FcRn. Do those proteins interfere with the expression, assembly and trafficking of FcRn? Second, do those proteins really block the FcRn functions, such as IgG transcytosis and IgG salvage from catabolism, especially in the context of viral infection? Third, since several HCMV viral Fc γ R_s can internalize IgG via endocytic pathway, do those viral Fc γ R_s collaborate with FcRn-targeting viral proteins in facilitating IgG degradation? Those questions will be addressed in Chapter 2 and Chapter 3.

Chapter 2: Human cytomegalovirus evades IgG antibody-mediated immunity through the endoplasmic reticulum-associated degradation of the neonatal Fc receptor (FcRn) for IgG

Abstract

Human Cytomegalovirus (HCMV) is known to evade host immunity, allowing it to persistently infect humans. Although the strategies of HCMV to evade cellular immunity is well studied, there is limited understanding on how HCMV antagonizes humoral immunity. The neonatal Fc receptor (FcRn), an MHC class I-related Fc γ R, plays a critical role in IgG-mediated humoral immunity. Through screening the HCMV proteome, we discovered that US11 specifically captured FcRn in both virally-infected and US11-expressing cells. US11 selectively inhibited the assembly of FcRn with β_2m , impaired FcRn IgG binding capacity and blocked FcRn trafficking to the endosome by retention of FcRn in ER. Furthermore, US11 recruited Derlin-1, a protein complex, as well as TMEM129, an ER-resident E3 ubiquitin ligase, to induce degradation of FcRn in US11⁺ or HCMV infected cells. This complex initiated the dislocation of FcRn from the ER to the cytosol and facilitated its degradation in an ubiquitination and proteasome-dependent manner. The cytosolic interaction between FcRn and Derlin-1 was shown necessary for degrading FcRn. Because FcRn is widely expressed in most cell types capable of supporting HCMV infection, including epithelial, endothelial and macrophage, we found that either HCMV infection or recombinant US11 expression significantly inhibited human IgG transcytosis across polarized human primary intestinal epithelial Caco-2 cells, Vascular endothelial HMEC-1 cells and placental trophoblast BeWo cells, and facilitated considerable IgG degradation inside endothelial HMEC-1 cells. Hence, our results show that HCMV exploits the Derlin-1/TMEM129

pathway through US11 to disable FcRn, thus revealing a novel strategy for viral evasion from antibody immunity, and having broad impact on the development of new treatment and vaccines for HCMV infection.

Introduction

Human cytomegalovirus (HCMV) is a herpesvirus found throughout the globe. HCMV infection can present with mononucleosis-like symptoms, progressing to latency, although infection in immunocompetent individuals is generally asymptomatic. However, both initial and reactivated HCMV infections pose a life-threatening risk in immunocompromised patients, such as transplant recipients, patients with uncontrolled HIV infection, and the elderly. In addition, due to its ability to infect the developing fetus *in utero* via placental transmission, HCMV is a cause of hydrops fetalis and is the leading infectious cause (97) of congenital abnormalities worldwide.

HCMV has been historically successful in infecting humans due to its ability to evade the immune system and establish latency. Viral infections are normally controlled through antibody-mediated immunity and cell-mediated immunity, which involves CD4⁺ and CD8⁺ T lymphocytes and natural killer (NK) cells. Cell-mediated immunity is essential for controlling viral infections (279, 280), and individuals with genetic defects affecting cell-mediated immunity display a high susceptibility to HCMV infection (281). HCMV normally inhibits T-cell activation by blocking TAP-dependent anterograde peptide transport into the endoplasmic reticulum (ER) (US6; 185,186), retaining newly synthesized MHC class I molecules in the ER (US3; 158, 270) and selectively degrading folded MHC class I molecules that have dislocated from the ER (US2 and US11; 161 and 174). HCMV US2 also destroys HLA-DR- α and DM- α , two components of the MHC class II pathway, preventing viral antigen recognition by CD4⁺ helper T-cells (172). In addition, the HCMV proteins

UL16, UL142, microRNA (miR)-UL112, US18, and US20 inhibit NK cell activation by moderating MICA, ULBP, and MICB, three ligands which normally engage the stimulatory NK cell receptor NKG2D (206, 213, 214). In total, by altering surface levels of T-cell and NK cell receptor ligands, HCMV interferes with the activation of cell-mediated immunity.

In addition to cell-mediated immunity, antibody-mediated immunity is also important for suppressing HCMV infection. Anti-virus IgG antibodies neutralize virions and stimulate immune cells expressing one or more Fc γ R, such as Fc γ RI, Fc γ RII and Fc γ RIII (282). Several reports have reported the importance of antibodies in controlling infection (283, 284). However, latent HCMV has been shown capable of reactivation and super-infection, even in the presence of HCMV-specific IgG (275, 276). Furthermore, HCMV can circumvent neutralizing antibodies (nAb), either by inhibiting their binding using a heavily glycosylated viral glycoprotein (221) or by integrating their Fc region into the viral envelope, thus increasing the efficiency of viral binding and infection in Fc γ R-expressing cells (222). Interestingly, the HCMV genome also encodes several decoy Fc γ Rs, which may indirectly prevent the Fc γ R-mediated effector consequences of anti-HCMV IgG antibodies (223, 226).

The neonatal Fc receptor (FcRn) is composed of a membrane-bound heavy chain (HC) in non-covalent assembly with a common β_2 -microglobulin (β_2 m) (5, 15). This association of FcRn HC with β_2 m is required for FcRn complex anterograde transport from the ER (271). Although FcRn shares structural characteristics with MHC class I molecules, it cannot present antigenic peptides to cognate T cells due to its narrowed antigen-binding groove (19). Instead, FcRn binds IgG antibodies in a pH-dependent manner, with FcRn binding to the Fc-region of IgG at pH below 6.5 and releasing IgG at higher pH (25).

In most cell types, FcRn is normally transported to early endosomes, with limited cell surface expression. Within these acidic endosomes, FcRn will bind endocytosed IgG (58). Depending on the cell type, FcRn will then either recycle IgG back to its original cell surface, as is the case with endothelial cells, or transport IgG to the opposite cell surface, as is the case with certain polarized epithelial cells. The near neutral pH of the extracellular environment then triggers the release of IgG from FcRn. Endocytosed IgG that does not bind FcRn moves to lysosomes, where it is degraded (51). FcRn, therefore, prolongs the half-life of IgG. As an antibody transporter, FcRn helps to establish passive immunity by carrying maternal IgG across the placental syncytiotrophoblast monolayer, as well as across polarized epithelium lining the neonatal respiratory, intestinal, and genital tracts (6, 9, 11 and 12). In all, FcRn plays a necessary role in establishing early neonatal immunity and is involved with immune responses to both infections and immunizations.

Little is currently known about the relationship between HCMV and FcRn. HCMV is known to infect placental trophoblasts, epithelial cells, endothelial cells, macrophages (Mφs), and dendritic cells (DCs) (93; 122), all cell types where FcRn is expressed (6, 11; 12). As FcRn is important in the generation of passive immunity, its inactivation could lead to superinfection of an unprotected developing fetus. Here, we have identified that the HCMV membrane glycoprotein US11 specifically captured human FcRn, inhibited its antibody trafficking functions, and caused its degradation. This process may be involved in limiting maternal IgG transport. We, therefore, propose a novel mechanism through which HCMV escapes antibody-mediated immunity.

Materials and Methods

Cell lines, Antibodies and virus

Human intestinal epithelial Caco-2 and HeLa cell lines were obtained from the American Type Culture Collection (Manassas, VA) and grown in complete DMEM. The human endothelial cell line HMEC-1, a dermal-derived microvasculature cell line, was provided by the Centers for Disease Control (Atlanta, GA) and was grown in complete DMEM medium. THP-1 cell line (kind gifts from Dr. Richard S. Blumberg, Harvard Medical School, Boston, MA) was grown in RPMI 1640 (Invitrogen) complete medium. Complete media were supplemented with 10 mM HEPES, 10% FCS (Sigma-Aldrich), 1% L-glutamine, nonessential amino acids, and 1% penicillin-streptomycin. Cells were grown in 5% CO₂ at 37 °C. The HeLa^{FcRn} cell line stably expressing human FcRn was established as previously described (12) and grown in complete DMEM supplemented with 0.5mg/ml G418 sulfate (KSE scientific). HeLa^{US11} cell line stably expressing wildtype US11 was established by the transfection of HeLa cells with a pEF6-HA-US11 plasmid (transfection protocol described below), whereas the HeLa^{US11*} cell line stably expressing the mutant US11Q192L, whose 192 Gln residue was replaced by Leu residue, was established by the transfection of HeLa cells with a pEF6-HA-US11Q192L plasmid. HeLa^{US11+FcRn} cell line stably co-expressing FcRn and US11 was established by the transfection of HeLa^{FcRn} cells with pEF6-HA-US11 plasmid, whereas the HeLa^{FcRn+US11*} cell line stably co-expressing FcRn and mutant US11Q192L was established by the transfection of HeLa^{FcRn} cells with the pEF6-HA-US11Q192L plasmid. The cell line Caco-2^{US11} expressing HA-tagged US11 was established by the transfection of intestinal epithelial Caco-2 cells with the pEF6-HA-US11 plasmid. The plasmids used for transfection for those stable cell lines are described below. After transfection cells were cultured under 10 µg/ml Blastocidin (Invitrogen). Surviving cell colonies were detected by immunofluorescence staining using the anti-HA antibody for US11 expression and cells with

high expression homogeneity were selected for subculture. Stable cell lines HeLa^{US11}, HeLa^{US11*} and Caco-2^{US11} were grown in complete DMEM medium supplemented with 5 µg/ml Blasticidin. Stable cell lines HeLa^{US11+ FcRn} and HeLa^{FcRn+US11*} were grown in complete DMEM medium supplemented with 5 µg/ml Blasticidin and 0.5mg/ml G418 sulfate.

Rabbit or rat anti-FLAG epitope (DYKDDDDK) antibody was purchased from Sigma-Aldrich and BioLegend. The hybridoma 12CA5 and its clone 3F10, both of which react with the influenza hemagglutinin (HA, YPYDVPDYA) epitope, were purchased from ATCC and Roche. Rabbit anti-Myc (EQKLISEEDL) antibody and mouse anti-Myc IgG_{2a} (clone 9B11) were from Cell Signaling. Mouse anti-human FcRn IgG_{2a} (clone B-8) antibody and mouse anti-ubiquitin IgG₁ (clone P4D1) were from Santa Cruz Biotechnology. Affinity purified polyclonal antibody against the cytoplasmic tail of human FcRn was described previously (63). Affinity purified polyclonal antibody against US11 was produced in mice as described below. Rabbit anti-TMEM129 polyclonal antibody was purchased from Sigma Aldrich. Mouse anti-MHC Class I (clone W6/32) antibody was from Enzo Life Sciences, Inc. Mouse anti-early endosomal Ag-1 (EEA1) and mouse anti-LAMP-1 were obtained from BD Biosciences. Mouse anti-HCMV pp65 IgG_{2a} antibody was purchased from Abcam. HRP-conjugated goat anti-mouse, rabbit or rat secondary antibody were purchased from Southern Biotech. Alexa Fluor 488-, Alexa Fluor 555-, and Alexa Fluor 633-conjugated secondary antibodies were purchased from Life Technologies.

The HCMV AD169 strain was purchased from ATCC. An HCMV clinical strain was obtained from Dr. Jeffrey Cohen (National Health of Institutes) and propagated in MRC-5 cells. At 10-14 day's post-infection, the cell-associated virus was harvested by sonicating cell pellets, and the cellular debris was removed by centrifugation at 6,000 rcf for 20 min. Virus particles were concentrated by centrifugation at 20,000 rcf for 2 hr through a 20% sucrose

cushion. Virus titer was determined by quantifying TCID₅₀ in MRC-5 cells using the Reed-Muench method.

Construction of protein expressing vectors

The construction of pcDNA-FLAG and human FcRn expression plasmid pcDNA-FLAG-FcRn was as previously described (12). Human HFE ORF was amplified from pCMV-Sport-HFE and cloned into pCDNA-Flag to construct the plasmid pCDNA-Flag-HFE encoding a Flag-tagged HFE. The encoding sequence for FcRn cytoplasmic tail knockout molecule FcRn CT^{-/-} or FcRn C-terminus amino acid deleted molecule FcRn 365A^{-/-} was amplified from pCDNA-FLAG-FcRn and cloned into pCDNA-Flag to construct the plasmid pCDNA-Flag-FcRnCT^{-/-} or pCDNA-Flag-FcRn365A^{-/-}. To construct pSectag2 -Derlin-1-Myc, Derlin-1 ORF was first amplified from HeLa cDNA and then amplified again by Derlin-1-Myc primers (Table 1.) that fused a Myc epitope with the C-terminus of Derlin-1. The encoding sequence for HCMV US2 or US11 was amplified from the cDNA of HCMV AD169-infected MRC-5 cells. The US2 ORF was further amplified by US2-HA primers (Table 1.) that fused an HA epitope with the C-terminus of US2 and cloned into the pEF6 to construct the plasmid pEF6-US2-HA. The US11 cDNA was inserted with an HA epitope sequence after the signal peptide sequence by US11-HA primers (Table 1.) through the site-directed mutagenesis (Clontech) PCR amplification and cloned into the pEF6 to construct the plasmid pEF6-HA-US11 encoding a N-terminal HA-tagged US11. The US11 cDNA was mutated by the US11 Q192L primers (Table 1) via site-directed mutagenesis (Clontech) PCR to generate the US11Q192L mutant cDNA and cloned into pEF6 to construct the plasmid pEF6-HA-US11Q192L. To construct a pGex4T1-US11, GST-US11 primers (Table 1) were used to amplify a truncated 438 bp DNA fragment encoding the extracellular domain of US11 gene and the DNA fragment was subsequently cloned into the pGEX4T-1 (Amersham

Pharmacia Biotech) expression vector. The plasmid pCD71(TFR)-GFP was obtained from Dr. Gary Banker (Oregon Health & Science University, Portland, Oregon).

Table II. I PCR primers used in this study

Genes	Forward Primer	Reverse Primer
US11 RT (1-675)	5'-GCTCGGATCCGCCACCATGAACCTTGTAAATGCTTATTC-3'	5'-GCCCTCTAGACTACCCTGGTCCGAAAAACATCCAGG-3'
US11-HA	5'-GTAGTCTGGCACATCATATGGGTATAATTCAGGCATACTACCCGGCAGAC-3'	5'-CCATATGATGTGCCAGACTACGGCATCCTTGACTCTTTTCGATGAAC-3'
US11 Q192L	5'-CAAAACACTAGAATCACTGCCACCATCATCAGCGTATACTGGCCGAC-3'	5'-CAGTGATTCTAGTGTTTTGGGGCTGTATGTGAAAGGTTGGCTG-3'
GST-US11 (93-531)	5'-GCGTGGATCCTTGGTGGAGACGGAGCCGTTACCCGCTC	5'-TTATGCGGCCCGGTGAGCGGTAGTAGCCATTAGAC-3'
US2 RT (1-600)	5'-ATGAACAATCTCTGGAAAAGCCTGG	5'-TCAGCACACGAAAAACCCGCATCCAC-3'
US2-HA	5'-ACGGGATCCGCCACCATGAACAATCTCTGGAAAAGC-3'	5'-GCGTCTAGACTATGCGTAGTCTGGCACATCATATGGGTAGCACACGAAAAACCCGCATCCACATC-3'
HFE (67-1035)	5'-GTCGAAGCTTCGCTTGCTGCTGCCTCACACTCTCTG-3'	5'-ACCGTCTAGACTACTCACGTTCCAGCTAAGACGTAGTG-3'
Deflin-1 RT (1-756)	5'-ATGTCGGACATCGGAGACTGGTTC-3'	5'-TCACTGGTCTCCAAGTCGAAAAGCC-3'
Deflin-1-Myc (1-756)	5'-GACGTCTAGAGCCACCATGTCGGACATCGGAGACTGGTTC-3'	5'-GAATCTCGAGTCACAGATCCTCTTCTGAGATGATTTTGTTCCTGGTCTCCAAGTCGAAAAGCC-3'
FeRnCT-/- (24-323)	5'-CTTGCCGCCGGCAGAAAAGCCACCTCTCCCTCCTG-3'	5'-ATCCTCTAGATTACCTTCTCCACAACAGAGCTCCTCC-3'
FeRn-365A ^{-/-} (24-364)	5'-CTTGCCGCCGGCAGAAAAGCCACCTCTCCCTCCTG-3'	5'-ATCCTCTAGATTAGGTGGCTGGAATCACATTTACATC-3'

Production of affinity-purified US11-specific Abs

Production of affinity-purified glutathione *S*-transferase fusion proteins was as previously described (63). Recombinant GST-US11 proteins were produced in BL21 cells (Invitrogen) following treatment with 0.2 mM IPTG (isopropyl- β -D-thiogalactopyranoside) for 16 hr. To produce anti-US11 antibodies, we immunized a mouse with the purified GST-US11 fusion protein. Anti-US11 antibodies were then affinity purified from the immunized mouse sera. This procedure was approved by the University of Maryland Institutional Animal Care and Use Committee (IACUC).

Transfection and proteins expression

Cells were transfected with recombinant plasmids (described above) along with PolyJet transfection reagent (SignaGen Laboratories, Rockville, MD). Cells were plated 18 to 24 hours prior to transfection. The PolyJet reagent (μ L) and the plasmid DNA (μ g) were mixed in serum-free DMEM at a ratio of 3: 1. After incubating for 10~15 minutes at room temperature, PolyJet/DNA mixture was dropped onto the medium and homogenize by gently swirling the cell culture plate. PolyJet/DNA complex-containing medium was replaced with fresh complete medium 12~18 hours post transfection. The transfection efficiency was examined by immunofluorescence or Western blot 24 to 48 hours post transfection.

SiRNA interference

Pre-designed siRNA products were synthesized from Genewiz (South Plainfield, NJ), including human TREM129 (#1: 5'- AUAGGCGAGAG UGAAGGUC -3'; #2: 5'- ACCGGUGGCAAACUUGUCA -3'), Ube2j1 (5'-UUAUUUGCCUAGCCAGUUC-3'), Ube2J2 (5'-UUGAACACUCGAGAAUAU-3') or HCMV US11 (#1:5'-

AGUCCCGGAGCCAFUAGCGUU-3'; #2:5'-UCGCACUCUACAUAUAAGUU-3'). Transfection of siRNA oligos against endogenous US11 and TREM129 genes was carried out using Lipofectamine 2000 Transfection Agent (Invitrogen) at a final concentration of 20 nM mixed siRNA oligomer #1 and #2 per well. Mock controls were transfected without adding the mixed siRNA oligomers. Each gene was targeted with two non-overlapping siRNAs to enhance effectiveness. Knockdown efficiency was confirmed by Western blot.

IgG binding Assay

A human IgG binding assay was performed as previously described (80). Cells were lysed in PBS (pH 6.0 or 7.4) with 0.5% CHAPS (Sigma-Aldrich) and protease inhibitor cocktail III (Calbiochem) mixture on ice for 1-2 hr. Post-nuclear supernatants containing 0.5 – 1 mg of soluble proteins were incubated with human IgG-Sepharose (Rockland Immunochemicals) at 4 °C overnight. Unbound proteins were washed off with PBS (pH 6.0 or 7.4) containing 0.5% CHAPS. Adsorbed proteins were boiled with Laemmli Sample buffer at 95 °C for 5 min. The eluted fractions were subjected to Western blot analysis as described below.

Gel electrophoresis, Western blotting, immunoprecipitation

Cell lines and transfectants were lysed in PBS with 0.5% CHAPS and protease inhibitor cocktail III. Protein concentrations were determined as described previously. The lysates were boiled with Laemmli Sample buffer at 95 °C and resolved on a 12% SDS-PAGE gel under reducing conditions. Proteins were transferred onto a nitrocellulose membrane (Schleicher & Schuell, Keene, NH, USA). All blocking, incubation and washing were performed in 5% non-fat milk and 0.05% Tween 20 in PBS). The membranes were blocked,

probed separately with specific primary antibody overnight at 4 °C, washed, and then probed with HRP-conjugated secondary antibody for 2 hours. Proteins were visualized using SuperSignal West Pico Chemiluminescent Reagent (Thermo Scientific). Chemiluminescence signal acquisition and densitometry analysis were conducted using the Image Lab, version 5.2 in a Chemi-Doc XRS imaging system (Bio-Rad Laboratories, Hercules, CA).

Analysis of N-linked glycosylation

N-linked glycosylation was analyzed as described previously (294). In brief, native FcRn in cell lysates or the proteins immunoprecipitated by HA murine antibodies were digested with N-acetylglucosaminidase H (Endo H; New England Biolabs) in digestion buffer (100 mM sodium acetate, pH 5, 150 mM NaCl, 1% Triton X-100, 0.2% SDS, 0.5 mM PMSF) or with peptide: N-glycosidase F (PNGase F; New England Biolabs) in 50 mM sodium phosphate, pH 7.5, with 1% NP-40. A mock digestion without enzymes was performed as a control. All digestions were performed for 2 hr at 37°C. Proteins were analyzed on a 12% SDS-PAGE gel under reducing conditions and immunoblotted as previously described.

Confocal immunofluorescence

Immunofluorescence was performed as previously described (Ye L, 2008). Briefly, cells were cultivated on coverslips for 24 hr. Subsequent procedures were done at room temperature. The cells were rinsed with PBS, cold fixed in 4% paraformaldehyde (Sigma-Aldrich) in PBS for 20 min, and quenched with glycine for 10 min. After two washes with PBS, the coverslips were permeabilized in solution (PBS containing 0.2% Triton X-100) for 5 min and then blocked with blocking buffer containing 3% normal goat serum (NGS) for 30 min. Antibodies diluted in blocking buffer were added onto the coverslips and incubated for 1 hr. Cells were then incubated with Alexa Fluor 488 or 555-conjugated goat secondary antibodies in blocking buffer. Cells were also stained by DAPI (4', 6-Diamidino-2-

Phenylindole, Dihydrochloride) for cell nucleus for 15 mins. After each step, cells were washed three times with 0.1% Tween 20 in PBS. Coverslips were mounted on slides with the ProLong antifade kit (Molecular Probes) and examined using a Zeiss LSM 510 confocal fluorescence microscope. Images were processed using LSM Image Examiner software (Zeiss). Quantitative colocalization measurements were performed using Zeiss LSM 510 Examiner Software. Pearson's correlation coefficient was calculated for describing the colocalization correlation of the intensity distributions between two channels, as previously described (Bai Y, 2011). In each quantitative experiment with transfected HeLa or infected Caco-2 cells, 100 representative cells were analyzed. A value of $p < 0.05$ was considered significant.

Flowcytometry analysis

Cells were washed with FACS washing buffer (2% FBS in PBS), if necessary detached by 10% EDTA for 20 mins and pelleted. For surface staining, cells were resuspended in FACS washing buffer with primary antibodies for 40 mins incubation at 4 °C. For intracellular staining, cells were resuspended with the Fixing/Permealizing Buffer (BD CytoFix/CytoPer Kit) for 20 mins incubation at 4 °C, washed and then were incubated in FACS washing buffer with primary antibodies for 40 mins at 4 °C. After 2 times wash, cells were incubated with FITC-conjugated secondary antibodies for 40 mins incubation at 4 °C and washed again, fixed in cold PBS with 2% paraformaldehyde, and analyzed using a FACSAria II and the software FlowJo.

Quantitative Cycloheximide (CHX) chase assay

Cells were treated with CHX (100 µg/ml) for the indicated hours and then lysed. The cell lysate was analyzed on a 12% SDS-PAGE gel under reducing conditions and immunoblotted with corresponding Abs. The expression levels of target proteins in cell lysate were quantified by the band density (relative band volume) measured by Image Lab 5.2. The levels of remaining target protein at different time points were calculated as the percentage of initial protein level (0 hour of CHX treatment).

Detection of protein ubiquitination in cultured cells

Cultured cells were transfected with plasmids expressing US11 along with a FLAG-tagged version of FcRn, HFE, and HLA-A2. 48 hr later, cells were treated with 50 µM MG132 (Calbiochem) for 2 hours and subsequently lysed in PBS with 0.5% CHAPS and protease inhibitor cocktail III. Protein concentrations were measured; the proteins (0.5-1mg) were precipitated with anti-FLAG Rabbit antibody. The cell lysate-bead mixtures were incubated at 4 °C overnight with continuous rotation. Immunoprecipitates were then washed three times and eluted from the protein G complex with Laemmli Sample buffer, heated at 95°C, run on SDS-PAGE, and subjected to the immunoblotting analysis to detect ubiquitin and the target proteins with respective antibodies.

Cell fraction

After a 4-hour incubation with or without 50 µM MG132 at 37 °C, cells were pelleted and fractured by three times freeze-thaw cycle on dry ice (245). Membrane fractions were pelleted from supernatants by ultracentrifugation at 100,000 × g (Beckman XL80, 28700 rpm) for 2 h. Soluble (cytosolic) fractions were collected and diluted in 1% Triton X-100. Pellet (Membrane) fractions were washed with PBS and resuspended in 1% Triton X-100.

Enzyme-linked immunosorbent assay (ELISA)

Human IgG was quantified using ELISA (Bethyl Laboratories, Montgomery, TX). ELISA plates (Nunc) were coated with 10 µg/ml goat anti-human IgG-Fc Ab overnight at 4 °C. Plates were washed three times with PBST (0.05% Tween 20 in PBS) and then blocked with 10% FBS in PBS for 1 hr at room temperature. Plates were washed with PBST three times and incubated with either an IgG standard or the transcytosis samples diluted in 10% FBS for 2 hr at 25°C. Plates were washed for five times with PBST and incubated with 0.1 µg/ml HRP-conjugated goat anti-human IgG-Fc Ab for 1 hr. After plates were washed with PBST seven times, we added the substrates tetramethylbenzidine and hydrogen peroxide to initiate a reaction. 1M sulphuric acid was added to stop the reaction. The colorimetric reaction was read at 450 nm using a Victor III microplate reader (Perkin Elmer).

In vitro human IgG transcytosis

IgG transcytosis was performed as previously described (Li, 2011). BeWo cells, Caco-2 cells or Caco-2 transfected with either pEF6 alone or pEF6-HA-US11 were grown onto 0.4 µm Transwell filter inserts (Corning Costar) to form a monolayer that exhibited a transepithelial electrical resistance (TER) of 600 ohms/cm² for Caco-2 and 400 ohms/cm² for BeWo, measured using planar electrodes (World Precision Instruments). Prior to infection, cell monolayers were washed twice with PBS and then were mock-infected or infected with HCMV clinical strain at an MOI of 10 for 2 hr. After washing, cells were incubated for 48 hr at 37 °C in an atmosphere of 5% CO₂. TER was assessed instantly after adding fresh complete medium to verify that monolayers had remained intact during the infection procedure. Human IgG was added to the medium at a final concentration of 0.5 mg/ml (for Caco-2 cells) or 0.25mg/ml (for BeWo cells) and monolayers were incubated for 2 hr at either 4 °C or 37 °C.

An aliquot of the buffer was collected into which apically-directed IgG transport was conducted. For detecting human IgG, the basolateral medium was concentrated with 0.5 ml Amicon Ultra 10K centrifugal filter (Millipore, Billerica MA). ELISA to quantify human IgG was performed according to the manufacturer instructions by Bethyl Laboratories (Montgomery, TX). Transported IgG proteins were analyzed by Western blot-ECL or ELISA.

In vitro human IgG protection

To perform the human IgG protection assay, either HEMC-1 cells (2.5×10^5 /ml), HeLa^{FcRn+US11} or HeLa^{FcRn} (10^6) were cultured in 2ml complete medium that contains 5% FBS with ultra-low IgG. After HEMC-1 cells were infected with 5 MOI of HCMV or Mock-infected for 48 hr, they were then incubated complete medium supplemented with 50 µg/ml human IgG for another 48 hours. During this incubation, the supernatant medium was sampled at 0, 12, 24, 36, 48 hr and the IgG concentration in each medium sample was measured by ELISA. To visualize human IgG trafficking inside the infected-HEMC-1 (5×10^4), we infected them with 5 MOI of HCMV or Mock-infected for 48 hr, then incubated in complete medium with 250 µg/ml human IgG for 1 hr at 37 °C. HeLa^{FcRn+US11}, HeLa^{FcRn} cells were also incubated in complete medium with 250 µg/ml human IgG for 1 hr at 37 °C. After washing, cells were incubated in complete medium without IgG for an additional 1 hr at 37 °C, then fixed and stained by immunofluorescence for the co-localization of human IgG with the early endosomal marker EEA1 or lysosomal marker LAMP1. For Pearson's correlation coefficient measurement, 10 scopes, each of which contains at least 10 cells, were measured for correlation efficiency rate.

Statistic

The differences between groups were tested by Student's t-test with a significance level of 0.05. Data are expressed as mean \pm SD. * $P < 0.05$, ** $P < 0.01$, and *** $P < 0.001$.

Results

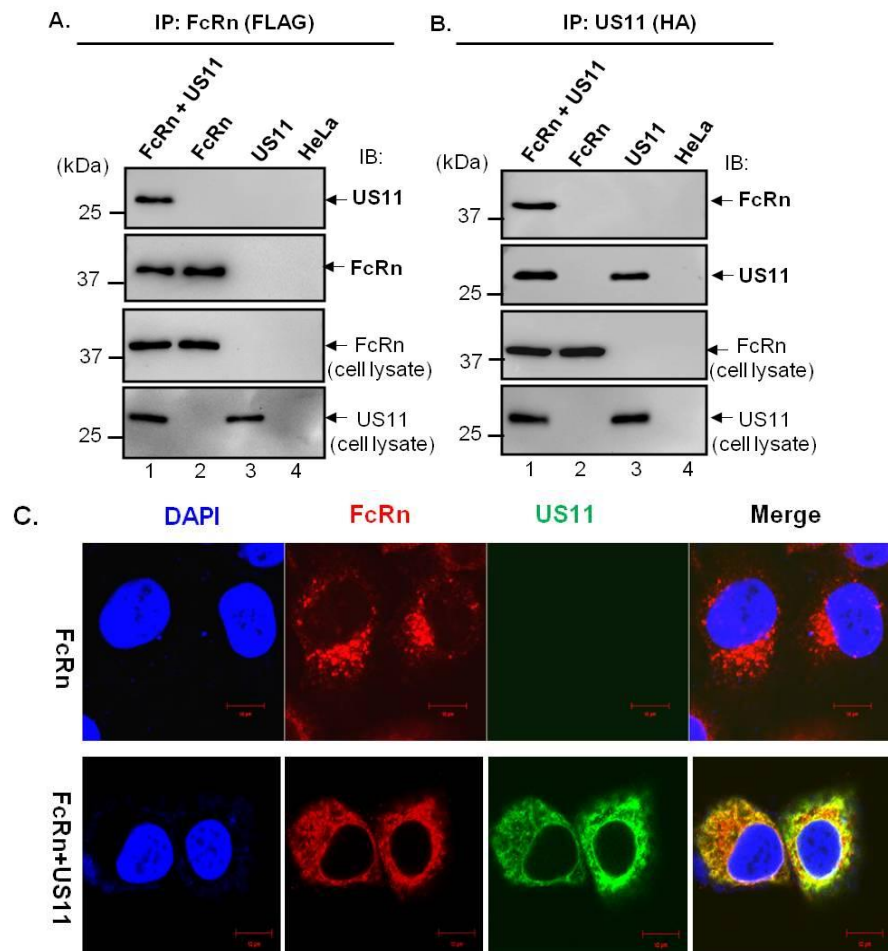
HCMV glycoprotein US11 interacts with FcRn

HCMV genes, US2, US3, US6, US10, US11, UL16, and UL18, were cloned by PCR amplification of viral DNA. We probed the interaction between FcRn and each HCMV individual protein. For screening purpose, the stable HeLa^{FcRn} cells were transfected with plasmids encoding each of the HA-tagged HCMV cDNAs. On the basis of strong binding to FcRn, we selected US11 gene in this study.

HeLa^{FcRn} or HeLa cells were transfected with plasmids encoding HA-tagged US11 cDNA. Cells were lysed with CHAPS buffer and used for immunoprecipitation with either anti-FLAG (for FcRn) (Fig. 2.1A) or anti-HA (for US11) (Fig. 2.1B) mAb. Immunoprecipitates were analyzed by blotting with anti-HA or Ab or anti-FLAG Ab. Anti-FLAG Ab coimmunoprecipitated US11 protein (Fig. 2.1A, *lane 1*) and anti-HA Ab coimmunoprecipitated FcRn heavy chain (HC) (Fig. 2.1B, *lane 1*). Colocalization between FcRn and US11 was also analyzed by confocal microscopy (Fig. 2.1C). FcRn appeared in a punctate or vesicular pattern within HeLa^{FcRn} cells. US11 (green) was highly colocalized with FcRn (*red*) in HeLa^{FcRn} cells expressing US11 (Fig. 2.1C, *right*). To show whether this interaction identified is specific, we co-expressed FcRn with US2 or US11 with another MHC-I-like molecule HFE molecule that regulates iron homeostasis at the similar expression levels in HeLa cells. We failed to detect the interaction of FcRn with US2 (Fig. 2.1D and E,

lanes 1) or HFE and US11 (Fig. 2.1F and G, lanes 1) in a reciprocal immunoprecipitation experiment.

Both US11 and FcRn are type I transmembrane glycoproteins. To understand how US11 and FcRn interact, GST-US11 or GST-FcRn CT fusion proteins were produced (Fig. 2.1H), where DNA encoding the extracellular domain of US11 or the cytoplasmic tail (CT) of FcRn was fused to GST. In pull-down assays, GST-US11 (Fig. 2.1I, lanes 1-2), but not GST alone (Fig. 2.1I, lanes 3-4), captured human FcRn from HeLa^{FcRn} (Fig. 2.1I, lane 1) cells. A GST fusion protein containing only the cytoplasmic tail of FcRn failed to pull down US11 from stable cell line HeLa^{US11} cells (Fig. 2.1J, lane 1). The results support a hypothesis that extracellular domains of US11 and FcRn are the main sites of contact.



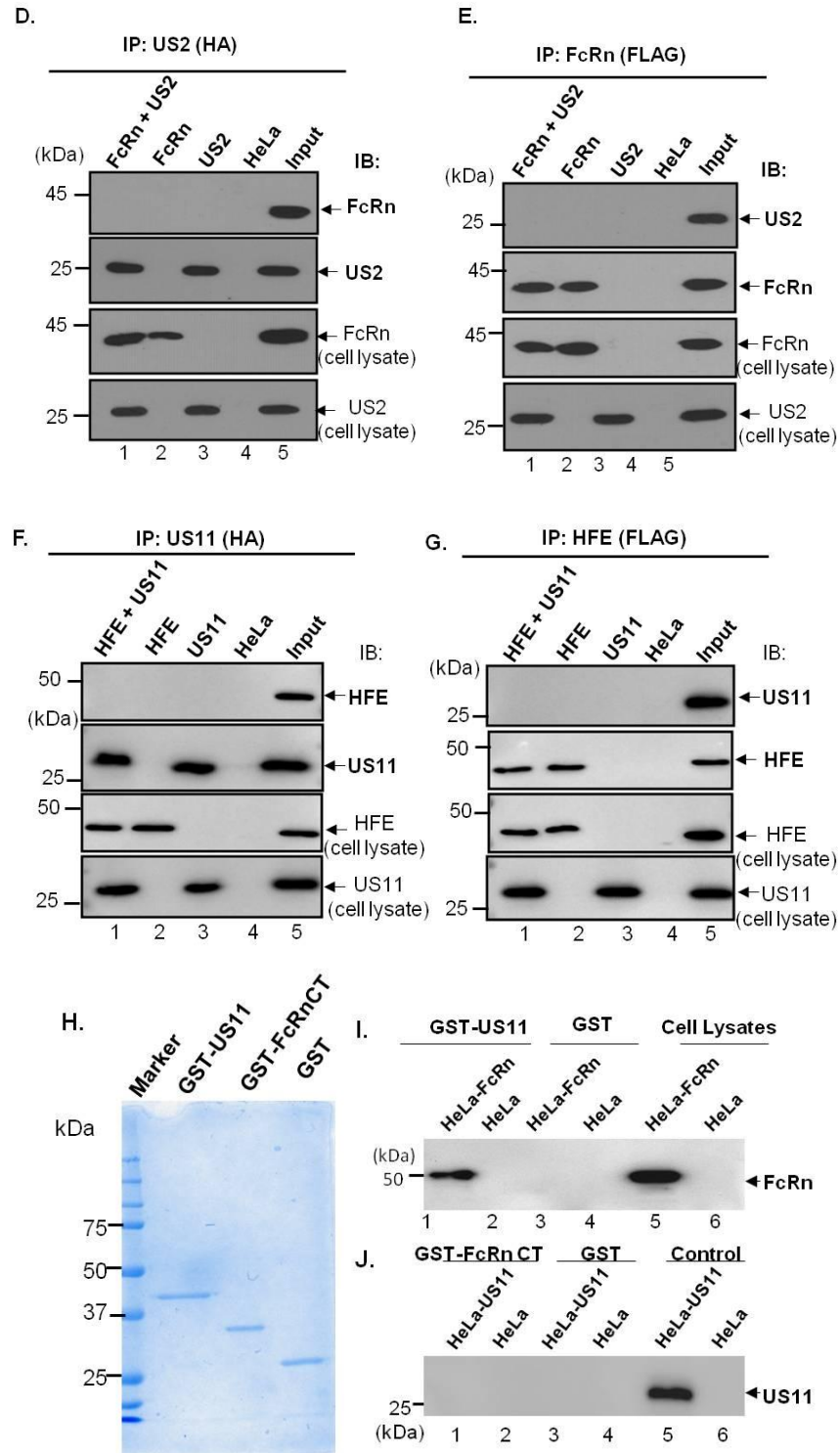


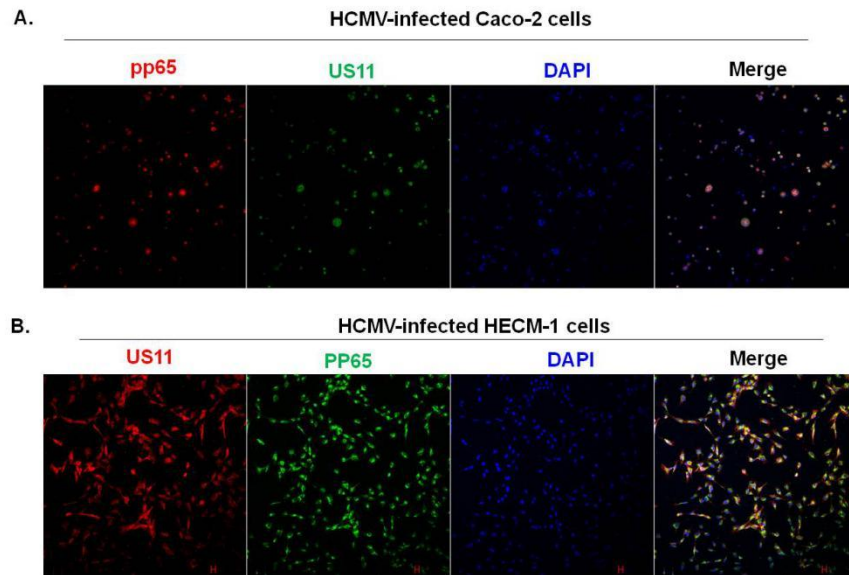
Figure 2.1 FcRn interacts with the HCMV US11. Cell lysates were immunoprecipitated (IP) with Abs and the immunoprecipitates were subjected to 12% SDS-PAGE electrophoresis under reducing conditions, then transferred to a nitrocellulose for Western blotting. Immunoblots (IB) were developed with ECL. Each experiment was performed at least 2-3 times. **A+B.** HeLa^{FcRn} is a HeLa stable cell line expressing the FcRn. HeLa^{FcRn}(US11) cells

were from HeLa^{FcRn} cells transfected with a pEF6-HA-US11 plasmid that expressed both FcRn and US11. HeLa (US11) cells were from HeLa cells transfected with a pEF6-HA-US11 plasmid that expressed US11. The cell lysates from HeLa^{FcRn} (US11) (lane 1), HeLa^{FcRn} (lane 2), HeLa (US11) (lane 3), and HeLa control (lane 4) were immunoprecipitated by mAb anti-HA for US11 or anti-FLAG for FcRn. The immunoprecipitates were subjected to Western blotting with anti-FLAG or HA mAb as indicated. **C.** Colocalization of FcRn and US11 in HeLa^{FcRn} (US11) cells. Cells grown on coverslips were fixed with 4% paraformaldehyde and permeabilized in 0.2% Triton X-100. Subsequently, the cells were incubated with affinity-purified anti-FLAG (FcRn) or anti-HA (US11) specific mAb, followed by Alexa Fluoro 488- or 555-conjugated IgG. Puncta that appear yellow in the merged images (*right panel*) indicate colocalization of FcRn with the US11 protein. The nuclei were stained with DAPI (blue). Scale bar represents 10 μ m. **D+E.** HeLa^{FcRn} (US2) cells were from HeLa^{FcRn} cells transfected with pEF6-US2-HA plasmid that expressed both FcRn and US2. HeLa (US2) cells were from HeLa cells transfected with pEF6-US2-HA plasmid that expressed US2. The cell lysates from HeLa^{FcRn} (US2) (lane 1), HeLa^{FcRn} (lane 2), HeLa (US2) (lane 3), and HeLa control (lane 4) were immunoprecipitated by mAb anti-HA for US2 or anti-FLAG for FcRn. The immunoprecipitates were subjected to Western blotting with anti-FLAG or HA mAb as indicated. **F+G.** HeLa (HFE+US11) cells were HeLa cells co-transfected with pCDNA-Flag-HFE and pEF6-HA-US11 plasmids that expressed both HFE and US11. HeLa (HFE) cells were from HeLa cells transfected with a pCDNA-Flag-HFE plasmid that expressed HFE. The cell lysates from HeLa (HFE+US11) (lane 1), (HFE) (lane 2), HeLa (US11) (lane 3), and HeLa control (lane 4) were immunoprecipitated by mAb anti-HA for US11 or anti-FLAG for HFE, respectively. The immunoprecipitates were subjected to Western blotting with anti-FLAG or HA mAb as indicated. The cell lysates (input) were blotted as controls. **H+I+J.** US11 interacts with FcRn through its ER-luminal domain. The cDNA fragment encoding extracellular domain of US11 or cytoplasmic tail of FcRn was fused to the GST and expressed as a GST fusion protein. Productions of GST fusion proteins are described in Materials and Methods. **H.** GST, GST-US11, and GST-FcRn CT fusion proteins were stained with Coomassie blue and used for in vitro pull-down assays. **I.** GST-US11 proteins were incubated with the cell lysates from HeLa^{FcRn} (lane 1) or FcRn-negative HeLa (lane 2) cells. GST proteins are shown as negative controls in lanes 3, 4, respectively. Cell lysates are used as loading control (lanes 5, 6). **J.** FcRn cytoplasmic tail (CT) expressed as a GST fusion protein were incubated with HeLa^{US11} (lane 1), HeLa (lane 2). GST protein is a control in lanes 3 and 4. HeLa^{US11} or HeLa cell lysates are used as loading control (lanes 5, 6). Beads were completely washed with buffers. In each experiment, GST-fusion protein binding was assessed by immunoblot as indicated.

US11 interacts with FcRn in HCMV-infected cells

To further verify whether US11 interacts with FcRn in HCMV-infected cells, human intestinal epithelial Caco-2 cells, vascular endothelial HMEC-1 cells and macrophage-like THP-1 cells were infected with HCMV clinical strain virus at an MOI of 5. The expression of the phosphoprotein 65 (PP65) protein, a most abundantly produced virion protein in *HCMV*, was used as an evidence for viral infection in epithelial and endothelial cells (Fig. 2.2A and B). At day 2 post-infection (p.i.), the cell lysates from infected or mock-infected cells were

immunoprecipitated by anti-US11 Ab (Fig. 2.2C) or anti-FcRn Ab (Fig. 2.2D). Consequently, anti-US11 Ab coimmunoprecipitated FcRn HC in the infected Caco-2 cells (Fig. 2.2C, *lane 1*) and HeLa^{FcRn} cells (Fig. 2.2C, *lane 3*). Similarly, anti-FcRn Ab also coimmunoprecipitated US11 protein in the infected Caco-2 cells (Fig. 2.2D, *lane 1*) and HeLa^{FcRn} cells (Fig. 2.2D, *lane 3*). The immunoprecipitations of the lysates from mock-infected Caco-2 or HeLa^{FcRn} cells failed to pull down either FcRn (Fig. 2.2C) or US11 (Fig. 2.2D). Importantly, this interaction between US11 and FcRn was not limited to HeLa or Caco-2 cell; their interactions were also identified in human endothelial HMEC-1 (Fig. 2.2E and F) and macrophage-like THP-1 (Fig. 2.2G and H) cell types. These results strongly showed that FcRn and US11 proteins specifically interact each other in the US11-transfected or HCMV-infected human cells.



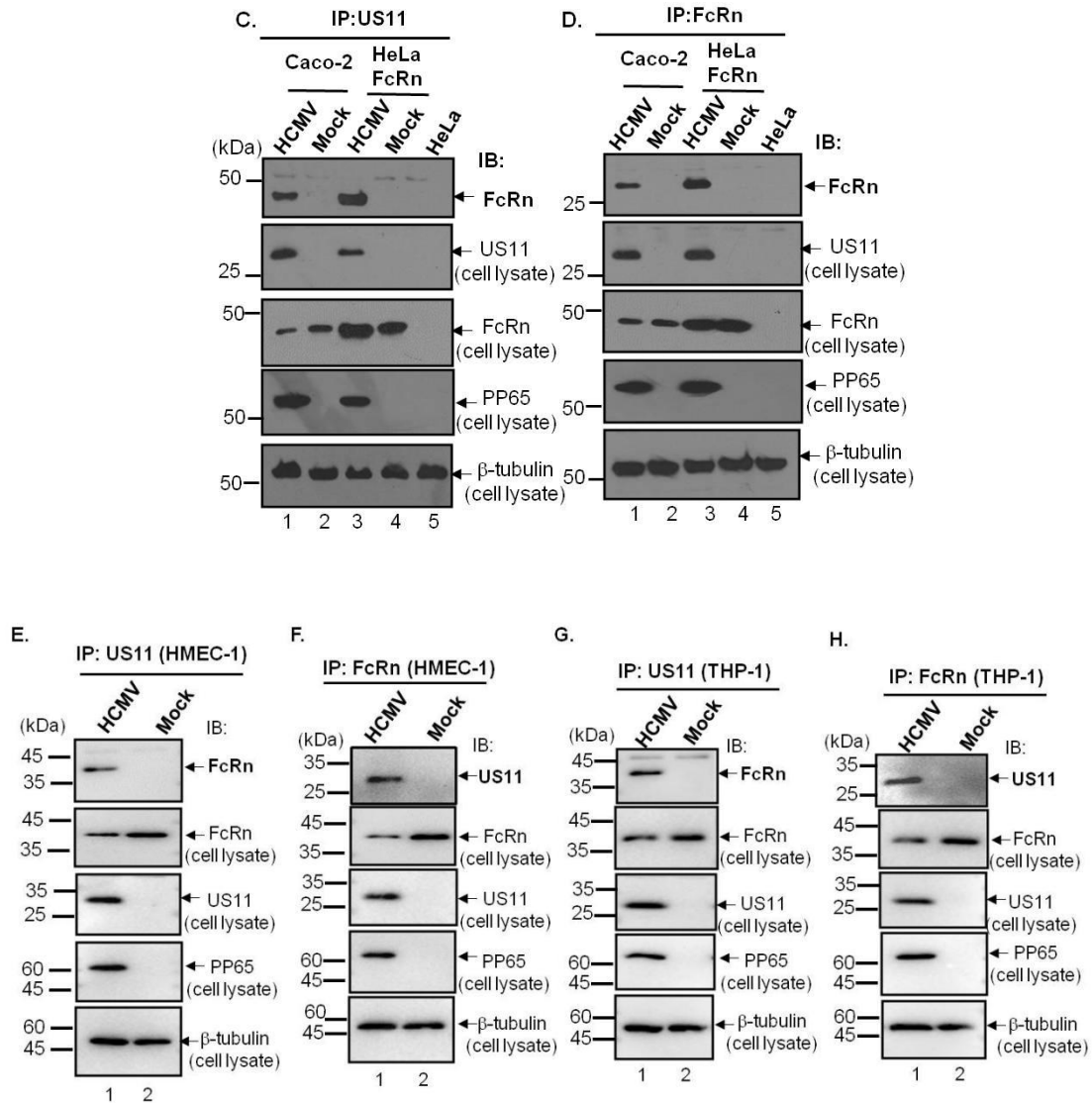


Figure 2.2 US11 interacts with FcRn in HCMV-infected cells. A+B. HCMV-infected Caco-2 and HECM-1. Caco-2 and HECM-1 cells were grown on glass coverslips and infected with HCMV at an MOI of 5. At day 2 p.i., monolayers were fixed with 4% paraformaldehyde, permeabilized in 0.2% Triton X-100. Subsequently, the cells were incubated with affinity-purified anti-US11 (green) or anti-pp65 (red) specific Ab, followed by Alexa Fluoro 488- or 555-conjugated IgG. The nuclei were stained with DAPI (blue). **C+D.** US11 interacts with FcRn in HCMV-infected cells. Human intestinal Caco-2 or HeLa^{FcRn} cells were infected with HCMV virus at an MOI of 5. At day 2 p.i. The cell lysates from infected or mock-infected Caco-2 cells, HeLa^{FcRn}, and HeLa cells were immunoprecipitated by anti-US11 Ab or anti-FcRn Ab. The immunoprecipitates were subjected to 12% SDS-PAGE electrophoresis under reducing conditions, then transferred to a nitrocellulose for Western blotting with anti-FcRn or US11 Ab as indicated. The cell lysates were blotted as controls. Immunoblots (IB) were developed with ECL. Each experiment was performed at least two times. **E+F+G+H.** The cell lysates from HMEC-1 and THP-1 cells were immunoprecipitated by US11 Ab or FcRn Ab. The immunoprecipitates were subjected to 12% SDS-PAGE electrophoresis under reducing conditions, then transferred to a

nitrocellulose for Western blotting with anti-US11 or FcRn as indicated. Immunoblots (IB) were developed with ECL. The 10 µg cell lysates (input) were blotted with the indicated Abs. The pp65, an HCMV major tegument protein, is used for monitoring viral infection. The location of the proteins is indicated by an arrow.

US11 expression inhibits FcRn trafficking to early endosomal compartments

In the majority of cell types, FcRn resides in acidic endosomes with a limited appearance on the cell surface. In early endosomes, FcRn binds IgG that entered into acidic vesicles after pinocytosis or endocytosis (58). When US11 binds FcRn HC, we reasoned FcRn distribution in the endosome would be affected. We therefore constructed stable cell line HeLa^{FcRn + US11} expressing both the FcRn and US11 cells and compared the cellular distribution of FcRn in HeLa^{FcRn} or HeLa^{FcRn + US11} cells. In HeLa^{FcRn + US11} cells, colocalization of FcRn and the early endosomal marker EEA1 was significantly decreased when compared with colocalization in HeLa^{FcRn} cells (Fig. 2.3A and B). This result suggests that US11 expression impairs FcRn trafficking to endosomes in most of the HeLa^{FcRn + US11} cells. Although the over-expression of FcRn protein does not affect its intracellular trafficking pattern, the over-expression of US11 protein may cause extensive remodeling of membranes within the cell. To exclude this possibility, we compared the colocalization of transferrin receptor (TfR1, CD71) with EEA1 marker between HeLa^{FcRn} and HeLa^{FcRn + US11} cells (Fig. 2.3C). We found there were no significant differences in co-localization of TfR1 with EEA1 proteins between HeLa^{FcRn} and HeLa^{FcRn + US11} cells (Fig. 2.3D). These results suggest the potential remodeling of cellular membranes by over-expression of US11 may not significantly affect endogenous protein trafficking into the endosome. Together, these data confirm that routing of FcRn to endosomes in human epithelial cells is significantly reduced by US11 expression.

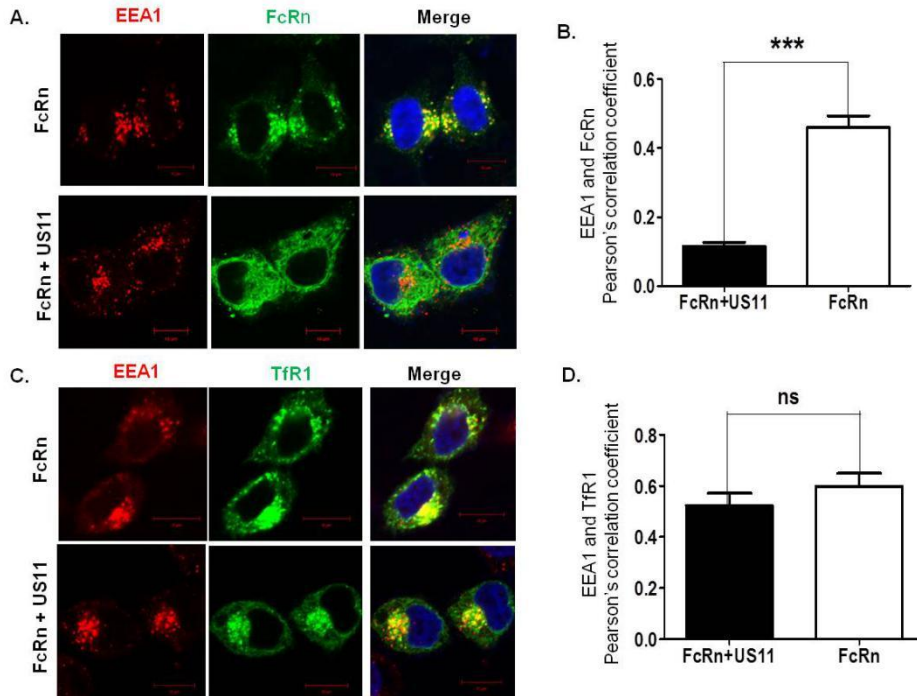


Figure 2.3 US11 expression inhibits FcRn trafficking to the early endosomal compartment. **A+B.** US11 reduces the trafficking of FcRn to the endosomal compartment. HeLa^{FcRn+US11} and HeLa^{FcRn} cells were immunostained for FcRn (*in green*) and EEA1 (*in red*) (**A**). EEA1: early endosome antigen 1. The nuclei were stained with DAPI (blue); Colocalization of two molecules appears in yellow. Scale bar represents 10 μ m. Similar images were seen from at least three independent staining. The colocalization degree of EEA1 with FcRn was quantified by the average Pearson's colocalization coefficients in HeLa^{FcRn+US11} and HeLa^{FcRn} cells (**B**). **C+D.** CD71 (transferrin receptor) trafficking to the early endosome. HeLa^{FcRn+US11} and HeLa^{FcRn} cells were transfected with a plasmid expressing human CD71-GFP (*green*) and immunostained for EEA1 (*in red*) (**C**) EEA1: early endosome antigen 1. The nuclei were stained with DAPI (blue); Colocalization of two molecules appears in yellow. Scale bar represents 10 μ m. Similar images were seen from at least three independent staining. The colocalization degree of EEA1 with CD71 was quantified by the average Pearson's colocalization coefficients in HeLa^{FcRn+US11} and HeLa^{FcRn} cells (**D**). For each assay, Pearson's correlation coefficient was measured by analyzing 100 cells (*in total*) in 10 different optical regions. Ns denotes no statistical significance. Star denotes statistical significance. * $P < 0.05$.

US11 blocks FcRn assembly with β_2m and retains FcRn in ER

The functional FcRn molecule consists of the heavy chain (HC) bound to β_2m . We tested whether US11 interacts with FcRn HC alone or FcRn- β_2m complex. Lysates from HeLa^{FcRn + US11} were immunoprecipitated with anti-HA (for US11) or anti- β_2m Ab and analyzed by blotting with anti-HA Ab to detect US11 (Fig. 2. 4A) or β_2m Ab (Fig. 2. 4B).

Immunoprecipitates were sequentially blotted with Abs against US11, FcRn, or β_2m (BBM1 mAb). As shown in Fig. 2. 4, an anti-HA Ab failed to co-immunoprecipitate β_2m (Fig. 2. 4A, *lane 1*); similarly, the BBM1 mAb did not pull down US11 protein either (Fig. 2. 4B, *lane 1*). However, an Ab against either HA or β_2m co-immunoprecipitated FcRn HC. These data strongly suggest that HCMV protein US11 only interacts with β_2m -free FcRn HC.

The FcRn has a single *N*-linked glycosylation site (27). FcRn in cells was tested by treating cell lysates with Endo H glycosidase that cleaves high mannose oligosaccharides formed only in the ER, or with PNGase amidase which cleaves high mannose, hybrid and complex oligosaccharides formed in both the ER and Golgi complexes. If the FcRn HC oligosaccharides is cleaved by Endo H or PNGase, the deglycosylated FcRn will show a faster mobility in SDS-PAGE. Although FcRn HC in HeLa^{FcRn + US11} or HeLa^{FcRn} cells exhibited a mixture of sensitivities to Endo H digestion (Fig. 2.4C, *top*), FcRn HC from HeLa^{FcRn + US11} cells was significantly more sensitive to Endo H digestion (Fig. 2.4D). As expected, FcRn from either of the above cells was sensitive to PNGase F digestion. We tested Endo H sensitivity of FcRn in anti-US11 immunoprecipitates from HeLa^{FcRn + US11} cells. As shown in Fig. 2.4C (*bottom*), Endo H-digested FcRn HC (*lane 2*) in a US11 immunoprecipitate from HeLa^{FcRn + US11} cells had a mobility similar to the band from PNGase F digestion (*lane 3*). The full sensitivity of FcRn HC to Endo H digestion conforms to an ER-specific glycosylation pattern of FcRn within the FcRn/US11 complex. Alternatively, Endo H sensitivity may also be accounted for inaccessibility of the glycosylation consensus sequence to the *N*-glycosylation machinery because of FcRn HC complex with US11. Overall, this is consistent with the ability of US11 to retain FcRn in the ER. These data strongly support the conclusion that the failure of newly synthesized FcRn to assemble with β_2m undergo maturation or transit the secretory pathway is due to its physical association with US11.

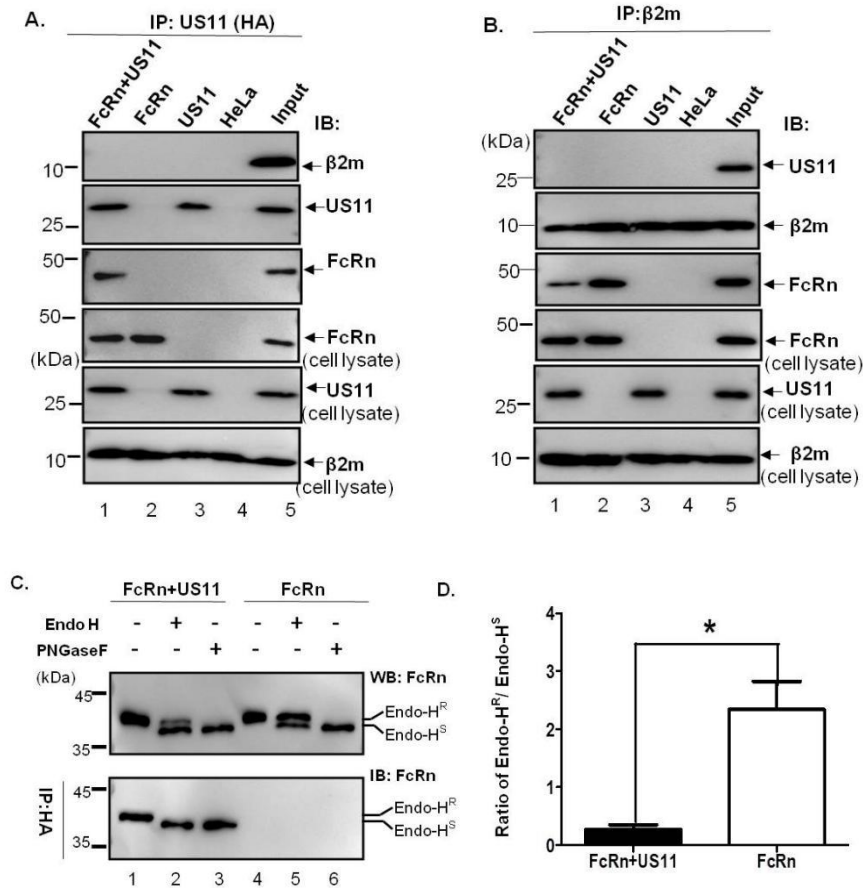


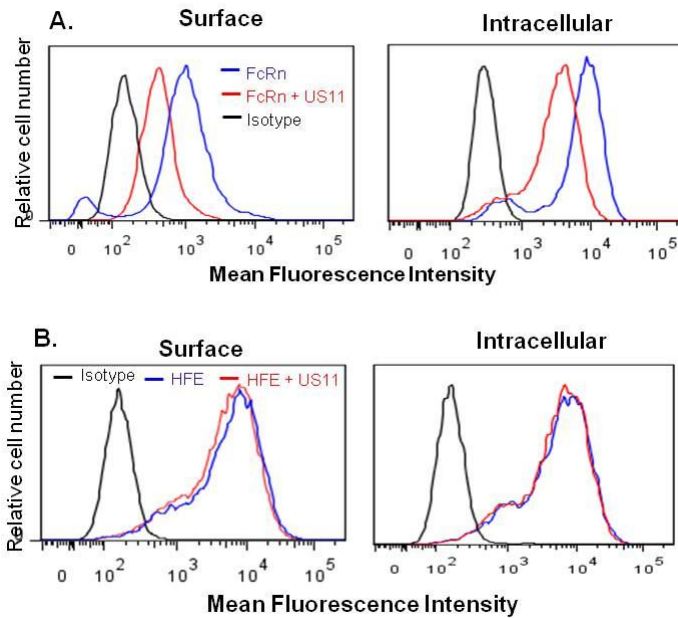
Figure 2.4 US11 blocks FcRn assembly with β ₂m and retains FcRn in ER. A+B. β ₂m or US11 does not coimmunoprecipitate with US11 or β ₂m protein. The cell lysates from HeLa^{FcRn+US11} (lane 1), HeLa^{FcRn} (lane 2), HeLa^{US11} (lane 3), and HeLa control (lane 4) were immunoprecipitated by anti-HA mAb (A), anti- β ₂m Ab (B). The immunoprecipitates and cell lysates (input) were subjected to 12% SDS-PAGE electrophoresis under reducing conditions, then transferred to a nitrocellulose for blotting with anti- β ₂m Ab, anti-FLAG (FcRn), anti-HA (US11), as indicated. Immunoblots were incubated with HRP-conjugated secondary antibody of the corresponding species and developed with ECL. C+D. The sensitivity of US11-associated FcRn HC to Endo-H digestion. The native FcRn in cell lysates (top panel) or the proteins immunoprecipitated by HA mAb (bottom panel) were digested by mock (lanes 1 and 4), Endo-H (lanes 2 and 5), PNGase F (lanes 3 and 6) for 2 h at 37°C, respectively (C). Proteins were analyzed on a 12% SDS-PAGE gel under reducing conditions and immunoblotted with FcRn-specific Ab. The digestion assay were independently performed for three times the figure C is representative of three independent experiments. The ratio of Endo H-resistant FcRn HC (Endo-H^R) to Endo H-sensitive FcRn HC (Endo-H^S) from HeLa^{FcRn+US11} or HeLa^{FcRn} cells was calculated by the ratio of the band density of glycosylated FcRn to that of the deglycosylated FcRn in the three independent digestion experiments (D). The band density (relative volume) was measured by the software Image Lab 5.2. Star denotes statistical significance. * $P < 0.05$.

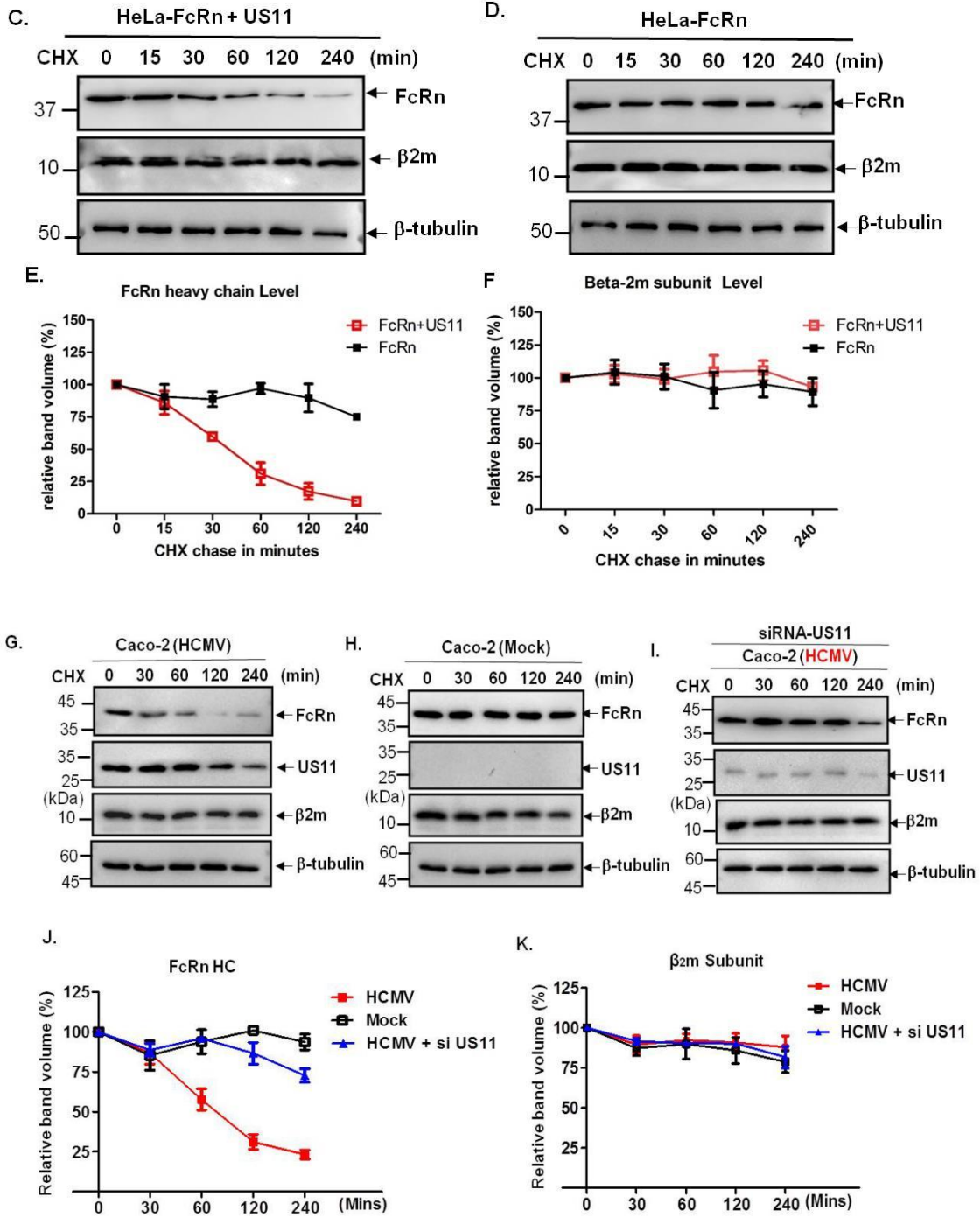
HCMV US11 is required for FcRn protein degradation.

To examine whether US11 affects FcRn expression, we first compared the surface or intracellular levels of FcRn expression in HeLa^{FcRn} or HeLa^{FcRn + US11} cells by flow cytometry. We found that US11 expression remarkably downregulated surface or intracellular expression level of FcRn molecules (Fig. 2.5A). In contrast, US11 did not affect either surface or intracellular expression level of HFE under the same conditions (Fig. 2.5B), suggesting the downregulation of FcRn by US11 is specific.

The steady-state level of a protein depends on rates of both protein synthesis and degradation. For this reason, a quantitative cycloheximide (CHX) chase is used to monitor the decay in the steady-state level of an FcRn HC in the absence of confounding synthesis. HeLa^{FcRn + US11} (Fig. 2.5C) and HeLa^{FcRn} (Fig. 2.5D) cells were treated with CHX (100 µg/ml); FcRn intensity was monitored for the indicated time thereafter. In US11-expressing HeLa^{FcRn + US11} cells, the expression of US11 induced a substantial and time-dependent decrease in FcRn protein levels in comparison with that of HeLa^{FcRn} (Fig. 2.5E). In US11-containing cells, FcRn protein had a shorter half-life of about 40 min, conversely, FcRn protein was highly stable in normal cells. Hence, the introduction of US11 into HeLa^{FcRn} cells stimulated FcRn protein turnover (Fig. 2.5E, *red*), indicating that US11 promotes FcRn protein degradation. We did not detect a significant change in the β_2m levels (Fig. 2.5F), suggesting that the effect of US11 expression on FcRn was not due to US11- or CHX-induced cytotoxicity. To further determine whether endogenous FcRn is downregulated by US11 in response to HCMV infection, we first subjected human intestinal Caco-2 epithelial cells endogenously expressing FcRn (272) to HCMV infection. At 48 hr after infection, the infected Caco-2 cells were similarly treated with CHX. FcRn HC protein levels were significantly decreased in HCMV-infected Caco-2 cells (Fig. 2.5G and J) in comparison with

that of mock-infected Caco-2 cells (Fig. 2.5H and J). The β_2m level was not significantly changed in either HCMV-infected or Mock-infected Caco-2 cells (Fig. 2.5K). In further confirming the role of US11 in down regulating FcRn, we knocked down ectopically expressed US11 in virally-infected cells by two independent US11 RNA-mediated interference (siRNA) species. The knockdown of US11 was verified by a Western blot (Fig. 2.5I). We found that FcRn degradation was significantly inhibited in US11 siRNA-treated cells (Fig. 2.5I and J). These results strongly show that the US11 is required for decreasing the intracellular concentration of FcRn protein. The US11-mediated down-regulation of FcRn was further confirmed by intracellular levels of FcRn expression in HCMV-infected THP-1 or HMEC-1 cells, as assessed by flow cytometry. We found that HCMV infections remarkably reduced the expression level of intracellular FcRn in both THP-1 (Fig. 2.5L) or HMEC-1 cells (Fig. 2.5M).





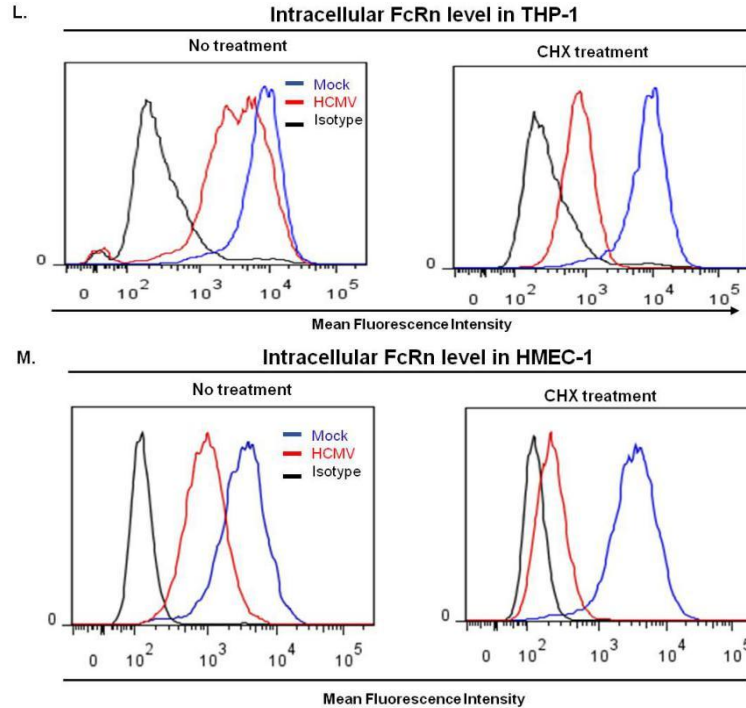


Figure 2.5 US11 protein mediates FcRn degradation. A+B. Cell surface and intracellular expression patterns of FcRn or HFE protein in the presence of US11 were measured by flow cytometry. Results are expressed as histograms of fluorescence intensity (log scale). The black histograms represent cells stained with isotype IgG. The staining was conducted three times with similar results. The mean fluorescence intensity (MFI) is shown on the x-axis, and the relative cell number on the y-axis. (A) HeLa^{FcRn+US11} and HeLa^{FcRn} cells were either nonpermeabilized for surface staining (Left panel) or permeabilized for intracellular staining (Right panel). The red or blue histograms represent staining of HeLa^{FcRn+US11} or HeLa^{FcRn} cells with anti-Flag specific Ab. (B) HeLa^{US11} (HFE) and HeLa (HFE) cells were either nonpermeabilized (Left panel) or permeabilized (Right panel). The red or blue histograms represent staining of HeLa^{FcRn+US11} or HeLa^{FcRn} cells with anti-Flag specific Ab. HeLa^{US11} (HFE) cells were from stable cell line HeLa^{US11} transfected with a pCDNA-Flag-HFE plasmid that expressed both HFE and US11. HeLa (HFE) cells were from HeLa cells transfected with the pCDNA-Flag-HFE plasmid that expressed HFE.

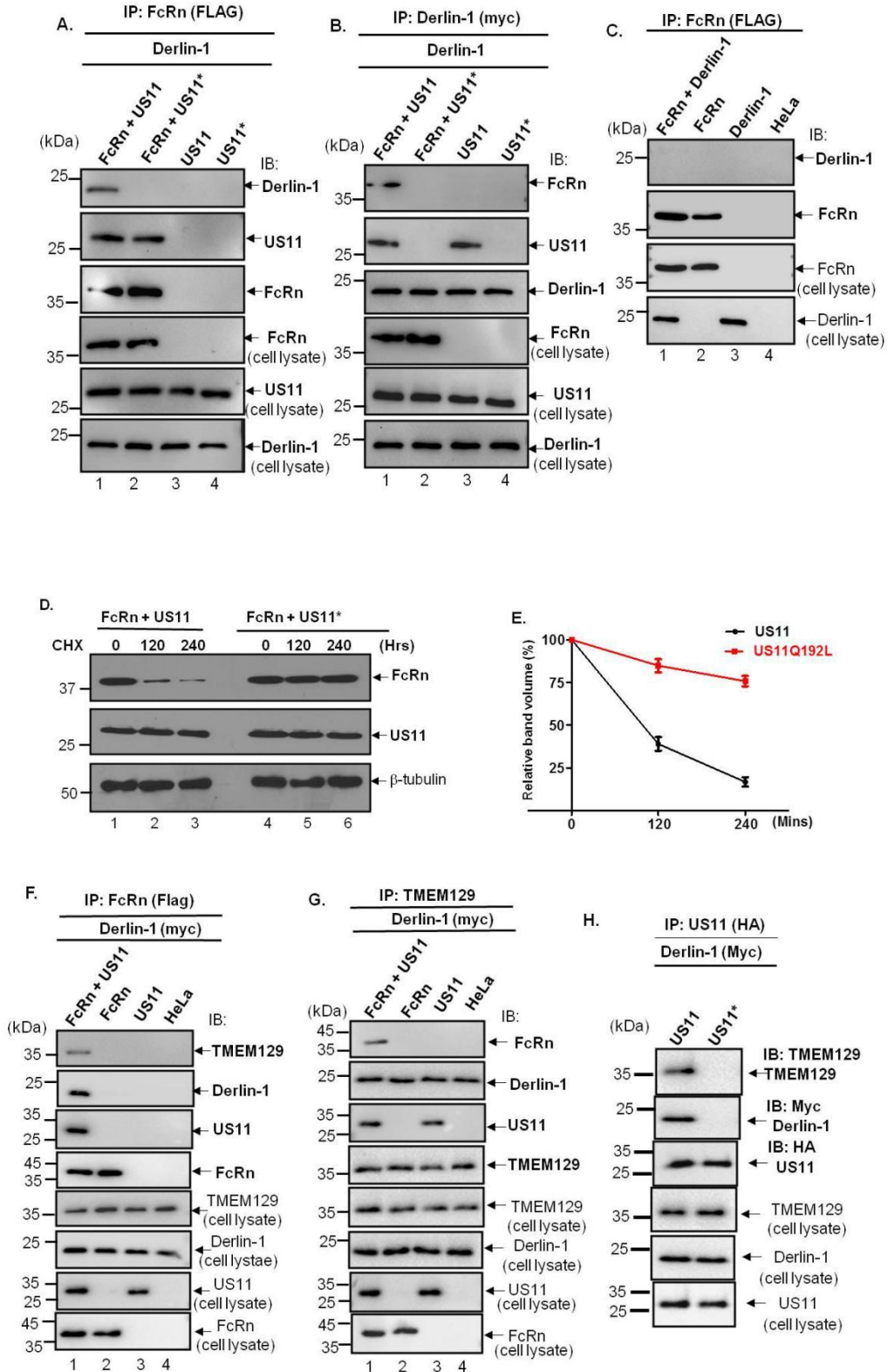
C+D+E+F+G+H+I+K+J. HeLa^{FcRn} cells were transfected with US11 plasmids for 24 h. HeLa^{FcRn+US11} (C) and HeLa^{FcRn} (D) cells were then treated with CHX (100 µg/ml) for the indicated time. Caco-2 cells were infected with HCMV (MOI 5) (G) or mock-infected (H) for 48 h. The infected cells were also transfected with 20 nM US11 siRNA oligomers (I). 48 h later, cells were then treated with CHX (100 µg/ml) for the indicated time. The cells were lysed after CHX treatment and the cell lysate was analyzed by immunoblotted with corresponding Abs. The CHX chase experiments were repeated independently for three times and the figures (C+D+J+H+I) are representative of three independent experiments. The expression level of FcRn or β_2m proteins in cell lysate from the three independent CHX chase experiments was quantified by the band density (relative band volume) measured by Image Lab 5.2. The level of remaining endogenous FcRn (E or J) and β_2m (F or K) at different time points was calculated as the percentage of initial protein level (0 h of CHX treatment). **L+M** Intracellular expression of FcRn in mock- or HCMV-infected THP-1 (A) and HMEC-1 (B) cells at MOI of 5 were measured by flow cytometry. 48 hr post infection, the equal number of

cells were treated with Cycloheximide (100µg/ml) or left untreated for 4 hr. Cells were then blocked with 2% FBS supplemented with 30µg /ml human Fc block and subsequently stained as described in Materials and Methods. Results are expressed as histograms of fluorescence intensity (log scale). The red or blue histograms represent staining of cells with anti-FcRn-specific Ab in the presence or absence of HCMV infection, and the black histograms represent cells stained with irrelevant IgG. The staining was conducted three times with similar results. The mean fluorescence intensity (MFI) is shown on the x-axis, and the relative cell number on the y-axis.

US11 recruits Derlin-1 and TMEM-129 to engage FcRn for degradation

Previous studies have shown that HCMV US11 interacts with Derlin-1 (177), SEL1L (258), AUP1, and UBXD8 (239). We screened that Derlin-1 is a potential partner of the FcRn-US11 complex. Derlin-1 is a component of the retrotranslocation complex in the ER (177, 239). The previous study shows that the US11–Derlin-1 interaction is dependent on a polar glutamine residue (Q192) in the US11 transmembrane (178). To confirm whether FcRn, US11, and Derlin-1 proteins form a complex, we expressed the US11 (Q192) mutant protein and test the interaction of Derlin-1 and FcRn in the in the presence of either a wild-type or mutant US11. We found that anti-FLAG Ab for FcRn coimmunoprecipitated US11 protein, derlin-1(Fig. 2.6A, *lane 1*), and mutant US11 protein (Fig. 2.6A, *lane 1*) and anti-Myc Ab for Derlin-1 coimmunoprecipitated FcRn HC and US11 (Fig. 2.6B, *lane 1*). However, anti-FLAG Ab for FcRn did not precipitate Derlin-1 in the presence of mutant US11 (Fig. 2.6A, *lane 2*) and anti-Myc Ab for Derlin-1 failed to pull down the FcRn and mutant US11 (Q192A) (Fig. 2.6B, *lane 2*). Further, anti-FLAG Ab for FcRn did not coimmunoprecipitate derlin-1 protein in the absence of US11 expression (Fig. 2.6C, *lane 1*). This data suggests that FcRn interacts with Derlin-1 in the presence of wild-type US11 and that mutant US11 (Q192A) abolishes FcRn interaction with Derlin-1 due to its incapability to bind Derlin-1. Consistently, the degradation effects of US11 on FcRn levels were abolished in HeLa^{FcRn+US11*} cells, confirming that FcRn level decrease is through US11 and Derlin-1 interaction (Fig. 2.6D and E). Together, these data suggest that the Derlin-1 binding activity of US11 is required for FcRn degradation.

Derlin-1 can interact with several E3 ligases, HUWE1, Hrd1 and Gp78, MARCH6, RNF5, TRC8, CHIP (230), and TMEM129 (183,184). By screening these candidates, the immunoprecipitation of FcRn (Fig. 2.6F) or TMEM129 (Fig. 2.6G) in the presence of both US11 and Derlin-1 showed that TMEM129 was recruited to the FcRn/US11/Derlin-1 complex. In the absence of US11 expression, the immunoprecipitation of FcRn failed to pull down TMEM129 (Fig. 2.6F *lane 2*). The immunoprecipitation of TMEM129 directly precipitated down the Derlin-1 in HeLa^{FcRn} cells (Fig 2.6G, *lane 2*), suggesting that TMEM129 binding to Derlin-1 is US11-independent. The recruitment of TMEM129 to the FcRn/US11 complex is through Derlin-1, as the wild-type US11 coprecipitated with the TMEM129 while the Derlin-binding mutant US11 (Q192A) failed to pull down the TMEM129 (Fig. 2.6 H). We further elected to test whether TMEM129 is indeed responsible for the down-regulation of FcRn in HeLa^{FcRn + US11} cells. We, therefore, depleted TMEM129 from cells with siRNA TMEM129 (Fig. 2.6I, *bottom*). Depletion of TMEM129 prevented the loss of FcRn expression in HeLa^{FcRn + US11} cells (Fig. 2.6I and J), suggesting a general requirement for TMEM129 in US11-mediated FcRn degradation activity. The specificity of TMEM129 for the US11-mediated FcRn degradation was confirmed, as a mock siRNA TMEM129 depletion did not evidently rescue FcRn expression in HeLa^{FcRn + US11} cells (Fig. 2.6I and J, *bottom*). Together, we conclude that TMEM129 is recruited to FcRn/US11 via Derlin-1 and is responsible for US11-mediated FcRn degradation.



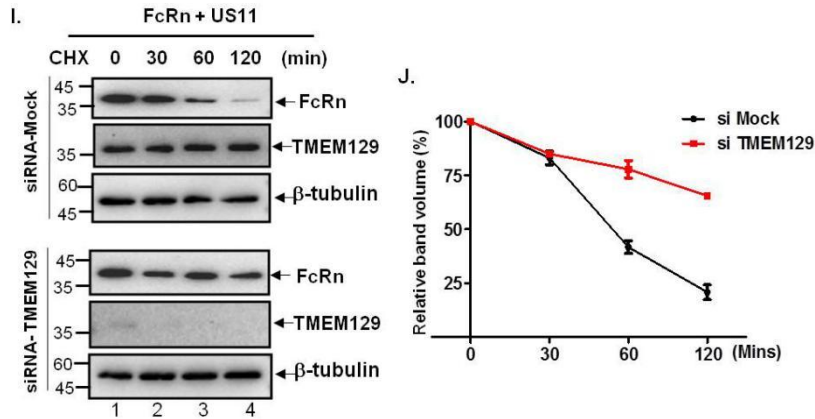


Figure 2.6 US11 recruits FcRn to Derlin-1 and TMEM129 protein complex. Each experiment was performed at least three times. **A+B.** US11 recruits FcRn to Derlin-1 complex. US11* represents a mutant US11 that the Q192 replaced with leucine, US11^{Q192L}. All stable HeLa^{FcRn+US11}, HeLa^{FcRn+US11*}, HeLa^{US11}, and HeLa^{US11*} cell lines were transiently transfected with a pSectag2-Derlin-1-Myc plasmid encoding a myc-tagged Derlin-1. After 48 hours transfection, the cell lysates (0.5 mg), as indicated, were immunoprecipitated by mAb anti-FLAG for FcRn (**A**) or anti-myc for Derlin-1 (**B**). All the precipitated products (**A**, **B**) were subjected to Western blotting with specific antibody as indicated. The cell lysates (input) were blotted as controls. **C.** FcRn does not interact with Derlin-1 in the absence of US11. HeLa^{FcRn} or HeLa cells were transfected with pSectag2-Derlin-1-Myc plasmid to become the HeLa^{FcRn} (Derlin-1) cells or HeLa (Derlin-1) cells. After 48 hours transfection, the cell lysates (0.5 mg), from the HeLa^{FcRn} (Derlin-1) cells (lane1), HeLa^{FcRn} (lane2), HeLa (Derlin-1) (lane3) and HeLa cells (lane4), were immunoprecipitated by mAb anti-FLAG for FcRn. **D+E.** Mutant US11^{Q192L} fails to degrade FcRn. HeLa^{FcRn+US11}, HeLa^{FcRn+US11*} cells were treated with CHX (100 μ g/ml) for the indicated time (**D**). The cells were lysed after CHX treatment and the cell lysate was analyzed by immunoblotting with corresponding Abs. The expression level of FcRn protein in cell lysate was quantified by the band density (relative band volume) measured by Image Lab 5.2 for three independent times. The level of remaining FcRn (**E**) at different time points was calculated as the percentage of initial protein level (0 h of CHX treatment). **F+G.** US11 recruits FcRn to TMEM129 complex. The HeLa^{FcRn+US11} (lane 1), HeLa^{FcRn} (lane 2), HeLa^{US11} (lane 3), and HeLa cells were transfected with Derlin-1 plasmid. 48 h later, the cell lysates were immunoprecipitated by mAb anti-FLAG for FcRn (**F**) or anti-TMEM129 Ab (**G**). The immunoprecipitates were subjected to 12% SDS-PAGE electrophoresis under reducing conditions, then transferred to a nitrocellulose for Western blotting with antibodies as indicated. The 50 μ g cell lysates (input) were blotted with the indicated Abs. Immunoblots (IB) were developed with ECL. **H.** The interaction between US11 and Derlin-1 is dependent on a polar glutamine residue in the US11 transmembrane domain. HeLa^{US11} or HeLa^{US11*} stable cells were lysed and US11 was immunoprecipitated and eluted in SDS sample buffer. Immune precipitates (top) and total lysates (bottom) were analyzed by SDS/PAGE and probed for TMEM129, Derlin-1, and US11. **I+J.** TMEM129 was involved in US11-mediated FcRn degradation. The HeLa^{FcRn+US11} cells were transfected with 20 nM TMEM129 siRNA oligomers (**I**, bottom). 48 h later, cells were then treated with CHX (100 μ g/ml) for the indicated time. The cells were lysed after CHX treatment and the cell lysate was analyzed by immunoblotting with corresponding Abs. The expression level of FcRn proteins in cell lysate was quantified by the band density (relative band volume) measured by Image Lab 5.2 for three independent times. The level of remaining FcRn (**J**) in TMEM129 siRNA-treated cells (*red*) or mock-treated cells (*black*)

at different time points was calculated as the percentage of initial protein level (0 hr of CHX treatment).

FcRn HC cytoplasmic tail is required for US11-mediated degradation

Previous data showed extracellular domains of US11 and FcRn are the main sites of interaction. However, it is unknown whether the cytoplasmic tail of FcRn will play a role in the US11-mediated degradation or not. To investigate the possible involvement of the cytoplasmic tail (CT) of FcRn HC, a deletion of all but five amino acids of the cytoplasmic tail of FcRn was generated (Fig. 2.7A). The remaining four residues were retained to facilitate the FcRn HC to properly insert in the membrane. We and others have shown that similarly truncated FcRn HC behaves like the full-length FcRn HC with respect to folding, assembling with β_2m , and pH-dependent binding to IgG (63). To examine whether deleting the FcRn CT affects US11-induced degradation, HeLa^{US11} cells were transfected with wild-type FcRn or with a tailless mutant of FcRn (FcRn-tailless) (Fig. 2.7B). The fate of full-length and tailless FcRn was further examined by a CHX-chase experiment. In the absence of proteasome inhibitor, the FcRn HC was initially degraded by 30-40 min of chase (Fig. 2.7B and C). This was in marked contrast with the tailless FcRn, which persisted in the presence of US11 (Fig. 2.7B and C). To identify the critical region within the FcRn CT that is responsible for degradation, we constructed a series of the C-terminal FcRn deletion mutants and examined their susceptibility to US11-mediated degradation. Furthermore, deleting a single C-terminal alanine residue affected its susceptibility to US11-induced degradation in a manner similar to that observed after deleting the entire FcRn CT (Fig. 2.7B and C). Indeed, the half-life of FcRn-365A^{-/-} was comparable with that of FcRn CT^{-/-} in HeLa^{US11} cells. Likewise, deleting the C-terminal 365 alanine residue rendered FcRn resistant to US11-induced degradation (Fig. 2.7B and C). Hence, we demonstrate that the cytoplasmic tail of the FcRn is required for its degradation.

FcRn HC interacts with Derlin-1 via US11 (Fig. 2.6A), US11 binds to the Derlin-1 via its transmembrane domain ((Fig. 2.6B). To further understand the mechanisms underlying the role of a cytoplasmic tail during the US11-induced degradation of FcRn HC, we first examined whether deleting the FcRn CT would abolish its interaction with US11. As shown by coprecipitation (Fig. 2.7D), the deletion of FcRn CT did not reduce the interaction between FcRn and US11, suggesting that the FcRn CT may serve as a point of contact for Derlin-1. Hence, we second examined whether deleting the FcRn CT affects its interaction with Derlin-1. Surprisingly, deleting the FcRn CT remarkably reduced, although not completely abolished, the interaction between FcRn and Derlin-1 (Fig 2.7E; compare lanes 1 and 2). Strikingly, we found that the deletion of a single C-terminal alanine residue from the FcRn also similarly decreased the interaction between FcRn and Derlin-1 (Fig 2.7E; compare lanes 1 and 3). Furthermore, the immunoprecipitation of tailless FcRn failed to precipitate TMEM129, suggesting the interaction of FcRn CT and derlin-1 is also important to recruit TMEM129 (Fig 2.7E). Taken together, these results suggest that the cytoplasmic tail of the FcRn HC is required for US11-induced degradation, perhaps it enables FcRn to bind tightly to Derlin-1.

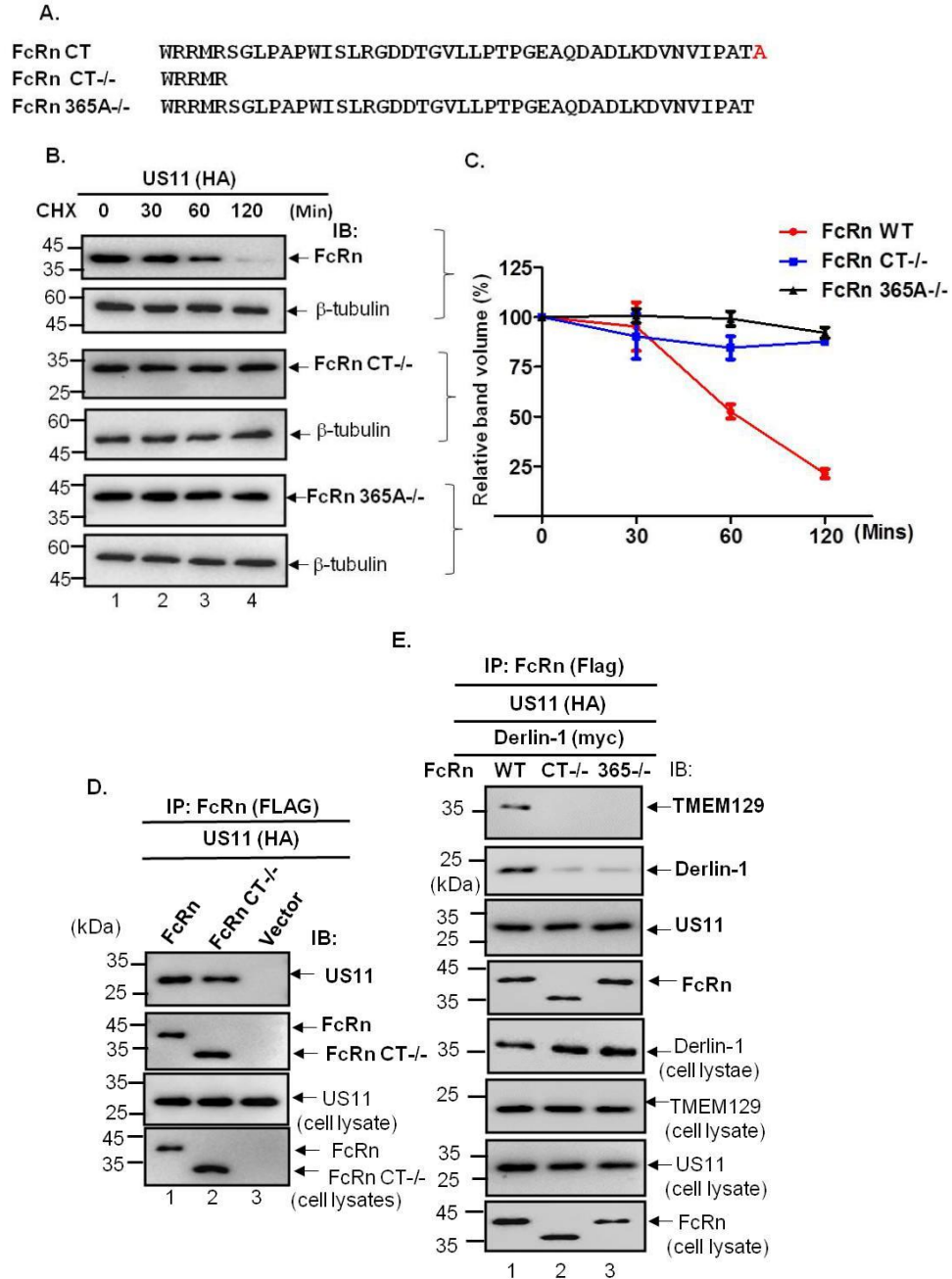


Fig 2.7 FcRn cytoplasmic tail is necessary for US11-mediated FcRn degradation. HeLa^{US11} (FcRn) were HeLa^{US11} cells transfected with plasmid pCDNA-Flag-FcRn encoding wild-type FcRn. HeLa^{US11} (FcRnCT^{-/-}) cells were HeLa^{US11} transfected with with plasmid pCDNA-Flag-FcRnCT^{-/-} encoding tailless FcRn. HeLa^{US11} (FcRn365A^{-/-}) cells were HeLa^{US11} cells transfected with plasmid pCDNA-Flag-FcRn365A^{-/-} encoding mutant FcRn 365A^{-/-} without the C-terminal alanine residue. **A.** Descriptions of tailless FcRn (CT^{-/-}) and FcRn HC deleting 365 alanine residue (365A^{-/-}) in the cytoplasmic tail. **B+C.** Tailless FcRn or FcRn 365A^{-/-} resists degradation in the presence of US11. HeLa^{US11} (FcRn) (**B, top**), HeLa^{US11} (FcRnCT^{-/-}) (**B, middle**), or HeLa^{US11} (FcRn365A^{-/-}) (**B, bottom**) were treated with CHX (100 μg/ml) and chased for the indicated time in the absence of

proteasome inhibitors. The cells were lysed after CHX treatment and the cell lysate was analyzed by immunoblotted with corresponding Abs. The expression levels of wild-type FcRn, tailless FcRn, and mutant FcRn 365A^{-/-} proteins in cell lysates were quantified by the band density (relative band volume) measured by Image Lab 5.2 for three independent times. The level of remaining wildtype FcRn (*C*, *red*), tailless FcRn (*C*, *blue*), and mutant FcRn 365A^{-/-} (*C*, *black*) in HeLa^{US11} cells at different time points was calculated as the percentage of initial protein level (0 hr of CHX treatment). **D.** US11 interacts with tailless FcRn protein. The cell lysates from HeLa^{US11} (FcRn) (lane 1), HeLa^{US11} (FcRnCT^{-/-}) (lane 2), and HeLa control (lane 3) were immunoprecipitated by anti-Flag Ab for FcRn. The immunoprecipitates and cell lysates (input) were subjected to 12% SDS-PAGE electrophoresis, then transferred to a nitrocellulose for blotting with anti-FLAG (FcRn), anti-HA (US11), as indicated. Immunoblots were incubated with HRP-conjugated 2nd Ab of the corresponding species and developed with ECL. The US11 molecules that coprecipitate in the complex are indicated. **E.** The cytoplasmic tail of the FcRn is required for tightly binding to Derlin-1 in the expression of US11. HeLa^{US11} (FcRn) (lane 1), HeLa^{US11} (FcRnCT^{-/-}) (lane 2), and HeLa^{US11} (FcRn365A^{-/-}) (lane 3) cells were transfected with pSectag2-Derlin-1-Myc plasmid for 48 hr. The cell lysates were immunoprecipitated by anti-Flag Ab for FcRn. The immunoprecipitates and cell lysates (input) were subjected to 12% SDS-PAGE electrophoresis, then transferred to a nitrocellulose for blotting with anti-TMEM129, anti-Myc (Derlin-1), anti-FLAG (FcRn), and anti-HA (US11), as indicated by arrows. Immunoblots were incubated with HRP-conjugated 2nd Ab of the corresponding species and developed with ECL.

US11/Derlin-1/TMEM129/Ube2J2 protein complex induces FcRn dislocation,
ubiquitylation, and degradation

Ubiquitination of the protein substrate provides a critical step in protein degradation (273). We then investigated whether US11 regulates FcRn turnover through an ubiquitination-dependent mechanism. We found that FcRn ubiquitination was efficiently induced by US11 in the presence of MG132 inhibitor (Fig. 2.8A). As expected, the US11 failed to induce HFE ubiquitination (Fig. 2.8B), further verifying specificity of FcRn ubiquitination induced by US11. Furthermore, a tailless FcRn (Fig. 2.8C, *lane 2*) or FcRn CT365A^{-/-} (Fig. 2.8C, *lane 3*) exhibited a much less ubiquitination in comparison with wild-type FcRn (Fig. 2.8C, *lane 1*), indicated that the cytoplasmic tail of FcRn is necessary for US11-induced FcRn ubiquitination.

We also detected FcRn proteins as slower and faster-migrating bands in our analysis (Fig. 2.8C, *lane 1, middle*). To verify this observation, we performed a CHX chase analysis. A faster-migrating band (Fig. 2.8D, *lane 1, middle*) appeared in the presence of proteasome inhibitor and the expression of US11, as FcRn molecules were also intensively ubiquitinated (Fig. 2.8C, *lane 4-6, top*). The HeLa^{FcRn + US11} cells contained the slower-migrating bands at early chase time points, which was then converted to the faster-migrating form at later time points. We reasoned this faster-migrating band might represent a dislocated and deglycosylated protein, which might result from cytosolic *N*-glycanase removal of the FcRn glycan. To prove this, HeLa^{FcRn+US11} or HeLa^{FcRn} cells were subjected to subcellular fractionation. The FcRn protein in the pellet (membrane) or soluble (cytosol) fraction were measured by western blotting analysis. We detected a faster FcRn migrating band in the cytosol fraction from HeLa^{FcRn + US11} cells rather than from HeLa^{FcRn} cells (Fig. 2.8E, *top, lanes 4 & 8*), indicating US11 induces FcRn dislocation from ER membrane into the cytosol fraction. A slower FcRn migrating band were detected in the membrane fraction from both the HeLa^{FcRn + US11} cells and HeLa^{FcRn} cells (Fig. 2.8E, *top, lanes 3 & 7*). As the slower-migrating band might be the glycosylated FcRn protein retained on ER membrane and the faster-migrating band might be a dislocated and deglycosylated FcRn protein, the subcellular fractionation products were analyzed by Endo H or PNGase F digestion. After PNGase F digestion, the FcRn protein from membrane fraction had a mobility similar to that from the cytosol fraction, as the PNGase F cleaved the glycan chain from FcRn (Fig. 2.8E, *bottom*). After Endo H digestion, only a portion of the FcRn protein from membrane fraction was EndoH-sensitive and showed a similar mobility to that from cytosol fraction (Fig. 2.8E, *middle*). However, membrane fraction FcRn from HeLa^{FcRn + US11} cells was much more sensitive to Endo H digestion than that from HeLa^{FcRn} cells (Fig. 2.8E, *middle*). Therefore, we conclude that the slower-migrating band represents a glycosylated form of FcRn which co-fractionates with the ER membrane and the-faster migrating band represents a deglycosylated

cytosolic form of FcRn which co-fractionates with the cytosol. The origin of the nonglycosylated FcRn form could be due to dislocation of FcRn from the ER, where the cytosolic *N*-glycanase removes the glycan chain from FcRn. It may represent an intermediate before its degradation because it accumulated only in the MG132 presence.

The E3 ligases are involved in protein ubiquitination (274); TMEM129 contains a novel and atypical RING domain with intrinsic protein E3 ubiquitin ligase activity (183). To show that TMEM129 was required for FcRn ubiquitination, we initially knocked down TMEM129 expression (Fig. 2.8F, *middle, lane 2*). We then immunoprecipitated FcRn and found the robust FcRn ubiquitination induced by US11 (Fig. 2.8F, *top, lane 1*) was abrogated in the TMEM129 siRNA-treated cells (Fig. 2.8F, *top, lane 2*). TMEM129 has an atypical RING-C2 domain which usually creates a binding platform for the E2 conjugating enzymes (184). We further tested a custom siRNA library targeting the E2 used by TMEM129. We explored the potential role of Ube2J1 or Ube2J2 in TEME129-mediated ubiquitination of FcRn. We confirmed that the knockdown of Ube2J2, but not Ube2J1, abolished US11-induced FcRn ubiquitination (Fig. 2.8G, *top, lane 1*) and rescued FcRn degradation in HeLa^{FcRn + US11} cells (Fig. 2.8H, *bottom*). Therefore, the E3 ligase TMEM129 recruits Ube2J2 for the US11-induced FcRn ubiquitination that drives ER dislocation and proteasomal degradation.

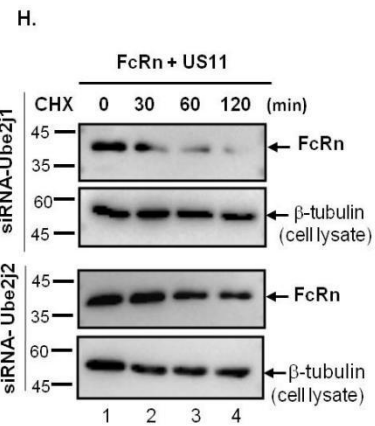
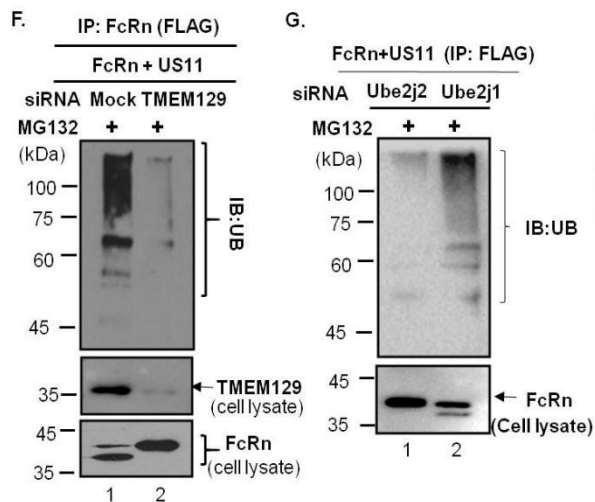
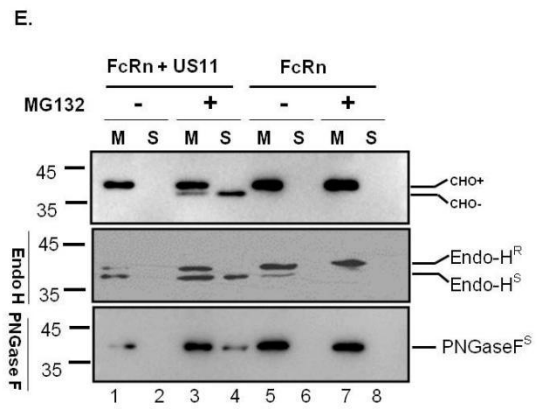
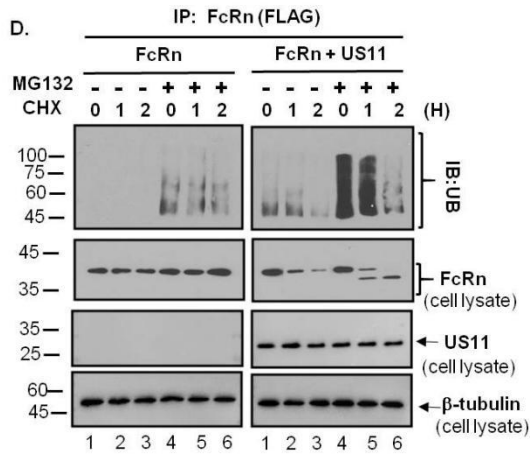
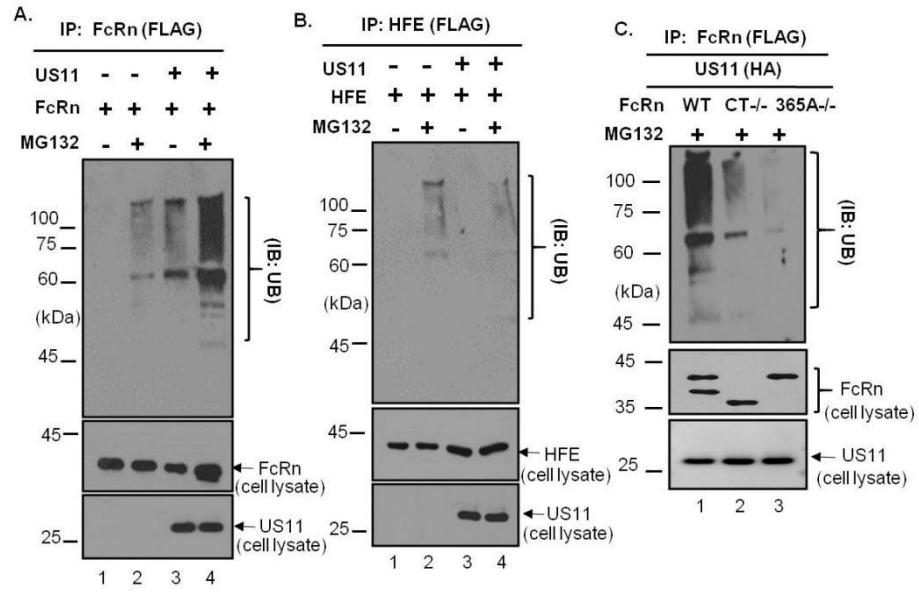


Figure 2.8 US11/Derlin-1/TMEM129/Ube2J2 protein complex induces FcRn dislocation, ubiquitylation, and degradation. A+B. FcRn is remarkably ubiquitinated in the presence of US11 expression and MG132 treatment. HeLa^{US11} (FcRn) were HeLa^{US11} cells transfected with plasmid pCDNA-Flag-FcRn encoding Flag-tagged FcRn. HeLa^{US11} (HFE) were HeLa^{US11} cells transfected with plasmid pCDNA-Flag-HFE encoding Flag-tagged HFE. HeLa^{US11} cells and HeLa^{US11} (FcRn) cells respectively were treated with or without MG132 (50Mm) for 2 hours (A). HeLa^{US11} cells and HeLa^{US11} (HFE) cells respectively were treated with or without MG132 (50μM) for 2 hours (B). The cell lysates (0.5 mg) were immunoprecipitated with mAb anti-FLAG for FcRn (A) or HFE (B). The immunoprecipitates were subjected to the electrophoresis and immunoblotting analysis to detect ubiquitin and the target proteins FcRn, HFE or US11 with respective Abs, as indicated. C. HeLa^{US11} (FcRn), HeLa^{US11} (FcRn CT^{-/-}) or HeLa^{US11} (FcRn 365A^{-/-}) cells were HeLa^{US11} cells transfected respectively with plasmid pCDNA-Flag-FcRn, pCDNA-Flag-FcRnCT^{-/-} or pCDNA-Flag-FcRn365A^{-/-}. HeLa^{US11} (FcRn) cells (lane 1.), HeLa^{US11} (FcRn CT^{-/-}) cells (lane 2) or HeLa^{US11} (FcRn 365A^{-/-}) cells (lane 3) respectively were treated with or without MG132 (50μM) for 2 hours. The cell lysates (0.5 mg) were immunoprecipitated with mAb anti-FLAG for wide-type FcRn, tailless FcRn CT^{-/-} or cytoplasmic tail mutant FcRn 365A^{-/-}. The immunoprecipitates were subjected to the electrophoresis and immunoblotting analysis to detect ubiquitin and the target proteins with respective Abs, as indicated. D. HeLa^{FcRn} cells or HeLa^{FcRn+US11} cells were respectively treated with or without MG132 (50μM) for 2 hours. Cells were subsequently treated with CHX (100 μg/ml) and chased for the indicated time in the presence of MG132. The cell lysates (0.5 mg) were immunoprecipitated with mAb anti-FLAG for FcRn. The immunoprecipitates were subjected to the electrophoresis and immunoblotting analysis to detect ubiquitin and the target proteins FcRn, US11 or β-tubulin with respective Abs, as indicated. E. Fractionations of FcRn HC. The HeLa^{FcRn}, HeLa^{US11+FcRn} cells were incubated in the presence or absence of the 50μM MG132 for 4 hr. The cells were then homogenized and the homogenates were fractionated by centrifugation (*see Materials and Methods*). Fractions were diluted by 1% Triton X-100 buffer. The FcRn in the membrane pellet (M, lanes 1, 3, 5, 7) and supernatant (S, lanes 2, 4, 6, 8) fractions were digested by mock (*top*), Endo-H (*middle*), PNGase F (*bottom*) enzymes for 2 h at 37°C, respectively. Proteins were analyzed on a 12% SDS-PAGE gel and immunoblotted with the FcRn-specific Ab. R: resistant; S: sensitive. F+G. TMEM129 and Ube2J2 are required for US11-induced FcRn ubiquitination. HeLa^{FcRn+US11} cells were transfected with 20 nM TMEM129, Ube2J1, Ube2J2 siRNA oligomers for 48 hr or an empty vector. Efficacy of TMEM129 silencing was analyzed 72 hr after transfection. Cells were subsequently treated with 50 μM MG132 for 4 hr and then lysed. After immunoprecipitation of FcRn with anti-FLAG, the immunoprecipitated complexes or cell lysates were analyzed by immunoblotting with the indicated antibodies, respectively. H. Ube2J2 are essential for US11-induced FcRn degradation and ubiquitination. HeLa^{US11+FcRn} cells were transfected with 20 nM Ube2J1 (*top*) and Ube2J2 (*bottom*) siRNA oligomers for 48 hr. Cells were then treated with CHX (100 μg/ml) and chased for the indicated time. Subsequently, cells were lysed in PBS with 0.5% CHAPS and protease inhibitor cocktail III. Cell lysates (20 μg) were probed with the Flag Ab for detection of FcRn level FcRn as indicated and developed with ECL. The β-tubulin (input) was blotted as controls.

US11 impairs FcRn IgG binding capacity

A hallmark of FcRn is that it binds IgG at acidic pH (≤ 6.5) and releases IgG at neutral or higher pH (25, 26). FcRn HC associating with β_2m is important for pH-dependent IgG binding. We further tested whether the association of FcRn with US11 affects FcRn binding to IgG. Lysates from HeLa cells expressing FcRn and/or US11 were incubated with IgG-Sepharose at pH 6.0 or pH 7.4; lysates from HeLa^{FcRn} cells were used as positive controls. The eluates from IgG binding and cell lysates were subjected to analysis by Western blot. As expected, FcRn from HeLa^{FcRn} cells bound IgG at pH 6.0 (Fig. 2.9A, *lane 2*) but not at pH 7.4 (Fig. 2.9B, *lane 2*). Similarly, β_2m from the IgG binding eluates was detected at pH 6.0 (Fig. 2.9A, *lane 2*) but not at pH 7.5 (Fig. 2.9B, *lane 2*). US11 proteins were not detected in the FcRn binding eluates of IgG beads at pH 6.0 (Fig. 2.9A, *lane 1*). Furthermore, FcRn and β_2m (Fig. 2.9A, *lane 1*) eluted from IgG beads was remarkably decreased in HeLa^{FcRn + US11} cells in comparison with these of HeLa^{FcRn} cells alone (Fig. 2.9A, *lane 2*), as measured by the quantitative method (Fig. 2.9C and Fig. 2.9D). These data strongly suggest the association of US11 with FcRn HC interferes with FcRn binding to IgG. Hence, when US11 binds FcRn, it prevents the formation of the FcRn/ β_2m complex and

consequently blocks functional binding to IgG.

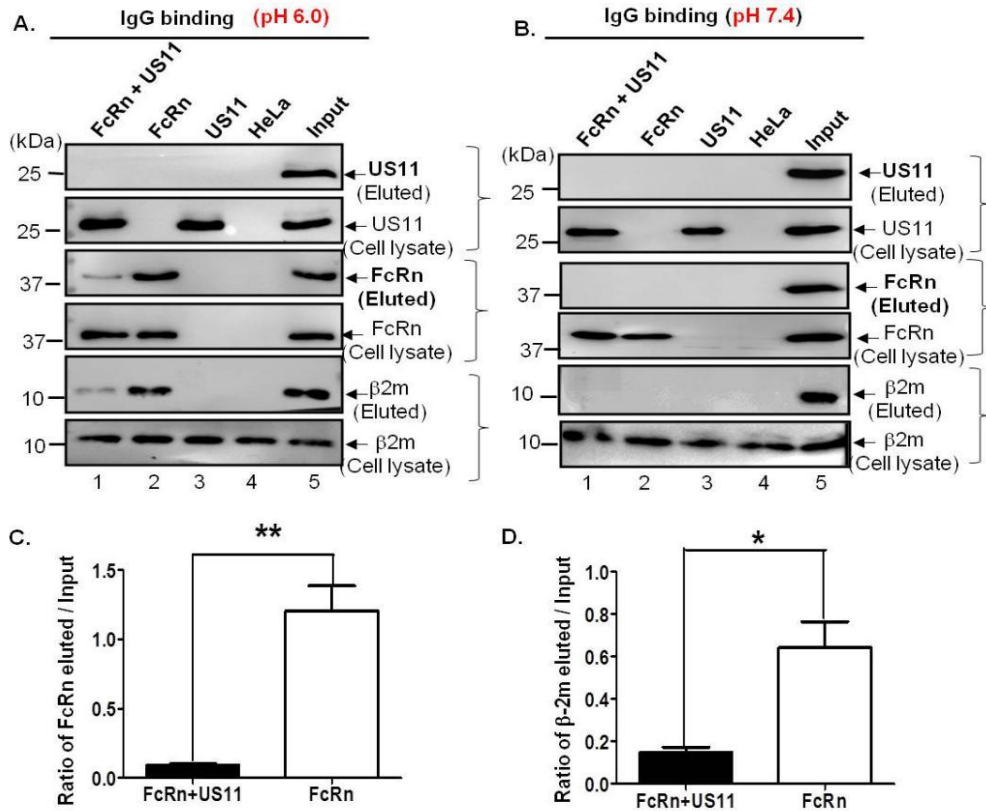


Figure 2.9 US11 impairs FcRn IgG binding capacity. The presence of US11 expression reduces FcRn binding to IgG. HeLa transfectants as indicated were lysed in sodium phosphate buffer pH 6.0 (A) or pH (B) with 0.5% CHAPS and fresh proteinase inhibitors. Approximately 0.5 mg of the soluble proteins were incubated with human IgG-Sepharose at 4 °C. Unbound proteins were washed off with PBS (pH6.0 or pH 7.4) containing 0.5% CHAPS. Human IgG-Sepharose adsorbed proteins were eluted by Laemmli Sample buffer at 95 °C for 5 mins. The eluted proteins were subjected to Western blotting analysis. Proteins were probed with rabbit anti-FLAG (FcRn), anti-HA (US11), anti- β_2m Ab and developed with HRP-conjugated secondary Abs of the corresponding species and ECL. Cell lysate from each sample with an equal amount of total protein was also tested by WB for FcRn, US11, and β_2m expression level. The locations of the human FcRn HC, US11, and β_2m proteins are indicated by arrows. The amount of eluted FcRn (C) or β_2m (D) protein from HeLa^{FcRn} and HeLa^{FcRn+US11} cells was compared by the ratio of the band density of eluded protein to that of the input protein. The band density of proteins (relative volume) was quantified by the software Image Lab 5.2. The binding experiments were independently repeated three times.

HCMV infection or US11 expression reduced IgG transcytosis in the polarized human epithelial monolayers

FcRn has been identified to transport IgG in polarized epithelial cells, namely from the apical to the basolateral direction or vice versa (272). HCMV is previously shown to infect Caco-2 cells at the basolateral membrane (58). We, therefore, explored the possibility that HCMV-infected Caco-2 epithelial cells have altered IgG transcytosis. In our assay, human IgG Abs were added to the apical surface of a Caco-2 cell monolayer and then we measured IgG transport into the opposite basolateral chamber using cells infected with HCMV. As expected, after 2 hr at 37 °C intact human IgG applied to the apical side was transported across the mock-infected monolayer (Fig. 2.10A, *lane 4*). IgG transport at 37 °C from the apical to basolateral direction was significantly decreased in HCMV-infected Caco-2 cells (Fig. 2.10A, *lane 2*) compared to mock-infected cell monolayers. There was no IgG transport across the HCMV-infected Caco-2 monolayer at 4 °C (Fig. 2.10A, *lane 1*), which precludes the possibility that infecting Caco-2 monolayers with HCMV for 48 hr might result in leaking of the IgG antibody. To further show whether US11 expression alone reduces IgG transcytosis, we stably expressed US11 in Caco-2 cells. Human IgG Ab (0.5 mg/ml) was apically added into the Caco-2^{US11} cell monolayer and further incubated for 2 hr to allow transcytosis. The basolateral medium was collected and human IgG content was measured by Western blot-ECL. Similar to HCMV-infected cells, IgG transport from the apical to basolateral direction was decreased in US11-expressing cells (Fig. 2.10C, *lane 2*) compared to mock-transfected cell monolayers (Fig. 2.10C, *lane 4*). Because FcRn transfers maternal IgG across placental epithelial cells, we finally showed that IgG transport from the apical to basolateral direction was decreased or blocked in HCMV-infected BeWo cells (Fig. 2.10E, *lane 3*) compared to mock-infected BeWo cell monolayers (Fig. 2.10E, *lane 1*). Human IgG was not transported at 4 °C in HCMV-infected (Fig. 2.10A, *lane 1*), US11-expressing (Fig.

2.10C, lane 1) Caco-2 cells or HCMV-infected BeWo cells (Fig. 2.10E, lane 4), suggesting that the transepithelial flux of IgG Abs by passive diffusion through intercellular tight junctions or monolayer leaks did not contribute to the amount of the IgG we detected. Furthermore, our Western blot data were verified by a more sensitive ELISA detection method (Fig. 2.10B, D and F). Hence, we concluded that HCMV infection or US11 decreases or blocks the IgG transport across the polarized epithelial cells.

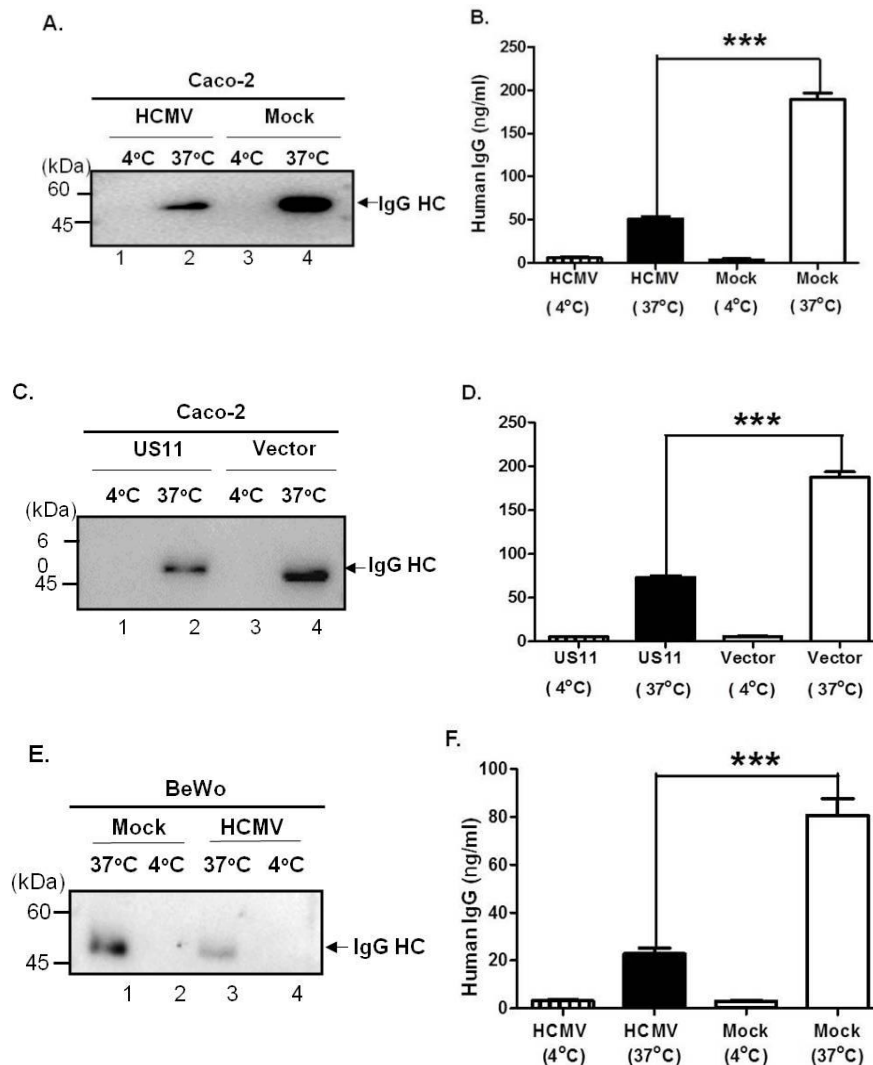


Figure 2.10 HCMV infection or US11 expression reduced IgG transcytosis in the polarized human epithelial monolayers. A+B. Caco-2 cells (2×10^4 /well) were grown in 0.4 μm transwell plate for 8 to 10 days to allow differentiation. When the transepithelial resistance of the Caco-2 monolayer reached above 600 ohms cm^2 , cells were basolaterally infected with HCMV (MOI 5) for 1 hr. After washing, cells were incubated for additional 48

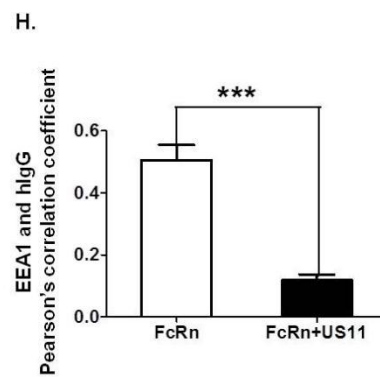
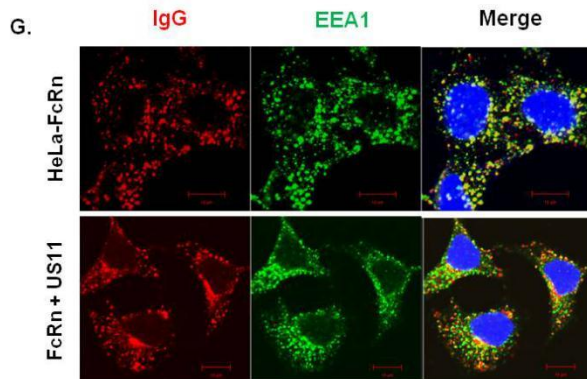
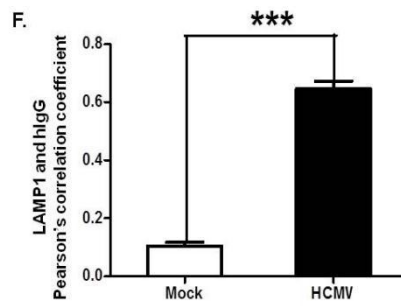
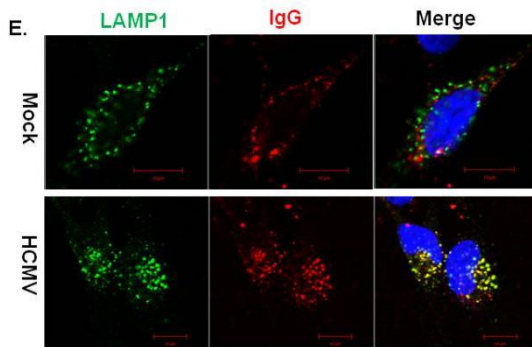
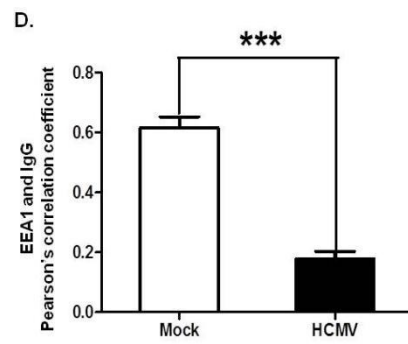
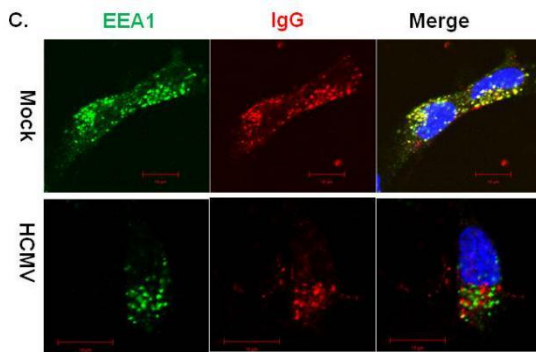
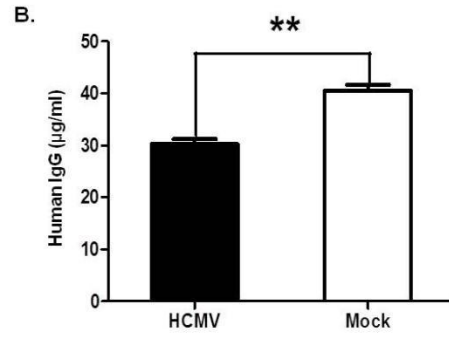
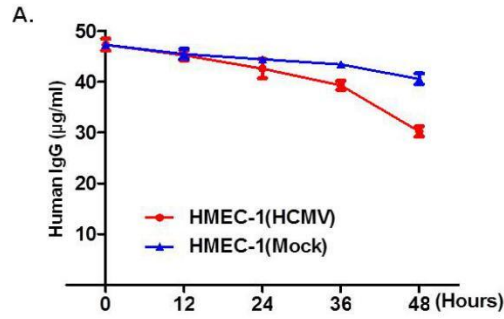
h. The infected or mock-infected Caco-2 cells were apically loaded with human IgG (*lanes 1-4*) (0.5 mg/ml) at 37 °C or 4 °C, respectively. The medium was collected from the basolateral compartment 2 hr later and subjected to Western blot-ECL (*A*) or ELISA (*B*) analysis. *C+D*. Caco-2 cells transfected with either pEF6 alone or pEF6-US11 was grown onto the transwell inserts as described above. The cells were incubated for 1 hr either at 37 °C or 4 °C, then human IgG (0.5 mg/ml) was apically added and further incubated for 2 hr to allow transcytosis. The basolateral medium was collected and human IgG content was measured by Western blot-ECL (*C*) or ELISA (*D*) analysis. The results are representative of at least three independent experiments. *E+F*. BeWo cells (10^5 /well) were grown in 0.4 μ m transwell plate for 4 days to allow differentiation. When the transepithelial resistance of the BeWo monolayer reached above 400 ohms cm^2 , cells were basolaterally infected with HCMV (MOI 5) for 1 hr. After washing, cells were incubated for additional 48 h. The infected or mock-infected BeWo cells were apically loaded with human IgG (*lanes 1-4*) (0.25 mg/ml) at 37 °C or 4 °C, respectively. The medium was collected from the basolateral compartment 2 hrs later and subjected to Western blot-ECL (*E*) or ELISA (*F*) analysis. All ELISA analyses were performed in triplicate. Star denotes statistical significance. *** $P < 0.001$.

HCMV infection or US11 expression facilitates IgG degradation

In addition to its transcytotic function, FcRn plays a critical role in IgG homeostasis by recycling IgG away from a catabolic pathway in vascular endothelium, thus extending its lifespan in circulation and ensuring long-lasting protective immunity after infection or immunization (57, 58). In the majority of cell types, FcRn resides primarily in early acidic endosomal vesicles (12, 18 and 52); FcRn binds to IgG that enters the cell by pinocytosis or endocytosis. Subsequently, FcRn efficiently recycles IgG back to the plasma membrane, where the near-neutral pH of the extracellular environment causes IgG release from FcRn. Any pinocytosed or endocytosed IgG that are not savaged in this manner are efficiently trafficked to the lysosomes for degradation (28, 57 and 58). If the US11 acts by preventing FcRn binding to IgG and trafficking to the endosome, it should accelerate the IgG degradation by promoting the pinocytosed IgG to the lysosomes.

To test this theory, HCMV-infected endothelial HMEC-1 cells were incubated with human IgG. The IgG concentration in the supernatant medium were subsequently measured by ELISA at indicated time points (Fig. 2.11A). We detected that, after 48 hours incubation, IgG concentration was significantly reduced in the medium from the HCMV-infected

HMEC-1 cells in comparison with that from mock-infected cells (Fig. 2.11B). To further understand this process, HCMV-infected HMEC-1 cells were stained with mAb anti-EEA1 to visualize human IgG trafficking to the endosomal compartment. We were able to easily detect human IgG (Fig. 2.11C, *yellow*) in the endosome of the mock-infected HMEC-1 cells, but not in the HCMV-infected HMEC-1 cells. Pearson correlation coefficient analysis indicated a significantly less colocalization of EEA1 and human IgG in the HCMV-infected HMEC-1 cells than that in the Mock-infected cells (Fig. 2.11D), suggesting that the HCMV infection impairs the IgG recycling in the endosome compartment. To further investigate the fate of IgG Ab, antibody against lysosome-associated membrane glycoprotein-1 (LAMP1), a lysosomal marker, was used to follow IgG trafficking to lysosomal sites. Transport of the human IgG to the lysosomes was negligible in mock-infected HMEC-1 cells during the incubation periods as indicated (Fig. 2.11E). However, the colocalization (Fig. 2.11E, *yellow*) of LAMP-1 and IgG Ab was prominent in HCMV-infected HMEC-1 cells. As showed in Pearson correlation coefficient analysis, the colocalization of LAMP1 and human IgG in the HCMV-infected HMEC-1 cells was significantly higher than that in the Mock-infected (Fig. 2.11F), indicating that the HCMV infection promotes the trafficking of IgG into the lysosomes. The human IgG trafficking patterns in HCMV-infected HMEC-1 cells were thoroughly verified in IgG-treated HeLa^{FcRn+US11} cells (Fig. 2.11G, H, I and J). Taken together, these data strongly suggest that the US11 protein or HCMV infection prevents FcRn trafficking to the endosome, possibly by retaining the FcRn in the ER compartment, ultimately resulting in the delivery of IgG Abs to lysosomes for degradation.



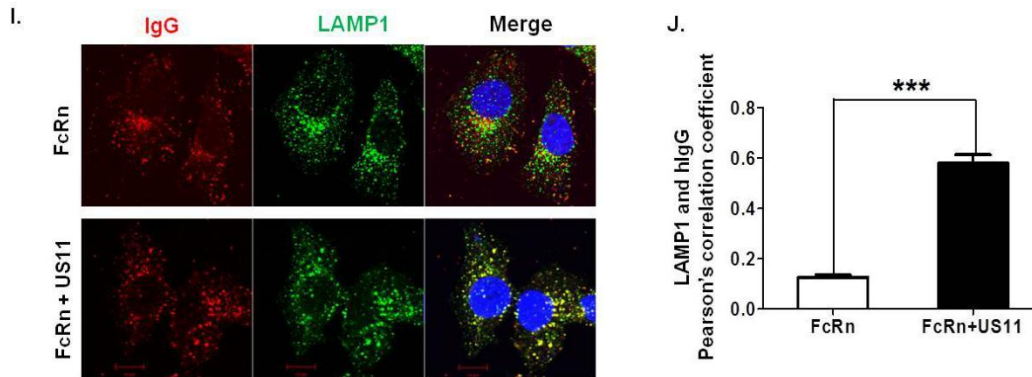


Figure 2.11 HCMV infection increased IgG catabolism in human endothelial cells.

A + B. HEMC-1 cells ($5 \times 10^5/2$ ml) were grown in the complete medium with 5% FBS with ultra-low IgG. After cells were initially infected with 5 MOI of HCMV or mock-infected for 48 hr, they were then incubated with complete medium supplemented with $50\mu\text{g/ml}$ human IgG for another 48 hours. During this incubation, the supernatant medium was sampled at 0, 12, 24, 36, 48 hr and the IgG concentration in each medium sample was measured by ELISA (**A**). The ELISA analyses were performed in triplicate. At 48 hr, the IgG concentration in the medium from the HCMV-infected and mock-infected cells were compared by t-test analysis (**B**). Star denotes statistical significance. $** P < 0.01$. **C+D+E+F.** To visualize human IgG trafficking inside the infected HEMC-1 (5×10^4) cells, they were infected with 5 MOI of HCMV for 48 hr and were then incubated with $250\mu\text{g/ml}$ human IgG for 1 hr at 37°C . After completely washing, cells were incubated in complete medium without IgG for an additional 1 hr, then fixed and stained by immunofluorescence for the co-localization of human IgG with the early endosomal marker EEA1 (**C**) or lysosomal marker LAMP1 (**E**). The nuclei were stained with DAPI (blue); Colocalization of two molecules appears in yellow. The colocalization degree of internalized IgG with EEA1 (**D**) or LAMP1 (**F**) was quantified by the average Pearson's colocalization coefficients in mock and viral-infected HMEC-1 cells. **G+H+I+J.** Human IgG trafficking inside HeLa^{FcRn+US11} and HeLa^{FcRn} cells. To visualize human IgG trafficking inside HeLa^{FcRn+US11}, HeLa^{FcRn} (1×10^5) cells, they were incubated with $250\mu\text{g/ml}$ human IgG for 1 hr at 37°C . After completely washing, cells were incubated with complete medium without IgG for an additional 1 hr, then fixed and stained by immunofluorescence for the co-localization of human IgG with the early endosomal marker EEA1 (**G**) or lysosomal marker LAMP1 (**I**). The nuclei were stained with DAPI (blue); Colocalization of two molecules appears in yellow. The colocalization degree of internalized IgG with EEA1 (**H**) or LAMP1 (**J**) was quantified by the average Pearson's colocalization coefficients in HeLa^{FcRn} and HeLa^{FcRn+US11} cells. For each assay, Pearson's correlation coefficient was measured by analyzing 100 cells (*in total*) in 10 different optical regions. Star denotes statistical significance. $*** P < 0.001$.

Discussion

Proteins inserted into the ER must fold and acquire their native state before further trafficking through the secretory pathway (291, 292). To remove the misfolded proteins, they are retrotranslocated across the ER-membrane for cytosolic proteasome degradation in a

process known as ER-associated degradation (ERAD) (230). Many pathogens take over the ERAD system, particularly to degrade components of the host immune system (293, 295). The FcRn plays a central role in IgG biology at all stages of life; it is the only known Fc receptor able to transport IgG across cell barriers and prolong IgG half-life (58). HCMV is a ubiquitous herpesvirus that establishes lifelong latent infections and, after periodic reactivation from latency. It causes life-threatening disease in patients who go through bone marrow or tissue transplantation or who have AIDS. HCMV uses a panel of immune evasion proteins to survive and replicate in the face of cellular immunity. In this study, we find that the HCMV infection can cause FcRn degradation through an ERAD mechanism.

Our first major finding is that FcRn and US11 proteins specifically interact in the US11 transfected HeLa or HCMV-infected human cells. *The* HCMV US11 protein binds FcRn HC in either transfected HeLa or HCMV-infected intestinal Caco-2, endothelial HMEC-1, and macrophage-like THP-1 cells. Monocyte/macrophages are important host cells for HCMV, serving as a latent reservoir and as a means of dissemination throughout the body. Important consequences of this interaction are that the US11 binding retains FcRn HC in the ER, so FcRn does not appear in the acidic endosomal compartment, an ideal compartment for FcRn binding to IgG. Several lines of evidence support this conclusion. First, US11 is colocalized with FcRn in transfected HeLa or HCMV-infected cells. Second, US11 expression impairs FcRn appearance in the early endosomes. Third, US11 interacts with the nascent FcRn HC but not with FcRn- β_2m , suggesting that US11 captures newly synthesized FcRn HC before it binds β_2m . Molecular interactions of US11 and FcRn are not exactly known but it seems that the US11 luminal domain interacts with the extracellular domain of FcRn. The contribution of the critical residue in their reciprocal bindings will be further investigated. Fourth, the glycosylation of FcRn complexed with US11 is restricted to early unmaturing forms, showing that the complex is retained in the ER. These findings agree with

that fact that the US11 is an ER resident protein, which the luminal domain of US11 is essential to confer ER localization (175). It is possible that a US11-deleted HCMV virus could be used to verify the function of US11 interacting with FcRn. However, additional HCMV proteins may affect FcRn expression and functions in US11 mutant virus-infected cells. We found that the HCMV genome encodes at least two additional proteins that interact with FcRn HC (unpublished data). Therefore, multiple HCMV proteins might interact with FcRn.

Our second major finding is that HCMV US11 protein initiates dislocation of newly translocated FcRn HC from the ER to the cytosol for proteasome-mediated degradation using an ERAD mechanism. Because binding between US11 and tailless FcRn is preserved, yet no degradation of FcRn HC was observed, we reason that US11 alone does not have the capability to mediate FcRn degradation. We find that US11 causes FcRn degradation in a CHX chase experiment and US11 engages a Derlin-1/TMEM129-dependent pathway that is required for FcRn degradation. This conclusion is supported by the evidence that a mutant US11 failing to interact with Derlin-1 fails to use FcRn degradation. Indeed, it remains unknown whether US11 remains bound to Derlin-1 even after the FcRn molecules dissociate from US11. Formation of the FcRn/US11/Derlin-1 complex is important for FcRn degradation. Thus, once captured by Derlin-1, MHC-I molecules are rapidly dislocated and ubiquitinated. Although Derlin-1 interacts with several ubiquitination E3 ligases, TMEM129's strong interaction with Derlin-1 suggest TMEM129 is a candidate. Bioinformatic analysis suggests that TMEM129 has three transmembrane domains and a long C-terminal tail which is predicted to contain conserved cysteine residues whose spacing is reminiscent of the RING family of E3 ligases (183). Linking FcRn with the TMEM129 cellular E3 ligase may provide a very efficient way to degrade FcRn. Thus, once captured by Derlin-1, FcRn HC are rapidly dislocated, ubiquitinated and, finally, extracted from the ER

membrane and released into the cytosol. We further show that the knockdown of TMEM129, together with its cognate E2 UBE2J2, abolishes FcRn ubiquitination in the presence of US11 and prevents FcRn degradation. Other ERAD E3 ligases cannot substitute for TMEM129, as depletion of neither Hrd1/Gp78, RMA-1, nor TRC8 prevents FcRn degradation, making it surprising that TMEM129 is the sole ligase responsible for US11-induced FcRn protein degradation. We reason that the major role of US11 is likely to be the delivery of FcRn HC to Derlin-1 or Derlin-1 bridges US11 to TMEM129, which then induces FcRn dislocation to the cytosol for proteasomal degradation. Also, US11 protein is shown to activate the unfolded protein response, which turns on the expression of genes involved in the ERAD pathway (285).

Our third major finding is that HCMV infected cells or US11 reduces FcRn-mediated IgG transport in epithelial monolayer and accelerates the IgG catabolism in human endothelial cells. We can envision the relevance of our findings *in vivo*. By transferring maternal IgG Ab across the placenta, FcRn provides passive protection to newborns before neonatal immunity develops. FcRn also transports IgG across other polarized epithelial cells lining the mucosal surfaces (38). In this way, FcRn ensures an effective IgG-mediated mucosal immune response to infection or vaccination. By extending IgG lifespan in circulation and local tissues, FcRn guarantees that pathogen-specific IgG Ab confers a durable protective immunity. Because HCMV establishes a lifelong persistent infection that frequently involves many cycles of latency and reactivation, HCMV triggers strong and long-lasting host immune responses, including IgG responses. As an opportunistic infectious agent, HCMV will increase susceptibility to secondary infections. Importantly, HCMV is a leading virus causing congenital diseases when it infects the uterine-placental interface syncytiotrophoblasts; this is associated with a variety of birth defects depending on the strength of maternal humoral immunity and gestational age (296). The US11 inhibition of

FcRn function would result in lower amounts of the high-avidity neutralizing Abs from maternal circulation getting to the fetal bloodstream. The US11 function undermines the mechanism for FcRn in syncytiotrophoblasts that are to import protective maternal Abs and inhibit viral replication in the placenta (32, 35). In order for HCMV to persist or evade pre-existing maternal immunity, viral immune evasion mechanisms must be developed to have a detrimental effect on FcRn functions. Until now, no viral mechanism able to evade FcRn functions has been described. Expression of US11 in cells reduced or abolished FcRn ability to transport and protect IgG. Thus, US11 may allow HCMV-infected cells to remain relatively 'invisible' to IgG, a property that would be important after virus reactivation, a property that would be important after virus reactivation. Our results, though limited to *in vitro* studies, point to a way that HCMV US11 could enable viral infections to persist by degrading FcRn function.

How FcRn is exactly extracted from the ER membrane and released into the cytosol for the degradation in the presence of US11 expression? US11 requires the cytosolic tail of the FcRn HC to drive FcRn into the ERAD pathway for degradation; however, the underlying mechanisms remain elusive. The cytoplasmic tail of the FcRn, although not required for interaction with US11, may be required for tight binding to Derlin-1. Our data show that deleting the cytoplasmic tail (or C-terminal amino acid) of FcRn markedly weakened its interaction with Derlin-1, suggesting the cytoplasmic tail of FcRn is required for FcRn tightly binding to Derlin-1 in the presence of US11. It is interesting to know whether deleting the C-terminal cytosolic region of Derlin-1 also prevents it from binding to FcRn HC. We reason that the interaction of cytoplasmic tails between FcRn and Derlin-1 may allow both molecules to engage the dislocation machinery because tailless FcRn seems to fail to complete the dislocation to the cytosol for proteasomal degradation. Also, for entry into the proteasome, the glycan in the FcRn could pose a steric constraint. The *N*-glycanase activity

likely acts immediately on removal of the glycans in the FcRn in the course of dislocation. Hence, the compromising of the proteasomal activity would accumulate the bulk of the dislocating FcRn that is transferred into the cytosol and as a deglycosylated polypeptide. We do detect the deglycosylated form of FcRn appears only in the cytosol during the cell fractionation (Fig. 2.8E). Because the cytosolic deglycosylated intermediates of the FcRn HC are not observed in the absence of proteasomal inhibitors, dislocation and degradation by the proteasome may be tightly coupled. This assumption is supported by the evidence that the C-terminal region of Derlin-1 interacts with the cytosolic AAA ATPase p97, a proteasomal protein; thus, the Derlin-1-bound FcRn HC may also physically interact with p97. It is possible that the p97 may provide the energy required for the dislocation (240). These interactions then allow p97 to extract FcRn from the ER membrane and release them into the cytosol for proteasomal degradation. Taken together, these results suggest that the cytosolic region of FcRn is involved in ERAD substrate binding and this interaction is critical for the Derlin-1-mediated dislocation of the FcRn to the cytosol during US11-induced FcRn degradation.

HCMV US11 has been shown to hijack the similar ERAD system to degrade MHC class I, thus preventing CD8⁺ T cells recognition of infected cells (285, 286). However, the discovery of the HCMV US11-mediated FcRn degradation is unexpected since FcRn protein has only limited homology with MHC-I molecules. Interestingly, US11 also utilizes a similar ERAD system to degrade MHC-I, which US11 binds to the MHC-I HC and Derlin-1 via its ER luminal domain and transmembrane domain, respectively (177, 178) and ubiquitinate MHC-I molecules for degradation by TMEM129 (184). The last two amino acids (valine or alanine) located at the C-terminus of the MHC-I molecules are conserved (176) and may be the target of Derlin-1 recognition (179). However, some differences also exist, for example, either US2 (289) or US11 is sufficient to induce the rapid degradation of newly synthesized

MHC-I. In contrast, we find HCMV US2 fails to cause FcRn degradation in our study. Perhaps MHC-I molecules are highly polymorphic, and HCMV is likely to use a “backup” immune-modulating protein to degrade MHC-I molecules. In contrast, FcRn is relatively non-polymorphic. Most surprisingly, HCMV employs a single US11 protein-mediated ERAD degradation system evades both cellular and antibody-mediated immunity, this may be due to HCMV encoding a limited number of immune evasion proteins.

Several questions remain and need further investigation. First, the role of ubiquitin in US11-induced FcRn degradation remains unknown. Human FcRn has one lysine residue in its cytoplasmic tail (33); whether this lysine residue is critical for FcRn ubiquitination or whether a major fraction of cytosolic FcRn HC that accumulates in the presence of proteasome inhibitors is an ubiquitinated form merit further investigation. If it is not, it should also not be surprised. Ubiquitin can be conjugated to nonlysine residues, including serine, threonine, or cysteine residues in the cytoplasmic tail and the protein N terminus (182). Both serine, threonine residues also appear in the cytoplasmic tail of FcRn (33), hence, FcRn tail seems to contain multiple potential ubiquitin acceptor sites. In addition, TMEM129 has an atypical RING-C2 domain and US11 is able to degrade a “lysine-less” MHC-I molecules (166), hence, TMEM129-dependent ubiquitination of FcRn HC might proceed on a combination of lysine and nonlysine residues, consistent with the detection of TMEM129’s cognate E2, Ube2J2, which is also recruited by the MHV γ 68 mK3 viral E3 ligase for ubiquitination of MHC-I on nonlysine residues (252). Secondly, is the US11 per se targeted by TMEM129 for the ubiquitination and degradation? It is shown that TMEM129 is unable to ubiquitinate US11 (184). In contrast, the HRD1/SEL1L complex mediates US11 degradation (245). Thirdly, HCMV US11 inhibits intracellular trafficking of FcRn leading to decreased reduced IgG transcytosis and increases IgG catabolism. The increase in IgG catabolism will reduce the levels of virus-neutralizing antibodies; the decrease in IgG transcytosis will lessen

the seeding of maternal and mucosal immunity. These mechanisms cannot be tested in vivo because HCMV is highly species specific and no animal model is available. However, CMV infects mouse or guinea pig; it is interesting to know whether these CMVs cause FcRn degradation in these species. Fourthly, it is reported that approximately 50% of rhesus macaques vaccinated with rhesus cytomegalovirus (RhCMV) vectors expressing SIV protein shows a durable control of infection with the highly pathogenic strain SIVmac239 (290). This seems paradoxical based on HCMV US11's potent ability to reduce MHC-I levels and alter antigen presentation and to block FcRn functions. However, in the context of RhCMV, it remains to know whether RhCMV US11 has the reciprocal function of HCMV US11. Lastly, the FcRn function is an important factor in autoimmune diseases (58) because the half-life of autoimmune IgG prolongs. From this view, the HCMV US11 might benefit the individuals by blocking FcRn function and facilitate the destruction of autoimmune IgG. Our findings may offer a new strategy for treating Ab-mediated autoimmune diseases.

In conclusion, we define a novel function and mechanism by which US11 suppresses antibody immunity through preventing normal function of FcRn. Thus, the role of US11 as a cellular immune suppressor may need to be reinterpreted in the light of the fact that US11 also suppresses FcRn-mediated IgG transport and protection. Based on our findings, we propose a working model that explains how HCMV US11 dislocates FcRn HC to the cytosol for proteasomal degradation (Fig. 2.12). In HCMV-infected cells, US11 captures FcRn HC and brings them to Derlin-1 via its direct binding to Derlin-1. During this transition, the C-terminal region of Derlin-1 may recognize and bind tightly to the cytosolic tail of the FcRn HC. The FcRn HC bound to Derlin-1 is then ubiquitinated and dislocated to the cytosol via a TMEM129-mediated mechanism. For dislocation of FcRn HC, the cytoplasmic tail of FcRn may provide a point of contact for the Derlin-1, likely more proteins, in the cytosol to pull out the FcRn HC from the ER membrane. Hence, our characterization of Derlin-1 and TMEM129

as a novel ERAD system of HCMV US11-induced FcRn ubiquitination, dislocation, degradation, therefore, not only uncovers a novel function for ERAD pathway but might help in future understanding HCMV pathogenesis, treating of viral diseases and vaccine design. Because of the HCMV infections in human population and the important role of FcRn in controlling IgG transport and catabolism, this study will have a broad impact on a variety of infectious diseases, autoimmune diseases, cancer immune therapy, and vaccine development.

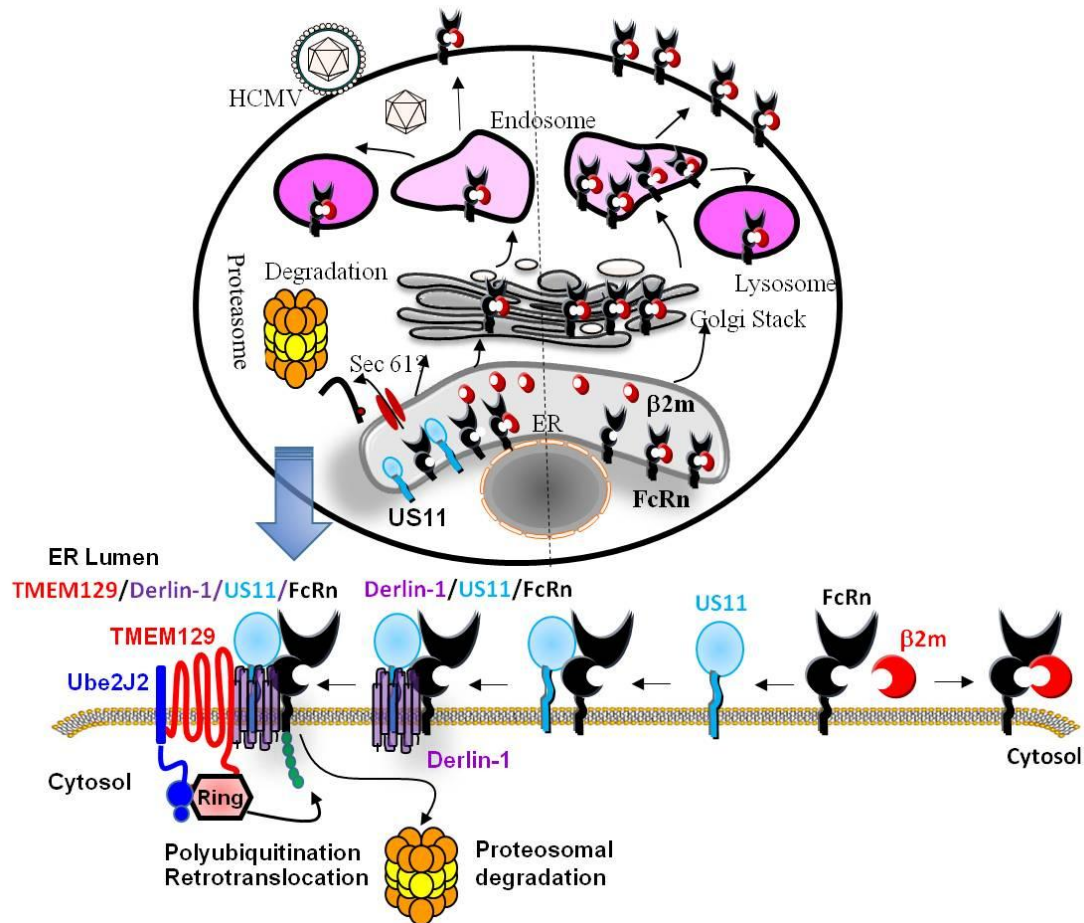


Figure 2.12 Proposed model for US11 interacting with FcRn. In cells without HCMV infection (*right*), FcRn routes to the endosome and reaches the cell surface through the secretory pathway and recycles between the plasma membrane and endosomes via endocytosis. In the presence of HCMV infection or US11 expression (*Left*), a portion of β_2m -free FcRn HC molecules is associated with the US11 in the ER. US11-bound MHC-I is rapidly ubiquitinated by the TMEM129 E3 ligase and subsequently retro-translocated to the cytosol for proteasomal degradation. TMEM129 is recruited to US11 via Derlin-1. The portion of FcRn engaged by US11 is targeted for proteasome degradation by ER ‘dislocation’ mechanism.

Chapter 3: HCMV Fc γ R cooperates with HCMV FcRn-targeting viral protein in facilitating host IgG degradation

Abstract

Human cytomegalovirus (HCMV) is widely spread across the world population. In immunocompromised individuals, HCMV infection poses a life-threatening risk. Moreover, HCMV can transmit across the placenta and is recognized as the leading infectious cause of congenital abnormalities worldwide. Antibody immunity is critical for controlling the HCMV infection and dissemination, However, HCMV has evolved a strategy to evade the antibody immunity by expressing viral Fc γ Rs gp34 and gp68 that can bind IgG and enhance the uptake of IgG via receptor-mediated endocytosis. The neonatal Fc receptor (FcRn), an MHC class I-related host Fc γ R can capture internalized IgG in acidified endosome and salvage IgG away from lysosome degradation. Although HCMV vFc γ Rs have been reported to internalize IgG via endocytosis, whether they facilitate IgG degradation in the presence of FcRn is still unknown. Interestingly, we found that in acidic pH (6.0) condition, the IgG binding capacity of gp34 was largely impaired while the IgG binding capacity of gp68 was not affected. Consequently, in the expression of FcRn, gp34 did not enhance IgG degradation whereas gp68 significantly promoted the IgG degradation. Furthermore, when the FcRn function was interfered by another HCMV viral protein US11, both gp34 and gp68 enhanced IgG degradation in FcRn⁺ cells.

Introduction

Human cytomegalovirus (HCMV), also known as Human herpes-virus 5 (HHV-5), is a member of the human pathogenic β -herpesvirus subfamily of Herpesviridae. HCMV is

widely spread across the world population (95), although infection in immunocompetent individuals is generally asymptomatic. However, both initial and reactivated HCMV infections pose a life-threatening risk in immunocompromised patients, such as organ transplant recipients (91) and HIV-infected patients (93). In addition, due to its ability to transmit across the placenta (128), HCMV is a cause of fetal damage and is the leading infectious cause of congenital abnormalities worldwide (97).

Antibody immunity is critical for controlling the HCMV infection and dissemination, as the viral specific IgG can either directly neutralize the HCMV virions or activate the immune cells, such as Macrophages or NK cells through the surface Fc γ Rs (219, 220). However, latent HCMV has been shown capable of reactivation and super-infection, even in the presence of HCMV-specific IgG (275, 276). Furthermore, HCMV can circumvent neutralizing antibodies (nAb), either by interfering with their binding using a heavily glycosylated viral glycoprotein (221), or by integrating their Fc region into the viral envelope, thus increasing viral binding and infection in Fc γ R-expressing cells (222). Interestingly, HCMV also encodes several viral Fc γ Rs, which may interfere with the Fc γ R-mediated effects by HCMV-specific antibodies (226). Two of the HCMV viral Fc γ Rs are gp34, a 34 kDa receptor encoding by the *RL11* gene (224), and gp68, a 68 kDa receptor encoding by the *UL119-UL118* gene (223). Both of the receptors can bind to human IgG efficiently and compete for IgG binding with host Fc γ Rs (225, 226). HCMV gp34 has a DxxxLL dileucine consensus motif in their cytoplasmic tail, indicating its role in internalizing IgG through the endocytic pathway (224). HCMV gp68 can uptake IgG-IC complex through receptor-mediated endocytosis and route IgG into lysosome for degradation (277). A recent report elucidated that gp34 and gp68 can compete with host Fc γ RIIIA (CD16) for binding to the viral-specific antibody on the cell surface, thus antagonizing the NK cell activation through antibody-dependent cellular cytotoxicity (ADCC) effect (226).

The neonatal Fc receptor (FcRn) is composed of a membrane-bound heavy chain (HC) in non-covalent assembly with a common $\beta 2$ -microglobulin ($\beta 2m$) (13, 15). The narrowed antigen-binding groove precludes the antigen-peptide loading to FcRn, instead, it enables FcRn to bind IgG (16, 17). FcRn binds IgG antibodies in a pH-dependent manner, binding to the Fc-region of IgG at acidic pH (< 6.5) and releasing IgG at neutral or higher pH (25, 26). In the majority of cell types, FcRn primarily resides in the early endosomal vesicles, where the acidic pH environment allows FcRn to capture IgG that enters the cell by pinocytosis or endocytosis (28). FcRn recycles IgG back to the cell surface, where the neutral pH extracellular environment enables FcRn to release IgG. Any internalized IgG that is not salvaged in this manner is efficiently trafficked to the lysosomes for degradation. By this way FcRn protects IgG from degradation and confers IgG a longer half-life (21 days in human) than other proteins in circulation (28, 56) and the major sites for IgG recycling by endogenous FcRn in vivo has been proved to be the endothelial cells (57).

Although HCMV gp34 or gp68 can mediate the IgG internalization into endosomes, previous studies are mostly performed in cells lacking FcRn expression (224, 225). After the viral Fc γ Rs deliver IgG into endosomes, the acidic pH environment may detach IgG from those receptors and the free IgG may be subsequently recycled by the FcRn in endosomes. Therefore, whether those receptors can really enhance IgG degradation in the presence of FcRn is unknown. This needs to be further determined, since HCMV can infect endothelial cells (121, 122) and express gp34 or gp68 to enhance IgG uptake into endothelial cells where FcRn is also expressed and actively salvage the IgG. Moreover, in HCMV-infected cells, viral protein US11 can interfere with FcRn trafficking to endosomes by retaining FcRn in ER (Data shown in Chapter 2). Whether gp34 or gp68 can enhance IgG degradation when FcRn is blocked also needs to be evaluated. In this study, we found that, at acidic pH condition, the

human IgG binding ability of gp34 was impaired while gp68 still efficiently bound human IgG. In FcRn⁺ cells, gp68 enhanced the IgG degradation while gp34 did not. In acidified endosomal compartments, gp34 probably released the internalized IgG, which was further protected by FcRn from lysosome degradation. When the FcRn trafficking to endosome was blocked by viral protein US11, both the gp34 and gp68 enhanced IgG degradation. Our discovery provides new knowledge that the HCMV viral protein US11 cooperates with viral Fc Receptors to enhance IgG degradation to evade antibody immunity.

Materials and Methods

Plasmids, cell lines and antibodies

The encoding DNA sequence for HCMV gp34 or gp68 was amplified by gp34 RT primer pair (5'-ATGCAGACCTACAGCACCCCCCTCAC-3' and 5'-TTACTGTAAATCCCCGTCCACCGTCAAC-3') or gp68 RT primer pair (5'-ATGTGTTCCGTACTGGCGATCGCGC-3' and 5'-CTACCATGCTTGAAGTAGGGCACC-3') from the cDNA of HCMV AD169-infected MRC-5 cells (Chapter 2. Materials and Methods). To construct the plasmid pSecTag2-Myc-gp34 that expresses an N-terminal Myc-tagged gp34 protein, the gp34 cDNA was further amplified by Myc-gp34 primer pair (5'-ACGAAGCTTAGAACAGAACTGATCTCTGAAGAAGACCTGGGTTTCATCGAACGCCGTCGAACC-3' and 5'-CTCCTCGAGTTACTGTAAATCCCCGTCCACCGTCAAC-3') that fused an Myc epitope at the N-terminus of gp34 major peptide and cloned into the pSecTag2/Hygro A (Invitrogen). To construct the plasmid pSecTag2-Myc-gp68 that expresses an N-terminal Myc-tagged gp68 protein, the gp68 cDNA was further amplified by Myc-gp68 primer pair (5'-ACGAAGCTTAGAACAAAACTCATCTCAG

AAGAGGATCTGAGCACCACAAGCGCCGTCCTTC-3' and 5'-CTCCTC
GAGCTACCACTGCTTGAAGTAGGGCAC-3') that fused an Myc epitope at the N-
terminus of gp68 major peptide and cloned into the pSecTag2/Hygro A.

HeLa cell lines were obtained from the American Type Culture Collection (Manassas, VA) and grown in complete DMEM. Complete media were supplemented with 10 mM HEPES, 10% FCS (Sigma-Aldrich), 1% L-glutamine, nonessential amino acids, and 1% penicillin-streptomycin. Cells were grown in 5% CO₂ at 37 °C. The HeLa^{FcRn} cell line stably expressing human FcRn was established as previously described (12) and grown in complete DMEM supplemented with 0.5mg/ml G418 sulfate (KSE scientific). The cell line HeLa^{US11+}^{FcRn} stably expressing human FcRn and HCMV US11 was established as previously described (Chapter 2. Materials and Methods) and grown in complete DMEM medium supplemented with 5 µg/ml Blasticidin (Invitrogen) and 0.5 mg/ml G418 sulfate. HeLa^{FcRn+gp34} cell line stably expressing human FcRn and HCMV US11 was established by the transfection of HeLa^{FcRn} cells with the pSecTag2-Myc-gp34 plasmid, whereas HeLa^{FcRn+gp68} cell line stably expressing human FcRn and HCMV gp68 was established by the transfection of HeLa^{FcRn} cells with the pSecTag2-Myc-gp68 plasmid. HeLa^{FcRn+US11+gp34} cell line stably expressing human FcRn and HCMV US11 was established by the transfection of HeLa^{FcRn+US11} cells with the pSecTag2-Myc-gp34 plasmid, whereas HeLa^{FcRn+US11+gp68} cell line stably expressing human FcRn and HCMV gp68 was established by the transfection of HeLa^{FcRn+US11} cells with the pSecTag2-Myc-gp68 plasmid. After transfection, cells were cultured under 200 µg/ml Hygromycin B (Invitrogen). Surviving cell colonies were detected by immunofluorescence staining using the anti-Myc antibody for gp34 or gp68 expression and cells with high expression homogeneity were selected for subculture. The HeLa^{FcRn+gp34} and HeLa^{FcRn+gp68} cell lines were grown in complete DMEM medium supplemented with 100 µg/ml Hygromycin B and 0.5 mg/ml G418 sulfate. The HeLa^{FcRn+US11+gp34} and HeLa^{FcRn+US11+gp68} cell

lines were grown in complete DMEM medium supplemented with 100 µg/ml Hygromycin B, 10 µg/ml Blasticidin and 0.5mg/ml G418 sulfate.

Rat anti-FLAG epitope (DYKDDDDK) IgG2a (clone L10) was purchased from BioLegend. Mouse anti-Myc epitope (EQKLISEEDL) IgG2a (clone 9B11) was from Cell Signaling. HRP-conjugated goat anti-mouse secondary antibody was purchased from Southern Biotech. Alexa Fluor 488-conjugated goat anti-Rat secondary antibody or Alexa Fluor 555-conjugated goat anti-mouse secondary antibody was purchased from Life Technologies.

Transfection and protein expression

Cells were transfected with recombinant plasmids (described above) along with PolyJet transfection reagent (SignaGen Laboratories, Rockville, MD). Cells were plated 18 to 24 hours prior to transfection. The PolyJet reagent (µL) and the plasmid DNA (µg) were mixed in serum-free DMEM at a ratio of 3: 1. After incubation for 10~15 minutes at room temperature, PolyJet/DNA mixture was dropped onto the medium and homogenize by gently swirling the cell culture plate. PolyJet/DNA complex-containing medium was replaced with fresh complete medium 12~18 hours post transfection. The transfection efficiency was examined by immunofluorescence or Western blot 24 to 48 hours post transfection.

Confocal immunofluorescence

Immunofluorescence was performed as previously described (Ye L, 2008). Briefly, cells were cultivated on coverslips for 24 hr. Subsequent procedures were done at room temperature. The cells were rinsed with PBS, cold fixed in 4% paraformaldehyde (Sigma-Aldrich) in PBS for 20 min, and quenched with glycine for 10 min. After two washes with

PBS, the coverslips were permeabilized in solution (PBS containing 0.2% Triton X-100) for 5 min and then blocked with blocking buffer containing 3% normal goat serum (NGS) for 30 min. 1 µg of first antibodies Rat anti-FLAG or Mouse anti-Myc were diluted in 200 µl blocking buffer were added onto the coverslips and incubated for 2 hr at room temperature. Cells were then incubated with Alexa Fluor 488-conjugated goat anti-Rat secondary antibody or Alexa Fluor 555-conjugated goat anti-mouse secondary antibody in blocking buffer. Cells were also stained by DAPI (4',6-Diamidino-2-Phenylindole, Dihydrochloride) for cell nucleus for 15 mins. After each step, cells were washed three times with 0.1% Tween 20 in PBS. Coverslips were mounted on slides with the ProLong antifade kit (Molecular Probes) and examined using a Zeiss LSM 510 confocal fluorescence microscope. Images were processed using LSM Image Examiner software (Zeiss).

Gel electrophoresis and Western blotting

Cell lines and transfectants were lysed in PBS with 0.5% CHAPS and protease inhibitor cocktail III. Protein concentrations were determined as described previously. The lysates were boiled with Laemmli Sample buffer at 95 °C and resolved on a 12% SDS-PAGE gel under reducing conditions. Proteins were transferred onto a nitrocellulose membrane (Schleicher & Schuell, Keene, NH, USA). All blocking, incubation and washing were performed in 5% non-fat milk and 0.05% Tween 20 in PBS). The membranes were blocked, probed separately with specific primary antibody overnight at 4 °C, washed, and then probed with HRP-conjugated secondary antibody for 2 hours. Proteins were visualized using SuperSignal West Pico Chemiluminescent Reagent (Thermo Scientific). Chemiluminescence signal acquisition was conducted using the Image Lab, version 5.2 in a Chemi-Doc XRS imaging system (Bio-Rad Laboratories, Hercules, CA).

IgG binding Assay

A human IgG binding assay was performed as previously described (80). Cells were lysed in PBS (pH 6.0 or 7.4) with 0.5% CHAPS (Sigma-Aldrich) and protease inhibitor cocktail III (Calbiochem) mixture on ice for 1-2 hr. Post-nuclear supernatants containing 0.5 – 1 mg of soluble proteins were incubated with human IgG-Sepharose (Rockland Immunochemicals) at 4 °C overnight. Unbound proteins were washed off with PBS (pH 6.0 or 7.4) containing 0.5% CHAPS. Adsorbed proteins were eluted by boiling in Laemmli Sample buffer at 95 °C for 15 min. The eluted fractions were subjected to Western blot analysis as described above.

In vitro human IgG protection

To perform the human IgG protection assay, stable cell lines HeLa^{FcRn}, HeLa^{FcRn+gp34}, HeLa^{FcRn+gp68} or HeLa^{FcRn+US11}, HeLa^{FcRn+US11+gp34}, HeLa^{FcRn+US11+gp68} (10⁶) were cultured in 2ml complete medium that contains 5% FBS with ultra-low IgG. Those cells were then incubated the complete medium supplemented with 50 µg/ml human IgG for 48 hours. During this incubation, the supernatant medium was sampled at 0, 12, 24, 36, 48 hr time point and the IgG concentration in each medium sample was measured by ELISA.

Enzyme-linked immunosorbent assay (ELISA)

Human IgG was quantified using ELISA (Bethyl Laboratories, Montgomery, TX). ELISA plates (Nunc) were coated with 10 µg/ml goat anti-human IgG-Fc Ab overnight at 4 °C. Plates were washed three times with PBST (0.05% Tween 20 in PBS) and then blocked with 10% FBS in PBS for 1 hr at room temperature. Plates were washed with PBST three times and incubated with either an IgG standard or the transcytosis samples diluted in 10%

FBS for 2 hr at 25°C. Plates were washed for five times with PBST and incubated with 0.1 µg/ml HRP-conjugated goat anti-human IgG-Fc Ab for 1 hr. After plates were washed with PBST seven times, we added the substrates tetramethylbenzidine and hydrogen peroxide to initiate a reaction. 1M sulphuric acid was added to stop the reaction. The colorimetric reaction was read at 450 nm using a Victor III microplate reader (Perkin Elmer).

Results

HCMV vFcRγs gp34 and gp68 colocalization with FcRn in the endosomes.

After the HCMV vFcRγs gp68 and gp34 bind the human IgG on the cell surface, they can internalize the IgG. The cytoplasmic tail of gp34 contains a DxxxLL dileucine consensus motif indicating a potential function in intracellular targeting of the protein to endocytic route (223,224). And gp68 has been reported to mediate endocytosis to transports antigen-bound IgG complexes into lysosome (277). To study the intracellular expression patterns of HCMV vFcRγs gp34 and gp68, we transfected the HeLa^{FcRn} cells with plasmid encoding myc-tagged gp34 or myc-tagged gp68 cDNA respectively. We found that the expressed gp34 and gp68 proteins showed a punctuate staining pattern that colocalized with the FcRn in HeLa^{FcRn} cells (Fig. 3.1A, *top* and B, *top*). As the majority of FcRn resides in acidic endosomes compartments (28), the colocalization of gp34 and gp68 with the FcRn indicates those viral Fc receptors are sorted into the endosomes vesicles after internalized from the cell surface. However, in the presence of US11 expression, the distribution pattern of FcRn appears as honeycomb with rare colocalization with gp34 and gp68 (Fig. 3.1A, *bottom* and B, *bottom*). This is consistent with previous data that US11 impairs FcRn trafficking into endosomes by retaining FcRn in ER (Data in Chapter 2). These data confirmed previous discovery that gp34 and gp68 can internalize the IgG from the cell surface into the endosomes vesicles.

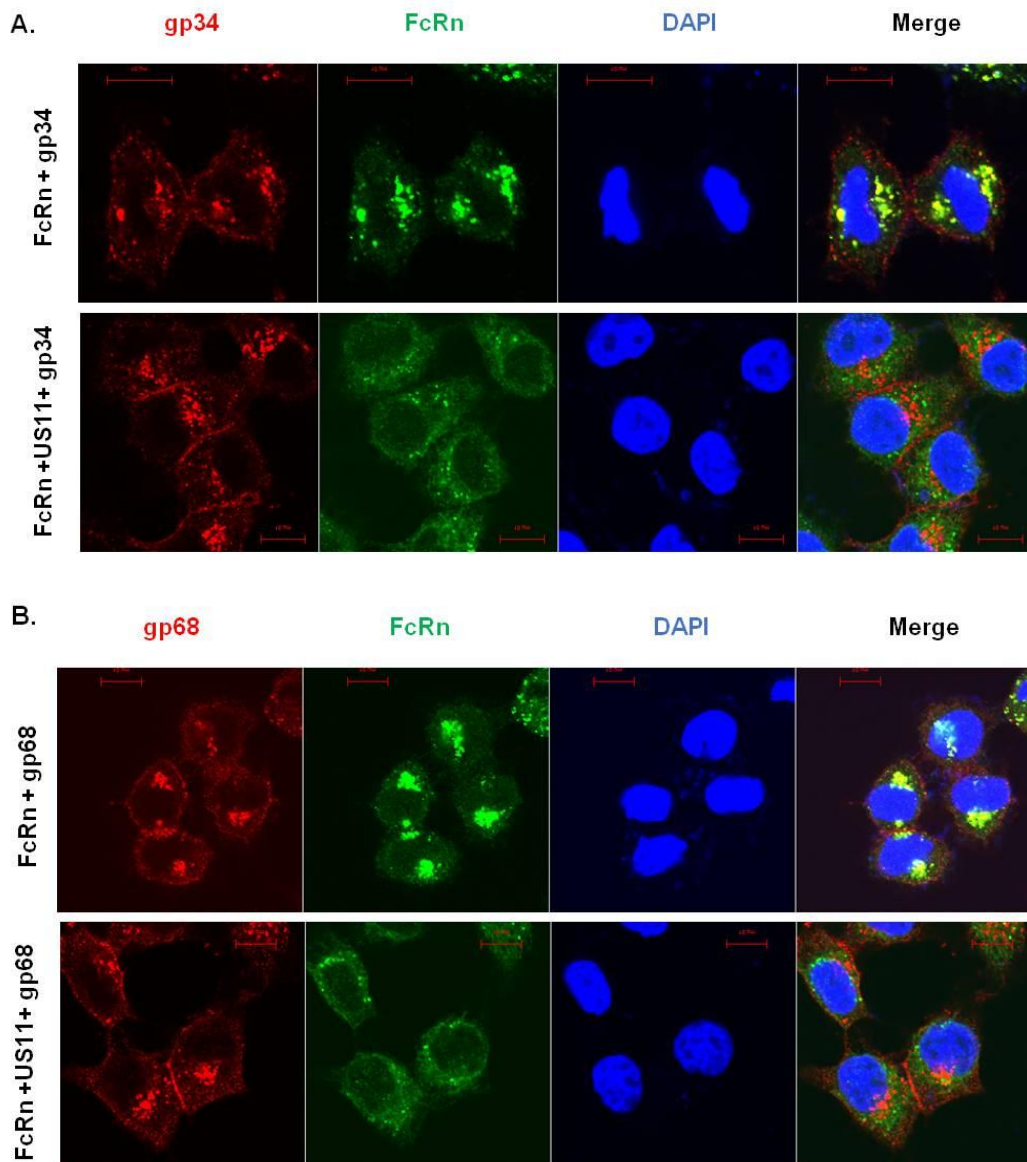


Figure 3.1. Intracellular staining pattern of gp68 and gp34. Immunofluorescence staining for the expression patterns of HCMV gp34 and FcRn in the HeLa^{FcRn} (gp34) cells (**A, top**) and HeLa^{FcRn+US11} (gp34) cells (**A, bottom**). Immunofluorescence staining for the expression patterns of HCMV gp68 and FcRn in the HeLa^{FcRn} (gp68) cells (**B, top**) and HeLa^{FcRn+US11} (gp68) cells (**B, bottom**). HeLa^{FcRn} (gp34) cells or HeLa^{FcRn} (gp68) cells are HeLa^{FcRn} cells transfected with plasmid pSecTag2-Myc-gp34 or plasmid pSecTag2-Myc-gp68. HeLa^{FcRn+US11} (gp34) cells or HeLa^{FcRn+US11} (gp68) cells are HeLa^{FcRn+US11} cells transfected with plasmid pSecTag2-Myc-gp34 or plasmid pSecTag2-Myc-gp68. Cells grown on coverslips were fixed with 4% paraformaldehyde and permeabilized in 0.2% Triton X-100. Subsequently, the cells were incubated with affinity-purified anti-Myc (gp34 or gp68) or anti-FLAG (FcRn) specific mAb, followed by Alexa Fluoro 555- or 488-conjugated IgG. Puncta that appear yellow in the merged images (*right panel*) indicate colocalization of FcRn with gp34 or gp68 proteins. The nuclei were stained with DAPI (blue). Scale bar represents 10 μ m.

The human IgG binding capacity of gp34 but not gp68 significantly decreases in acidic pH condition

After entering the endosome, gp68 continues to route the IgG into lysosome, as the gp68 binds IgG very stably from pH 5.6 to pH 8.1 (225). To verify whether HCMV vFcγR gp34 can still bind IgG or not in the acidic pH condition in endosome compartment, we performed IgG binding assay for gp34 and gp68 proteins at either acidic pH (6.0) or neutral pH(7.4). At pH 7.4, both gp34 and gp68 bound efficiently to human IgG, as very large amounts of those proteins were eluted from human IgG-sepharose after the binding assay (Fig. 3.2A, *lane 4 and Fig. 3.2B, lane 4*). However, at pH 6.0, the amount of gp34 proteins eluted from the IgG-sepharose was remarkably reduced compared to that at pH 7.4 (Fig. 3.2A, *lane 3 and 4*), indicating that the IgG binding capacity of gp34 was significantly impaired in the acidic pH environment. In contrast, the amount of gp68 proteins eluted from the IgG-sepharose was not significantly changed between the pH 6.0 and pH 7.4 (Fig. 3.2B, *lane 3 and 4*), consistent with previous discovery that gp68-IgG complex is stable at acidic pH (225). Therefore, after internalizing IgG into endosomes, gp34 is very likely to release the IgG in the acidic environment in endosome vesicles, and the free IgG in endosome may be recycled in the presence of FcRn. In contrast, gp68 can still bind IgG in the acidic endosome vesicles and sort IgG according to its own trafficking pathway.

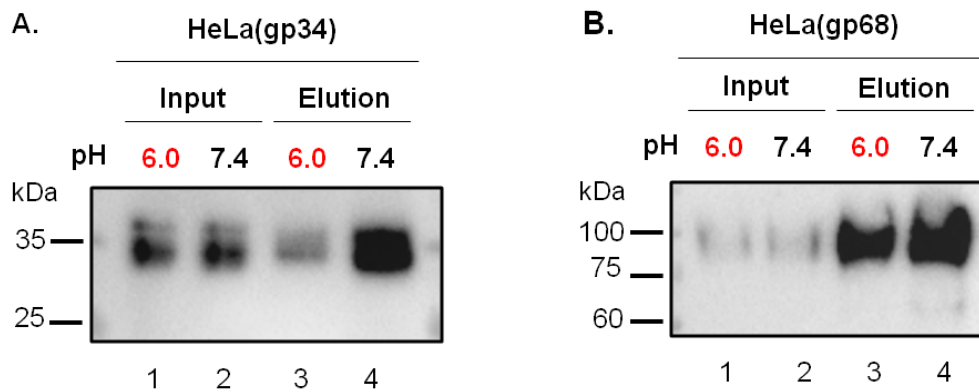


Figure 3.2. The human IgG binding capacity of gp34 but not gp68 significantly decreases in acidic pH condition. HeLa (gp34) cells or HeLa (gp68) cells were from HeLa cells transfected with either pSecTag2-Myc-gp34 plasmid or pSecTag2-Myc-gp68 plasmid. HeLa (gp34) cells expressing myc-tagged gp34 (**A**) or HeLa (gp68) cells expressing myc-tagged gp68 (**B**) were lysed in sodium phosphate buffer pH 6.0 or pH 7.4 with 0.5% CHAPS and fresh proteinase inhibitors. From each cell lysate, approximately 0.5 mg of the soluble proteins were incubated with human IgG-Sepharose at 4 °C. Unbound proteins were washed off with PBS (pH6.0 or pH 7.4) containing 0.5% CHAPS. Human IgG-Sepharose adsorbed proteins were eluted by Laemmli Sample buffer at 95 °C for 15 mins. The eluted proteins were subjected to Western blotting analysis with mouse anti-Myc specific antibody. Cell lysate from each sample with an equal amount of total protein was also tested by WB by Myc antibody.

HCMV gp34 and gp68 enhance IgG degradation when FcRn is blocked by US11 expression

To test whether gp34 and gp68 can enhance the IgG degradation in the presence of FcRn expression. We construct the stable cell line HeLa^{FcRn+gp34} expressing the gp34 and FcRn proteins and the stable cell line HeLa^{FcRn+gp68} expressing the gp68 and FcRn proteins. HeLa^{FcRn} (as control), HeLa^{FcRn+gp34} cells and HeLa^{FcRn+gp68} cells were incubated with human IgG respectively. The IgG concentration in the supernatant medium from the cell culture were subsequently measured by ELISA at indicated time points (Fig. 3.3A). After 48 hours incubation, IgG concentration was significantly reduced in the medium from the HeLa^{FcRn+gp68} cells in comparison with that from HeLa^{FcRn} cells (Fig. 3.3B). In contrast, IgG concentration in the medium from the HeLa^{FcRn+gp34} showed no significant changes and comparable to that from HeLa^{FcRn} cells (Fig. 3.3B). This result indicates that in the presence of FcRn, gp68 enhances IgG degradation whereas gp34 does not. This may be explained by our previous data that the acidic pH in endosomes impairs gp34 IgG binding capacity. The internalized IgG by gp34 is released in endosomes and subsequently recycled by FcRn to cell surface instead of being sorted into lysosome for degradation. Whereas gp68 binds IgG very stably at acidic pH (225) and is still able to deliver IgG into lysosome even in the presence of FcRn expression.

In HCMV infection, the viral protein US11 can interfere with FcRn function by retaining FcRn in the ER and blocking FcRn trafficking to endosomes (data in Chapter 2). We hypothesized that in the presence of US11, the IgG internalized into endosomes by gp34 is not be salvaged by FcRn, but delivered into lysosome for degradation. Therefore, to test whether gp34 can enhance the IgG degradation or not when FcRn is blocked by HCMV protein US11, we constructed the stable cell line HeLa^{FcRn+US11+gp34} expressing the gp34, US11 and FcRn proteins and the stable cell line HeLa^{FcRn+US11+gp68} expressing the gp68, US11 and FcRn proteins. HeLa^{FcRn+US11} (as control), HeLa^{FcRn+US11+gp34} cells and HeLa^{FcRn+US11+gp68} cells were incubated with human IgG respectively. The IgG concentration in the supernatant medium from the cell culture were subsequently measured by ELISA at indicated time points (Fig 3.3C). After 48 hours incubation, IgG concentrations in the medium from both the HeLa^{FcRn+US11+gp34} cells and HeLa^{FcRn+US11+gp68} cells were significantly decreased in comparison with that from HeLa^{FcRn+US11} cells (Fig 3.3 D), and the IgG decrease in in the medium from the HeLa^{FcRn+US11+gp34} showed equal level to that from HeLa^{FcRn+US11+gp68} cells (Fig 3.3 D). Thus, we conclude that both the gp34 and gp68 receptor can efficiently enhance the IgG degradation when FcRn function is blocked by the expression of HCMV protein US11.

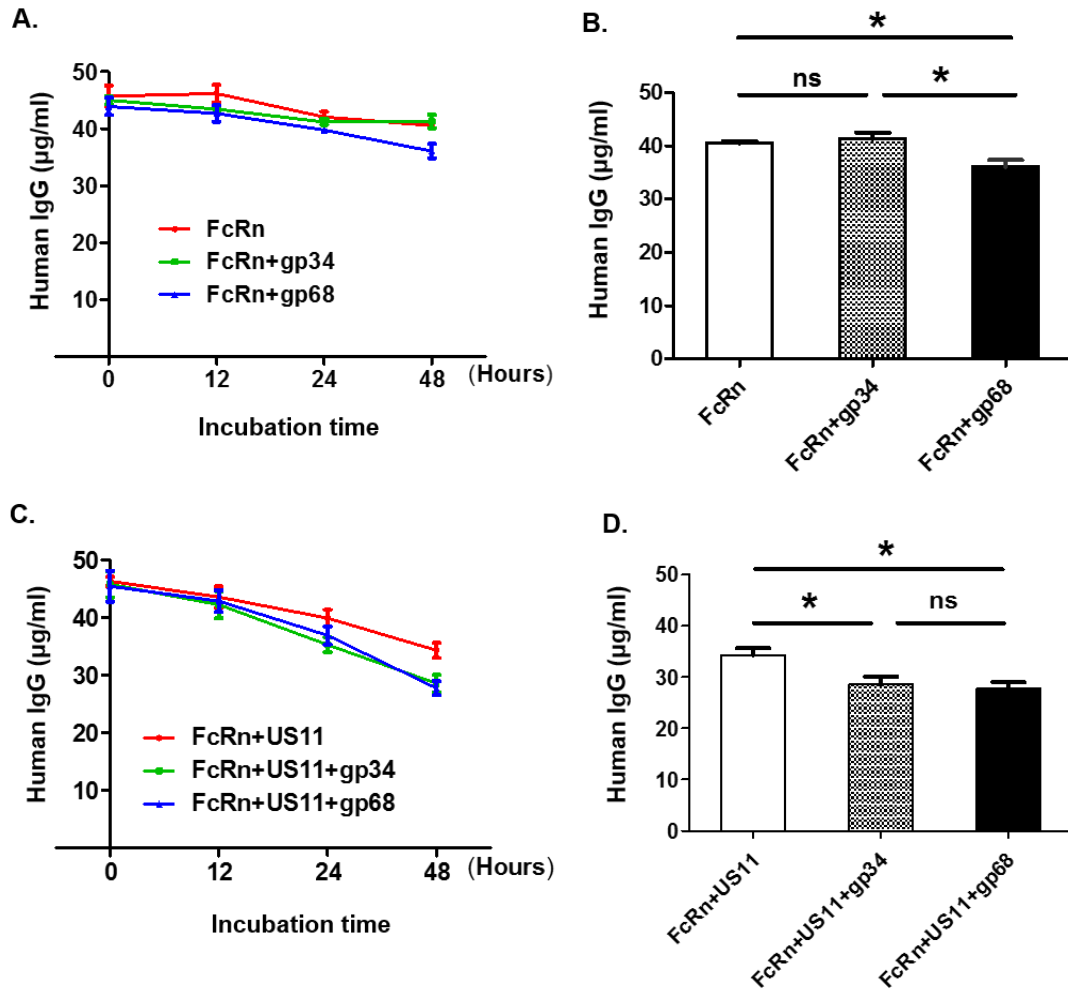


Figure 3.3 HCMV gp34 and gp68 enhance IgG degradation when FcRn is blocked by US11 expression.

HeLa^{FcRn} cells, HeLa^{FcRn+gp34} cells and HeLa^{FcRn+gp68} cells ($10^6/2$ ml) respectively were grown in the complete medium with 5% FBS with ultra-low IgG, which were then supplemented with 50 µg/ml human IgG for 48 hours incubation. During this incubation, the supernant medium was sampled at 0, 12, 24, 36, 48 hr and the IgG concentration in each medium sample was measured by ELISA (A). At 48 hr, the IgG concentration in the medium from the HeLa^{FcRn} cells, HeLa^{FcRn+gp34} cells and HeLa^{FcRn+gp68} cells were compared by t-test analysis (B). HeLa^{FcRn+US11} cells, HeLa^{FcRn+US11+gp34} cells and HeLa^{FcRn+US11+gp68} cells ($10^6/2$ ml) were grown in the complete medium with 5% FBS with ultra-low IgG, which were then supplemented with 50 µg/ml human IgG for 48 hours incubation. During this incubation, the supernant medium was sampled at 0, 12, 24, 36, 48 hr and the IgG concentration in each medium sample was measured by ELISA (C). At 48 hr, the IgG concentration in the medium from the HeLa^{FcRn+US11} cells, HeLa^{FcRn+US11+gp34} cells and HeLa^{FcRn+US11+gp68} cells were compared by t-test analysis (D). All the ELISA analyses were performed in triplicate. Ns denotes no statistical significance. Star denotes statistical significance. * P < 0.05.

Discussion

HCMV has evolved strategies to evade the antibody immunity. One strategy is to express viral Fc γ Rs that can bind IgG antibodies as efficiently as host Fc γ Rs (223, 225). However, those viral Fc γ Rs cannot activate immune response as their host counterparts, instead they can enhance the IgG degradation through the receptor-mediated endocytosis (277). The MHC-I related molecule, FcRn can efficiently bind IgG at acidic pH condition and mainly resides in early endosomes vesicle in most cell types (25, 26). In the acidified endosomes, FcRn can capture IgG internalized via pinocytosis or endocytosis and salvage IgG from lysosome degradation by recycling IgG back to cell surface (28, 56). In our study, we found that HCMV viral Fc γ R gp68 but not gp34 can facilitate IgG degradation in FcRn⁺ cells (Fig 3. 3 A and B). However, when the FcRn function is blocked by viral protein US11, both gp34 and gp68 can significantly enhance the IgG degradation in FcRn⁺ cells (Fig 3. 3 C and D).

HCMV gp34 has an endocytic motif in its cytoplasmic tail for endocytosis and gp68 has been reported to deliver the IgG-IC complex into lysosome through receptor-mediated endocytosis (277). We verified the internalization of gp34 and gp68 into endosomes, as both of those receptors colocalized with FcRn which mainly resides in endosome vesicles (Fig 3. 1). After IgG is uptaken by viral Fc γ Rs into endosomes, the acidic pH environment may impair the stability of IgG-vFc γ Rs complex and detaches IgG from those vFc γ Rs as it does to the host Fc γ Rs (58). According to our data, gp34 showed impaired IgG binding capacity at acidic pH and most of the IgG bound to gp34 was released at pH 6.0 (Fig 3. 2 A). In contrast, the IgG binding capacity for gp68 was very stable in acidic pH and gp68 can still efficiently bind IgG at pH 6.0 (Fig 3.2 B). Therefore, we speculate that IgG internalized by gp34 is released in acidified endosome and captured by FcRn which protects IgG from further

lysosome degradation. However, gp68 can bind IgG very tightly at acidified endosome environment and thus continually route the IgG to lysosome for degradation. Consistent with our hypothesis, gp34 did not significantly enhance IgG degradation in FcRn⁺ cells while gp68 promoted the IgG degradation even in the presence of FcRn (Fig 3.3 A and B).

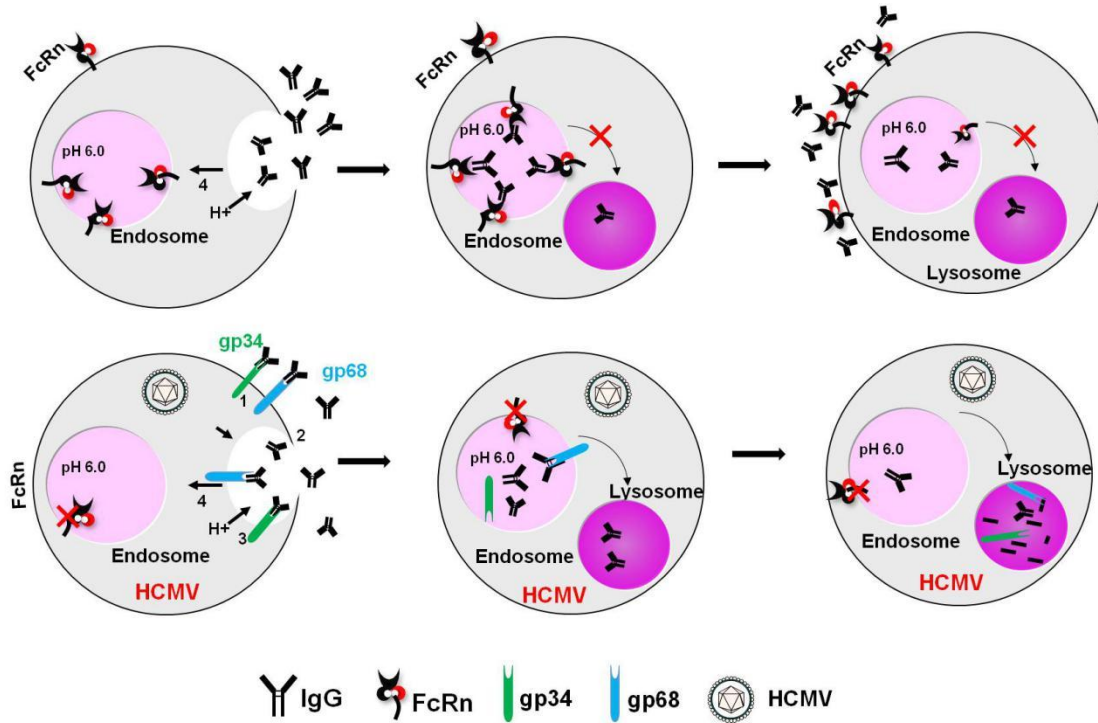


Figure 3.4 Proposed role of HCMV Fc γ Rs in IgG evasion in cooperation of HCMV FcRn-targeting viral proteins. In uninfected cells, IgG that enters the endosome through pinocytosis will be captured by FcRn and recycled back to cell surface, precluding IgG degradation in lysosome. In HCMV-infected cells, when FcRn will be retained in ER and degraded by US11, both of the vFc γ Rs gp34 and gp68 can mediated the IgG internalization via receptor-mediated endocytosis and facilitate IgG degradation in lysosome.

In the context of HCMV infection, the expression of viral protein US11 can interfere with FcRn trafficking into endosomes by retaining FcRn in the ER (Data shown in Chapter 2). After the expression of US11 in FcRn⁺ cells, both the viral Fc γ Rs gp34 and gp68 can significantly enhance the IgG degradation (Fig 3.3C and D). As the IgG that is internalized and released into endosome by gp34 is not salvaged when FcRn is blocked by viral protein

US11, the free IgG in endosome is delivered into lysosome for degradation (28). In uninfected cells, IgG that enters the endosome through pinocytosis is captured by FcRn and recycled back to cell surface, precluding IgG degradation in lysosome (Fig 3.4 *top*). In HCMV-infected cells, the FcRn is retained in ER and degraded by US11 (Fig 3.4 *bottom*). Although both of vFcγRs gp34 and gp68 can mediate the IgG internalization via receptor-mediated endocytosis, those two receptors utilize different pathway to facilitate IgG degradation (Fig 3.4 *bottom*). The vFcγRs gp34 releases the internalized IgG in the acidic pH condition in endosome vesicles, thus requiring the cooperation of viral protein US11 to block FcRn function to facilitate IgG lysosome degradation. In contrast, vFcγRs gp68 can efficiently bind IgG even in the acidified endosome environment and can directly deliver IgG into lysosome. Therefore gp68-mediated degradation of IgG does not rely on the inhibition of FcRn by US11 protein.

Chapter 4: Conclusion and Perspective

Human cytomegalovirus (HCMV) is widely spread across the world population (95). Although HCMV infection in immunocompetent individuals is generally asymptomatic, it poses a life-threatening risk in immunocompromised individuals (96), such as organ transplant recipients and HIV-infected patients. Moreover, due to its ability to transmit across placenta, HCMV causes congenital infection in fetus and is believed to be the leading infectious cause of congenital abnormalities worldwide (97). So far, the major drugs for treating HCMV infection are too toxic for fetus and no HCMV vaccine appears to be approaching the clinical licensure (91, 92). The major reason for HCMV persistence in human population is that this virus has evolved sophisticated strategies for evading immune system. It is known that HCMV encodes multiple proteins to interfere with classical and non-classical MHC-I molecules, thus impairing the CD8⁺ T and NK cells-mediated cellular immunity (155). Moreover, HCMV also expresses several viral FcγRs to counteract with the host FcγRs and inhibit the effects of antibody mediated-immunity (226).

FcRn is a non-classical MHC-I molecule and can efficiently bind IgG at acidic pH condition (pH<6.5) (26). In the majority of cell types, FcRn mainly resides in early endosomes, where the acidic pH environment allows FcRn to capture IgG internalized by pinocytosis or endocytosis (28) and recycle IgG to the cell surface. By this way, FcRn can transport IgG across the mucosal barriers and confers IgG a longer half-life in circulation by the salvage of endocytosed IgG from lysosome degradation. Overall, FcRn plays an important role in antibody-mediated immunity.

In this study (Chapter 2), we discovered that HCMV protein US11 can specifically interact with FcRn in both virally-infected and US11-expressing cells. US11 selectively

inhibits the assembly of FcRn with β_2m subunit and retains FcRn in the ER, consequently blocking FcRn intracellular sorting to the endosome. Furthermore, US11 recruits Derlin-1, a transmembrane dislocon, as well as TMEM129, an ER-resident E3 ubiquitin ligase, to form a complex with FcRn. This initiates the dislocation of FcRn from the ER to the cytosol and facilitates its degradation in an ubiquitination and proteasome-dependent manner. The interaction between FcRn cytosolic tail and Derlin-1 was shown to be necessary for US11-mediated degradation of FcRn. Because FcRn is widely expressed in the same cell types capable of supporting HCMV infection, including epithelial, endothelial, macrophage and dendritic cells, we found that either HCMV infection or recombinant US11 expression in these cells inhibited pH-dependent IgG-FcRn binding. Importantly, this significantly inhibits human IgG transcytosis across polarized human intestinal epithelial cells Caco-2 and placenta trophoblast cells BeWo monolayerlining, leading to considerable IgG degradation inside vascular endothelial cells HMEC-1. Hence, our results reveal that HCMV infection exploits a Derlin-1/TMEM129 pathway through US11 to disable FcRn. Because FcRn is vital to IgG transport and homeostasis, these results proposes a new mechanism for viral evasion against antibody immunity via the interference with the expression and trafficking of FcRn molecule and will have a broad impact on the development of new therapies or vaccines against HCMV.

Nevertheless, several interesting questions still remain to be solved. Firstly, apart from US11, are there any other HCMV proteins targeting FcRn? HCMV encodes redundant proteins to target and interfere with the classical and non-classical MHC-I molecules. Specifically, HCMV utilizes several viral proteins, such as US2 (161), US3 (158), US6 (186) and US11 (174) to interfere with the expression, assembly and trafficking of MHC-I, and also employs viral proteins UL16 (205), UL142 (212), US18, US20 (214) and even microRNA (miR)-UL112 (213) to downregulate the expression of non-classical MHC-I molecules,

NKG2D ligands (155). Therefore, it is reasonable to speculate that HCMV may also utilize more than one protein to inhibit FcRn function. To solve this question, mass spectrometry analysis is needed to compare the proteins precipitated by FcRn from HCMV-infected and Mock-infected cells. To test the potential involvement of microRNAs in FcRn downregulation, FcRn mRNA levels in the expression of all 30 HCMV microRNA species (278) should be monitored. Secondly, although our data showed the ER luminal domain of US11 interacts with the extracellular domain of FcRn, the key amino acid residues that mediate their interaction remain unknown. Surprisingly, the exact residues for the US11 binding to the classical MHC-I is still not identified (175,176), despite the fact that the interaction of US11 with MHC-I has been discovered for decades. Are the amino acid residues for US11 binding to MHC-I different from those binding to FcRn? Therefore, it is interesting to explore the US11-binding sites for both the MHC-I and FcRn molecules probably through site-directed mutagenesis. Thirdly, the deletion of FcRn tail significantly impairs the interaction of FcRn with derlin-1 in the presence of US11, suggesting that the cytoplasmic tail is the site for FcRn to engage derlin-1. However, the sites in the Derlin-1 molecule involved in the engagement of FcRn cytoplasmic tail is not determined, as Derlin-1 is a multi-transmembrane protein that has two cytoplasmic tails at the C-terminus and the N-terminus. Mutagenesis at the C-terminal or N-terminal sequence of Derlin-1 will provide answer for this question. Fourthly, since ubiquitination is a key step for US11-mediated FcRn and degradation by proteasome, the ubiquitin acceptor sites for FcRn needs further identification. The cytoplasmic tail of FcRn is the putative site targeted by the E3 ligase TMEM129, as the catalytic ring domain of TMEM129 is in the ER cytosol side (183,184). There is only one lysine residue in FcRn cytoplasmic tail, however, nonlysine residues, including serine/threonine and cysteine are also potential sites for ubiquitination, as reported in MHC-I ubiquitination (182). Thus, those nonlysine residues should also be considered in the screening for ubiquitination sites of FcRn.

Recently, there are numerous attempts to interfere with FcRn function so as to modulate the self-specific IgG level for the treatment of autoimmune diseases, such as myasthenia gravis, rheumatoid arthritis and systemic lupus, since FcRn can prolong the half-life of IgG in circulation (85, 86). HCMV protein US11 is the only currently known viral protein that can negatively regulate FcRn by ER retaining and proteasome degradation. Therefore, along with the development and maturation of gene therapy technologies, the delivery and expression of US11 in the autoimmuned individuals will provide a novel strategy for the treatment of autoimmune diseases.

In the second study (Chapter 3), we discovered that HCMV viral Fc γ Rs gp34 cooperates with FcRn-targeting protein US11 to facilitate the IgG degradation, whereas gp68 alone can significantly promote IgG degradation. We found that in acidic pH (6.0) condition, the IgG binding capacity of gp34 was largely impaired while the IgG binding capacity of gp68 was not affected. Consequently, in the expression of FcRn, gp34 did not enhance IgG degradation whereas gp68 significantly promoted the IgG degradation. Furthermore, when the FcRn function was interfered by another HCMV viral protein US11, both gp34 and gp68 enhanced IgG degradation in FcRn⁺ cells. Several questions remain to be solved. First, the intracellular trafficking pathway for IgG internalized by gp34 or gp68 is not elucidated. Does IgG really detach from gp34 and salvaged in the presence of FcRn in early endosome? Does the gp68 stably bind IgG through the endocytic pathway following the sequence from early endosome to late endosome and finally into the lysosome? The survey of the colocalization rate of IgG with endosome or lysosome markers will provide a clearer view on the routing pathway of IgG internalized by those two vFc γ Rs. Secondly, although the gp34 cytoplasmic tail has an endocytic motif DxxxLL (223), gp68 does not contain any canonic sequence for endocytosis in its cytoplasmic tail, such as tyrosine-based NPXY or YXX ϕ

motifs (66) or dileucine-based [DE]XXXL[LI] or DXXLL motifs (68). HCMV gp68 may employ a novel endocytic pathway, which needs further investigation. Thirdly, recently HCMV RL13 and RL12 have been identified as new vFcγRs, which contribute to HCMV antibody evasion (227). It is interesting to investigate whether RL13 and RL12 can enhance IgG degradation in the absence or presence of FcRn.

Bibliography

1. Brambell, F. W., W. A. Hemmings, M. Henderson, and R. A. Kekwick. 1953. Electrophoretic studies of serum proteins of foetal rabbits. *Proc. R. Soc. Lond. B Biol. Sci.* 141: 300–314.
2. Brambell, F. W., W. A. Hemmings, C. L. Oakley, and R. R. Porter. 1960. The relative transmission of the fractions of papain hydrolyzed homologous gammaglobulin from the uterine cavity to the foetal circulation in the rabbit. *Proc. R. Soc. Lond. B Biol. Sci.* 151: 478–482.
3. Brambell, F. W., W. A. Hemmings, and I. G. Morris. 1964. A theoretical model of gamma-globulin catabolism. *Nature* 203: 1352–1354.
4. Brambell, F. W. 1966. The transmission of immunity from mother to young and the catabolism of immunoglobulins. *Lancet* 2: 1087–1093.
5. Simister, N. E., and K. E. Mostov. 1989. An Fc receptor structurally related to MHC class I antigens. *Nature* 337: 184–187.
6. Story, C.M., J.E. Mikulska, and N.E. Simister. 1994. A major histocompatibility complex class I-like Fc receptor cloned from human placenta: possible role in transfer of immunoglobulin G from mother to fetus. *J. Exp. Med.* 180:2377-2381.
7. Kandil, E., M. Egashira, O. Miyoshi, N. Niikawa, T. Ishibashi, and M. Kasahara. 1996. The human gene encoding the heavy chain of the major histocompatibility complex class I-like Fc receptor (FCGRT) maps to 19q13.3. *Cytogenet. Cell Genet.* 73: 97–98.

8. Ahouse, J.J., C.L. Hagerman, P. Mittal, D.J. Gilbert, N.G. Copeland, N.A. Jenkins, and N.E. Simister. 1993. Mouse MHC class I-like Fc receptor encoded outside the MHC. *J Immunol* 151:6076-6088.
9. Hornby, P. J., Cooper, P. R., Kliwinski, C., Ragwan, E., Mabus, J. R., Harman, B., et al. 2014. Human and non-human primate intestinal FcRn expression and immunoglobulin G transcytosis. *Pharm Res* 31(4), 908–922
10. Spiekermann, G.M., P.W. Finn, E.S. Ward, J. Dumont, B.L. Dickinson, R.S. Blumberg, and W.I. Lencer. 2002. Receptor-mediated immunoglobulin G transport across mucosal barriers in adult life: Functional expression of FcRn in the mammalian lung. *Journal of Experimental Medicine* 196:303-310.
11. Borvak, J., Richardson, J., Medesan, C., Antohe, F., Radu, C., Simionescu, M., et al. 1998. Functional expression of the MHC class I-related receptor, FcRn, in endothelial cells of mice. *Int Immunol* 10(9), 1289–1298.
12. Zhu, X., Meng, G., Dickinson, B. L., Li, X., Mizoguchi, E., Miao, L., et al. 2001. MHC class I-related neonatal Fc receptor for IgG is functionally expressed in monocytes, intestinal macrophages, and dendritic cells. *J Immunol* 166(5), 3266–3276
13. Simister, N. E., and K. E. Mostov. 1989. An Fc receptor structurally related to MHC class I antigens. *Nature* 337:184-187.
14. Ghetie, V., and E.S. Ward. 2000. Multiple Roles for the Major Histocompatibility Complex Class I-Related Receptor FcRn. *Annual Review of Immunology* 18:739-766.

15. Burmeister, W.P., L.N. Gastinel, N.E. Simister, M.L. Blum, and P.J. Bjorkman. 1994. Crystal structure at 2.2 Å resolution of the MHC-related neonatal Fc receptor. *Nature* 372:336-343.
16. Plaksin, D., K. Polakova, M.G. Mage, and D.H. Margulies. 1997. Rigidification of the alpha(2) helix of an MHC class I molecule by a valine to proline mutation in position 165 does not prevent peptide-specific antigen presentation. *Journal of Immunology* 159:4408-4414.
17. Sand, K. M. K., Bern, M., Nilsen, J., Noordzij, H. T., Sandlie, I., & Andersen, J. T. 2015. Unraveling the interaction between FcRn and albumin: Opportunities for design of albumin-based therapeutics. *Front Immunol* 5(JANUARY), 1–21.
18. Burmeister WP, Huber AH, Bjorkman PJ. Crystal structure of the complex of rat neonatal Fc receptor with Fc. 1994. *Nature*. 372(6504):379-83.
19. Z.-H. Zeng, A. R. Castano, B. W. Segelke, E. A. Stura, P. A. Peterson, I. A. Wilson. 1997. Crystal structure of mouse CD1: an MHC-like fold with a large hydrophobic binding groove. *Science*: 277:339-345.
20. West, A. P., Jr., and P. J. Bjorkman. 2000. Crystal structure and immunoglobulin G binding properties of the human major histocompatibility complex-related Fc receptor. *Biochemistry* 39: 9698–9708.
21. Wines, B. D., M. S. Powell, P. W. Parren, N. Barnes, and P. M. Hogarth. 2000. The IgG Fc contains distinct Fc receptor (FcR) binding sites: the leukocyte receptors Fc gamma RI and Fc gamma RIIa bind to a region in the Fc distinct from that recognized by neonatal FcR and protein A. *J. Immunol.* 164: 5313– 5318.

22. Raghavan, M., M.Y. Chen, L.N. Gastinel, and P.J. Bjorkman. 1994. Investigation of the interaction between the class I MHC-related Fc receptor and its immunoglobulin G ligand. *Immunity* 1:303-315.
23. Jin-Kyoo Kim, M.F.C.G.R.C.-H.K.V.G.E.S.W. 1999. Mapping the site on human IgG for binding of the MHC class I-related receptor, FcRn. *European Journal of Immunology* 29:2819-2825.
24. Vaughn, D. E., C. M. Milburn, D. M. Penny, W. L. Martin, J. L. Johnson, and P. J. Bjorkman. 1997. Identification of critical IgG binding epitopes on the neonatal Fc receptor. *J Mol Biol* 274:597-607.
25. Raghavan, M., L. N. Gastinel, and P. J. Bjorkman. 1993. The class I major histocompatibility complex related Fc receptor shows pH-dependent stability differences correlating with immunoglobulin binding and release. *Biochemistry* 32:8654-8660.
26. Vaughn, D. E., and P. J. Bjorkman. 1998. Structural basis of pH-dependent antibody binding by the neonatal Fc receptor. *Structure* 6:63-73.
27. Martin, W. L., A. P. West, Jr., L. Gan, and P. J. Bjorkman. 2001. Crystal structure at 2.8 Å of an FcRn/heterodimeric Fc complex: mechanism of pH-dependent binding. *Mol. Cell* 7: 867–877.
28. Roopenian, D. C., and S. Akilesh. 2007. FcRn: the neonatal Fc receptor comes of age. *Nat Rev Immunol* 7:715-725.
29. Gill, R. K., S. Mahmood, C. P. Sodhi, J. P. Nagpaul, and A. Mahmood. 1999. IgG binding and expression of its receptor in rat intestine during postnatal development. *Indian J Biochem Biophys* 36:252-257

30. Kim, J. K., M. F. Tsen, V. Ghetie, and E. S. Ward. 1994. Localization of the site of the murine IgG1 molecule that is involved in binding to the murine intestinal Fc receptor. *Eur J Immunol* 24:2429-2434.
31. Israel, E. J., V. K. Patel, S. F. Taylor, A. Marshak-Rothstein, and N. E. Simister. 1995. Requirement for a beta 2-microglobulin-associated Fc receptor for acquisition of maternal IgG by fetal and neonatal mice. *J Immunol* 154:6246-6251.
32. Palmeira, P., Quinello, C., Silveira-Lessa, A. L., Zago, C. A., & Carneiro-Sampaio, M. 2012. IgG placental transfer in healthy and pathological pregnancies. *Clin Dev Immunol* 2012, 985646
33. Simister, N. E., C. M. Story, H. L. Chen, and J. S. Hunt. 1996. An IgG transporting Fc receptor expressed in the syncytiotrophoblast of human placenta. *Eur J Immunol* 26:1527-1531.
34. Simister, N. E., and C. M. Story. 1997. Human placental Fc receptors and the transmission of antibodies from mother to fetus. *J Reprod Immunol* 37:1-23.
35. Leach, J. L., D. D. Sedmak, J. M. Osborne, B. Rahill, M. D. Lairmore, and C. L. Anderson. 1996. Isolation from human placenta of the IgG transporter, FcRn, and localization to the syncytiotrophoblast: implications for maternal fetal antibody transport. *J Immunol* 157:3317-3322.
36. Simister, N. E. 2003. Placental transport of immunoglobulin G. *Vaccine* 21:3365-3369.
37. Shah U, Dickinson BL, Blumberg RS, Simister NE, Lencer WI, Walker WA. 2003. Distribution of the IgG Fc receptor, FcRn, in the human fetal intestine. *Pediatr Res*. Feb;53(2):295-301.

38. Dickinson, B. L., K. Badizadegan, Z. Wu, J. C. Ahouse, X. Zhu, N. E. Simister, R. S. Blumberg, and W. I. Lencer. 1999. Bidirectional FcR-dependent IgG transport in a polarized human intestinal epithelial cell line. *J Clin Invest* 104:903-911
39. Robert-Guroff, M. 2000. IgG surfaces as an important component in mucosal protection. *Nat. Med.* 6:129–130.
40. Merrill, W.W., G.P. Naegel, J.J. Olchowski, and H.Y. Reynolds. 1985. Immunoglobulin G subclass proteins in serum and lavage fluid of normal subjects. Quantitation and comparison with immunoglobulins A and E. *Am. Rev. Respir. Dis.* 131:584–587.
41. Kitz, R., P. Ahrens, and S. Zielen. 2000. Immunoglobulin levels in bronchoalveolar lavage fluid of children with chronic chest disease. *Pediatr. Pulmonol.* 29:443–451.
42. Groothuis, J.R., E.A. Simoes, M.J. Levin, C.B. Hall, C.E. Long, W.J. Rodriguez, J. Arrobio, H.C. Meissner, D.R. Fulton, R.C. Welliver, et al. 1993. Prophylactic administration of respiratory syncytial virus immune globulin to high-risk infants and young children: the respiratory syncytial virus immune globulin study group. *N. Engl. J. Med.* 329:1524–1530
43. Mascola, J. R., G. Stiegler, T. C. VanCott, H. Katinger, C. B. Carpenter, C. E. Hanson, H. Beary, D. Hayes, S. S. Frankel, D. L. Birx, and M. G. Lewis. 2000. Protection of macaques against vaginal transmission of a pathogenic 165 HIV-1/SIV chimeric virus by passive infusion of neutralizing antibodies. *Nat Med* 6:207-210.
44. Ben Suleiman, Y., M. Yoshida, S. Nishiumi, H. Tanaka, T. Mimura, K. Nobutani, K. Yamamoto, M. Takenaka, A. Aoganghua, I. Miki, et al. 2012. Neonatal Fc

receptor for IgG (FcRn) expressed in the gastric epithelium regulates bacterial infection in mice. *Mucosal Immunol.* 5: 87–98.

45. Armitage, C. W., C. P. O’Meara, M. C. Harvie, P. Timms, R. S. Blumberg, and K. W. Beagley. 2014. Divergent outcomes following transcytosis of IgG targeting intracellular and extracellular chlamydial antigens. *Immunol. Cell Biol.* 92: 417–426

46. Burton, D. R., A. J. Hessel, B. F. Keele, P. J. Klasse, T. A. Ketas, B. Moldt, D. C. Dunlop, P. Poignard, L. A. Doyle, L. Cavacini, et al. 2011. Limited or no protection by weakly or nonneutralizing antibodies against vaginal SHIV challenge of macaques compared with a strongly neutralizing antibody. *Proc. Natl. Acad. Sci. USA* 108: 11181–11186.

47. Yoshida M, Claypool SM, Wagner JS, Mizoguchi E, Mizoguchi A, Roopenian DC, et al. Human neonatal Fc receptor mediates transport of IgG into luminal secretions for delivery of antigens to mucosal dendritic cells. *Immunity.* 2004;20(6):769–83.

48. Yoshida M, Kobayashi K, Kuo TT, et al. Neonatal Fc receptor for IgG regulates mucosal immune responses to luminal bacteria. *J Clin Invest.* 2006;116(8):2142–51.

49. Roopenian, D. C., G. J. Christianson, T. J. Sproule, A. C. Brown, S. Akilesh, N. Jung, S. Petkova, L. Avanesian, E. Y. Choi, D. J. Shaffer, P. A. Eden, and C. L. Anderson. 2003. The MHC class I-like IgG receptor controls perinatal IgG transport, IgG homeostasis, and fate of IgG-Fc-coupled drugs. *J Immunol* 170:3528-3533.

50. Pyzik M, Rath T, Lencer WI, Baker K, Blumberg RS. 2015. FcRn: The architect behind the immune and non-immune functions of IgG and albumin. *J Immunol* 194: 4595-4603.

51. Ghetie, V., J. G. Hubbard, J. K. Kim, M. F. Tsen, Y. Lee, and E. S. Ward. 1996. Abnormally short serum half-lives of IgG in beta 2-microglobulin-deficient mice. *Eur J Immunol* 26:690-696.
52. Ober, R. J., C. Martinez, C. Vaccaro, J. Zhou, and E. S. Ward. 2004. Visualizing the site and dynamics of IgG salvage by the MHC class I-related receptor, FcRn. *J Immunol* 172:2021-2029.
53. Zhou, J., J. E. Johnson, V. Ghetie, R. J. Ober, and E. S. Ward. 2003. Generation of mutated variants of the human form of the MHC class I-related receptor, FcRn, with increased affinity for mouse immunoglobulin G. *J Mol Biol* 332:901-913.
54. Ward, E. S., J. Zhou, V. Ghetie, and R. J. Ober. 2003. Evidence to support the cellular mechanism involved in serum IgG homeostasis in humans. *Int Immunol* 15:187-195.
55. Ober, R. J., C. Martinez, X. Lai, J. Zhou, and E. S. Ward. 2004. Exocytosis of IgG as mediated by the receptor, FcRn: an analysis at the single-molecule level. *Proc Natl Acad Sci U S A* 101:11076-11081. 158
56. Prabhat, P., Z. Gan, J. Chao, S. Ram, C. Vaccaro, S. Gibbons, R. J. Ober, and E. S. Ward. 2007. Elucidation of intracellular recycling pathways leading to exocytosis of the Fc receptor, FcRn, by using multifocal plane microscopy. *Proc Natl Acad Sci U S A* 104:5889-5894.
57. Montoyo, H. P., C. Vaccaro, M. Hafner, R. J. Ober, W. Mueller, and E. S. Ward. 2009. Conditional deletion of the MHC class I-related receptor FcRn reveals the sites of IgG homeostasis in mice. *Proc Natl Acad Sci U S A* 106:2788-2793.

58. Akilesh, S., G. J. Christianson, D. C. Roopenian, and A. S. Shaw. 2007. Neonatal FcR expression in bone marrow-derived cells functions to protect serum IgG from catabolism. *J. Immunol.* 179: 4580–4588.
59. Qiao, S. W., K. Kobayashi, F. E. Johansen, L. M. Sollid, J. T. Andersen, E. Milford, D. C. Roopenian, W. I. Lencer, and R. S. Blumberg. 2008. Dependence of antibody-mediated presentation of antigen on FcRn. *Proc. Natl. Acad. Sci. USA* 105: 9337–9342.
60. Baker, K., S. W. Qiao, T. T. Kuo, V. G. Aveson, B. Platzer, J. T. Andersen, I. Sandlie, Z. Chen, C. de Haar, W. I. Lencer, et al. 2011. Neonatal Fc receptor for IgG (FcRn) regulates cross-presentation of IgG immune complexes by CD8⁺ CD11b⁺ dendritic cells. *Proc. Natl. Acad. Sci. USA* 108: 9927–9932.
61. Baker, K., T. Rath, M. B. Flak, J. C. Arthur, Z. Chen, J. N. Glickman, I. Zlobec, E. Karamitopoulou, M. D. Stachler, R. D. Odze, et al. 2013. Neonatal Fc receptor expression in dendritic cells mediates protective immunity against colorectal cancer. *Immunity* 39: 1095–1107.
62. Weflen, A. W., N. Baier, Q. J. Tang, M. Van den Hof, R. S. Blumberg, W. I. Lencer, and R. H. Massol. 2013. Multivalent immune complexes divert FcRn to lysosomes by exclusion from recycling sorting tubules. *Mol. Biol. Cell* 24: 2398–2405
63. Ye, L., Liu, X., Rout, S., Li, Z., Yan, Y., Lu, L., Kamala, T., Song, W., Samal, K. S. and Zhu, X..2008.The MHC Class II-Associated Invariant Chain Interacts with the Neonatal Fcγ Receptor and Modulates Its Trafficking to Endosomal/Lysosomal Compartments. *J. Immunol* 181: (4) 2572-2585;

64. Trowbridge, I. S., J. F. Collawn, and C. R. Hopkins. 1993. Signal-Dependent Membrane Protein Trafficking in the Endocytic Pathway. *Annual Review of Cell Biology* 9:129-161.
65. Pandey, K. N. 2009. Functional roles of short sequence motifs in the endocytosis of membrane receptors. *Front Biosci* 14: 5339–5360.
66. Chen, W., J. Goldstein, and M. Brown. 1990. NPXY, a sequence often found in cytoplasmic tails, is required for coated pit-mediated internalization of the low density lipoprotein receptor. *J. Biol. Chem.* 265:3116-3123.
67. Letourneur, F., and R. D. Klausner. 1992. A novel di-leucine motif and a tyrosine-based motif independently mediate lysosomal targeting and endocytosis of CD3 chains. *Cell* 69:1143-1157.
68. Bonifacino, J. S., and L. M. Traub. 2003. signals for sorting of transmembrane proteins to endosomes and lysosomes *. *Annual Review of Biochemistry* 72:395-447.
69. Puertollano, R., N. N. van der Wel, L. E. Greene, E. Eisenberg, P. J. Peters, and J. S. Bonifacino. 2003. Morphology and Dynamics of Clathrin/GGA1- coated Carriers Budding from the Trans-Golgi Network. *Mol. Biol. Cell* 14:1545-1557.
70. Ohno, H., J. Stewart, M. Fournier, H. Bosshart, I. Rhee, S. Miyatake, T. Saito, A. Gallusser, T. Kirchhausen, and J. Bonifacino. 1995. Interaction of tyrosinebased sorting signals with clathrin-associated proteins. *Science* 269:1872- 1875.
71. Kirchhausen, T. 1999. ADAPTORS FOR CLATHRIN-MEDIATED TRAFFIC. *Annual Review of Cell and Developmental Biology* 15:705-732.

72. Puertollano, R., R. C. Aguilar, I. Gorshkova, R. J. Crouch, and J. S. Bonifacino. 2001. Sorting of Mannose 6-Phosphate Receptors Mediated by the GGAs. *Science* 292:1712-1716.
73. Zhao, Y., I. Kacs Kovics, Z. Zhao, and L. Hammarstrom. 2003. Presence of the dileucine motif in the cytoplasmic tail of the pig FcRn alpha chain. *Vet Immunol Immunopathol* 96:229-233.
74. Wu, Z., and N. E. Simister. 2001. Tryptophan- and dileucine-based endocytosis signals in the neonatal Fc receptor. *J Biol Chem* 276:5240-5247.
75. Dickinson, B. L., S. M. Claypool, J. A. D'Angelo, M. L. Aiken, N. Venu, E. H. Yen, J. S. Wagner, J. A. Borawski, A. T. Pierce, R. Hershberg, R. S. Blumberg, and W. I. Lencer. 2008. Ca²⁺-dependent calmodulin binding to FcRn affects immunoglobulin G transport in the transcytotic pathway. *Mol Biol Cell* 19:414-423.
76. Dall'Acqua, W. F., Kiener, P. A., & Wu, H. 2006. Properties of human IgG1s engineered for enhanced binding to the neonatal Fc receptor (FcRn). *J Biol Chem* 281(33), 23514–23524.
77. Hinton, P. R., Xiong, J. M., Johlfs, M. G., Tang, M. T., Keller, S., & Tsurushita, N. 2006. An engineered human IgG1 antibody with longer serum half-life. *J. Immunol* 176(1), 346–356
78. Strohl, W. R. Fusion proteins for half-life extension of biologics as a strategy to make biobetters. 2015. *BioDrugs* 29(4), 215–239.
79. Bai, Y., Ye, L., Tesar, D. B., Song, H., Zhao, D., Bjorkman, P. J., et al. 2011. Intracellular neutralization of viral infection in polarized epithelial cells by neonatal

Fc receptor (FcRn)-mediated IgG transport. *Proc Natl Acad Sci U S A* 108(45), 18406–18411.

80. Li, Z., Palaniyandi, S., Zeng, R., Tuo, W., Roopenian, D. C., & Zhu, X. 2011. Transfer of IgG in the female genital tract by MHC class I-related neonatal Fc receptor (FcRn) confers protective immunity to vaginal infection. *Proc Natl Acad Sci U S A* 108(11), 4388–4393

81. Ben Suleiman, Y., Yoshida, M., Nishiumi, S., Tanaka, H., Mimura, T., Nobutani, K., et al. 2012. Neonatal Fc receptor for IgG (FcRn) expressed in the gastric epithelium regulates bacterial infection in mice. *Mucosal Immunol* 5(1), 87–98.

82. Palmeira P, Quinello C, Silveira-Lessa AL, Zago CA, Carneiro-Sampaio M. 2012. IgG placental transfer in healthy and pathological pregnancies. *Clin Dev Immunol*. 2012:985646

83. Pereira L, Petitt M, Tabata T. 2013. Cytomegalovirus infection and antibody protection of the developing placenta..*Clin Infect Dis*. 57 Suppl 4:S174-7.

84. Ye, L., Zeng, R., Bai, Y., Roopenian, D. C., & Zhu, X.. 2011. Efficient mucosal vaccination mediated by the neonatal Fc receptor. *Nat Biotechnol* 29(2), 158–163.

85. Rosenblum, M. D., Remedios, K. A., Abbas, A. K. 2015. Mechanisms of human autoimmunity. *J Clin Invest* 125(6):2228–2233

86. Yu, Z., and V. A. Lennon. 1999. Mechanism of Intravenous Immune Globulin Therapy in Antibody-Mediated Autoimmune Diseases. *N Engl J Med* 340:227-228.

87. Vaccaro, C., J. Zhou, R.J. Ober, and E.S. Ward. 2005. Engineering the Fc region of immunoglobulin G to modulate in vivo antibody levels. *Nature Biotechnol* 23:1283-1288.

88. Getman, K. E., and J. P. Balthasar. 2005. Pharmacokinetic effects of 4C9, an anti-FcRn antibody, in rats: implications for the use of FcRn inhibitors for the treatment of humoral autoimmune and alloimmune conditions. *J Pharm Sci* 94:718-729.
89. Murphy E, Rigoutsos I, Shibuya T, Shenk TE. 2003. Reevaluation of human cytomegalovirus coding potential. *Proc. Natl. Acad. Sci. U.S.A* 100:13585-90.
90. Varnum SM, Streblow DN, Monroe ME, Smith P, Auberry KJ, Pasa-Tolic L, Wang D, Camp DG 2nd, Rodland K, Wiley S, Britt W, Shenk T, Smith RD, Nelson JA. 2004. Identification of proteins in human cytomegalovirus (HCMV) particles: the HCMV proteome. *J Virol* 78:10960-10966.
91. Mocarski ES, Shenk T, Pass RF (2006) Cytomegaloviruses. In: Knipe DM (ed) *Fields virology*. Lippincott Williams and Wilkins, Philadelphia, pp 2701-2772
92. Pierre M Jean Beltran and Ileana M Cristea. 2014. The life cycle and pathogenesis of human cytomegalovirus infection: lessons from proteomics. *Expert Rev. Proteomics* 11(6), 697–711.
93. Sinzger C, Digel M, Jahn G. 2008. Cytomegalovirus cell tropism. *Curr Top Microbiol Immunol* 325:63-83
94. Reeves M, Sinclair J. 2008. Aspects of human cytomegalovirus latency and reactivation. *Curr Top Microbiol Immunol* 325: 297-313
95. Goodrum F, Caviness K, Zagallo P. 2012. Human cytomegalovirus persistence. *Cell Microbiol* 14:644-55.
96. Kenneson A, Cannon MJ. 2007. Review and meta-analysis of the epidemiology of congenital cytomegalovirus (CMV) infection. *Rev Med Virol* 17:253-76

97. Lanzieri TM, Dollard SC, Bialek SR, Grosse SD. 2014. Systematic review of the birth prevalence of congenital cytomegalovirus infection in developing countries. *Int J Infect Dis* 22:44-8
98. Biron, K. K. 2006. Antiviral drugs for cytomegalovirus disease. *Antivir Res* 71:154-163
99. Isaacson MK, Juckem LK, Compton T. Virus entry and innate immune activation. *Curr Top Microbiol Immunol* 2008;325: 85-100.
100. Bechtel JT, Shenk T. 2002. Human cytomegalovirus UL47 tegument protein functions after entry and before immediate-early gene expression. *J Virol* 76:1043–1050.
101. Li T, Chen J, Cristea IM. 2013. Human cytomegalovirus tegument protein pUL83 inhibits IFI16-mediated DNA sensing for immune evasion. *Cell Host Microbe* 14:591-9.
102. Terhune S, Torigoi E, Moorman N, Silva M, Qian Z, Shenk T, Yu D. 2007. Human cytomegalovirus UL38 protein blocks apoptosis. *J Virol* 81:3109–3123.
103. Hwang J, Kalejta RF. 2007. Proteasome-dependent, ubiquitin-independent degradation of Daxx by the viral pp71 protein in human cytomegalovirus-infected cells. *Virology* 367:334-8.
104. Cristea IM, Moorman NJ, Terhune SS, et al. Human cytomegalovirus pUL83 stimulates activity of the viral immediate-early promoter through its interaction with the cellular IFI16 protein. *J Virol* 2010;84:7803-14.

105. Milbradt J, Auerochs S, Marschall M. 2007. Cytomegaloviral proteins pUL50 and pUL53 are associated with the nuclear lamina and interact with cellular protein kinase C. *J Gen Virol* 88: 2642-50.
106. Milbradt J, Kraut A, Hutterer C, et al. 2014. Proteomic analysis of the multimeric nuclear egress complex of human cytomegalovirus. *Mol Cell Proteomics* 13(8):2132-46.
107. Alwine JC. 2012. The human cytomegalovirus assembly compartment: a masterpiece of viral manipulation of cellular processes that facilitates assembly and egress. *PLoS Pathog* 8:e1002878.
108. Das S, Vasanthi A, Pellett PE. 2007. Three-dimensional structure of the human cytomegalovirus cytoplasmic virion assembly complex includes a reoriented secretory apparatus. *J Virol* 81:11861-9.
109. Das S, Pellett PE. 2011. Spatial relationships between markers for secretory and endosomal machinery in human cytomegalovirus-infected cells versus those in uninfected cells. *J Virol* 85:5864-7.
110. C. C. Rossetto, M. Tarrant-Elorza, and G. S. Pari. 2013. Cis and Trans Acting Factors Involved in Human Cytomegalovirus Experimental and Natural Latent Infection of CD14 (+) Monocytes and CD34 (+) Cells. *PLoS Pathog* 9:e1003366.
111. G. Hahn, R. Jores, and E. S. Mocarski. 1998. Cytomegalovirus remains latent in a common precursor of dendritic and myeloid cells. *Proc. Natl. Acad. Sci. U.S.A* 95: 3937–3942.

112. R. T. Saffert, R. R. Penkert, and R. F. Kalejta. 2010. Cellular and viral control over the initial events of human cytomegalovirus experimental latency in CD34⁺ cells. *J Virol* 84:5594–04.
113. M. B. Reeves, P. A. MacAry, P. J. Lehner, J. G. P. Sissons, and J. H. Sinclair. 2005. Latency, chromatin remodeling, and reactivation of human cytomegalovirus in the dendritic cells of healthy carriers. *Proc. Natl. Acad. Sci. U.S.A* 102: 4140–45.
114. M. B. Reeves, P. J. Lehner, J. G. P. Sissons, and J. H. Sinclair. 2005. An in vitro model for the regulation of human cytomegalovirus latency and reactivation in dendritic cells by chromatin remodeling. *J Gen Virol* 86:2249–54.
115. Hamprecht K, Maschmann J, Vochem M, Dietz K, Speer CP, Jahn G. 2001. Epidemiology of transmission of cytomegalovirus from mother to preterm infant by breastfeeding. *Lancet* 357:513-518.
116. Sinzger C, Grefte A, Plachter B, Gouw AS, The TH, Jahn G. 1995. Fibroblasts, epithelial cells, endothelial cells and smooth muscle cells are major targets of human cytomegalovirus infection in lung and gastrointestinal tissues. *J Gen Virol* 76:741-750.
117. Emery VC, Cope AV, Bowen EF, Gor D, Griffiths PD. 1999. The dynamics of human cytomegalovirus replication in vivo. *J Exp Med* 190:177-182.
118. Riegler S, Hebart H, Einsele H, Brossart P, Jahn G, Sinzger C. 2000. Monocyte-derived dendritic cells are permissive to the complete replicative cycle of human cytomegalovirus. *J Gen Virol* 81:393-399.

119. Halwachs-Baumann G, Wilders-Truschnig M, Desoye G, Hahn T, Kiesel L, Klingel K, Rieger P, Jahn G, Sinzger C. 1998. Human trophoblast cells are permissive to the complete replicative cycle of human cytomegalovirus. *J Virol* 72:7598-7602
120. Wang D, Shenk T. 2005. Human cytomegalovirus virion protein complex required for epithelial and endothelial cell tropism. *Proc. Natl. Acad. Sci. USA.* 102: 18153–18158.
121. Hahn G, Revello MG, Patrone M, et al. 2004. Human cytomegalovirus UL131–128 genes are indispensable for virus growth in endothelial cells and virus transfer to leukocytes. *J Virol* 78: 10023–10033.
122. Ryckman BJ, Rainish BL, Chase MC, et al. 2008. Characterization of the human cytomegalovirus gH/gL/UL128–131 complex that mediates entry into epithelial and endothelial cells. *J Virol* 82: 60–70.
123. Cannon MJ, Hyde TB, Schmid DS. 2011. Review of cytomegalovirus shedding in bodily fluids and relevance to congenital cytomegalovirus infection. *Rev Med Virol* 21: 240–255.
124. Boppana SB, Rivera LB, Fowler KB, et al. 2001. Intrauterine transmission of cytomegalovirus to infants of women with preconceptional immunity. *N Engl J Med* 344: 1366–1371.
125. Vries JJ, van Zwet EW, Dekker FW, et al. 2013. The apparent paradox of maternal seropositivity as a risk factor for congenital cytomegalovirus infection: a population-based prediction model. *Rev Med Virol* 23: 241–249

126. Dahle AF, Fowler KB, Wright JD, Boppana SB, Britt WJ, Pass RF. 2000. Longitudinal investigation of hearing disorders in children with congenital cytomegalovirus. *J Am Acad Audiol* 11:283-290
127. Noyola DE, Demmler GJ, Nelson CT, Griesser C, Williamson WD, et al. 2001. Early predictors of neurodevelopmental outcome in symptomatic congenital cytomegalovirus infection. *J Pediatr* 138:325-331.
128. Boppana SB, Fowler KB, Vaid Y, Hedlund G, Stagno S, Britt WJ, Pass RF. 1997. Neuroradiographic findings in the newborn period and long-term outcome in children with symptomatic congenital cytomegalovirus infection. *Pediatrics* 99:409-414.
129. Atabani SF, Smith C, Atkinson C, et al. 2012. Cytomegalovirus replication kinetics in solid organ transplant recipients managed by preemptive therapy. *Am J Transpl* 12: 2457–2464.
130. Grundy JE, Lui SF, Super M, et al. 1998. Symptomatic cytomegalovirus infection in seropositive kidney recipients: reinfection with donor virus rather than reactivation of recipient virus. *Lancet* 2: 132–135.
131. Singh N. 2005. Late-onset cytomegalovirus disease as a significant complication in solid organ transplant recipients receiving antiviral prophylaxis: a call to heed the mounting evidence. *Clin Infect Dis* 40:704-708.
132. Schmidt GM, Horak DA, Niland JC, Duncan SR, Forman SJ, Zaia JA. 1991. A randomized, controlled trial of prophylactic ganciclovir for cytomegalovirus pulmonary infection in recipients of allogeneic bone marrow transplants; The City of Hope-Stanford-Syntex CMV Study Group. *N Eng J Med* 324:1005-1011.

133. Jacobson MA, Mills J, Rush J, Peiperl L, Seru V, Mohanty PK, Hopewell PC, Hadley WK, Broadus VC, Leoung G et al. 1991. Morbidity and mortality of patients with AIDS and first-episode *Pneumocystis carinii* pneumonia unaffected by concomitant pulmonary cytomegalovirus infection. *Am Rev Respir Dis* 144:6-9
134. Dieterich DT, Rahmin M. 1991. Cytomegalovirus colitis in AIDS: presentation in 44 patients and a review of the literature. *J AIDS* 4: S29-S35.
135. Wilcox CM, Chalasani N, Lazenby A, Schwartz DA. 1998. Cytomegalovirus colitis in acquired immunodeficiency syndrome: a clinical and endoscopic study. *Gastrointest Endos* 48:39-43.
136. Pecorella I, Ciardi A, Garner A, McCartney AC, Lucas S. 2000. Postmortem histological survey of the ocular lesions in a British population of AIDS patients. *Br J Ophthalmol* 84:1275-1281.
137. Kimberlin DW, Lin CY, Sanchez PJ, et al. 2003. Effect of ganciclovir therapy on hearing in symptomatic congenital cytomegalovirus disease involving the central nervous system: a randomized, controlled trial. *J Pediatr* 143: 16–25.
138. Whitley RJ, Cloud G, Gruber W, et al. 1997. Ganciclovir treatment of symptomatic congenital cytomegalovirus infection: results of a phase II study. National Institute of Allergy and Infectious Diseases Collaborative Antiviral Study Group. *J Infect Dis* 175: 1080–1086.
139. Britt WJ, Vugler L, Butfiloski EJ, Stephens EB. 1990. Cell surface expression of human cytomegalovirus (HCMV) gp55-116 (gB): use of HCMV-recombinant vaccinia virus-infected cells in analysis of the human neutralizing antibody response. *J Virol* 64:1079-1085

140. Pass RF, Zhang C, Evans A, et al. 2009. Vaccine prevention of maternal cytomegalovirus infection. *N Engl J Med* 360:1191–1199.
141. Nigro G, Adler SP, La Torre R, Best AM. 2005. Passive immunization during pregnancy for congenital cytomegalovirus infection. *N Engl J Med* 353:1350-62.
142. Visentin S, Manara R, Milanese L, et al. 2012. Early primary cytomegalovirus infection in pregnancy: maternal hyperimmunoglobulin therapy improves outcomes among infants at 1 year of age. *Clin Infect Dis* 55:497-503.
143. Revello MG, Lazzarotto T, Guerra B, et al. 2014. A randomized trial of hyperimmune globulin to prevent congenital cytomegalovirus. *N Engl J Med* 370: 1316–1326
144. Boehme KW, Guerrero M, Compton T. 2006. Human cytomegalovirus envelope glycoproteins B and H are necessary for TLR2 activation in permissive cells. *J Immunol* 177:7094–7102
145. Laroux FS. 2004. Mechanisms of inflammation: the good, the bad and the ugly. *Front Biosci* 9:3156–3162
146. Taylor RT, Bresnahan WA. 2006. Human cytomegalovirus IE86 attenuates virus- and tumor necrosis factor alpha-induced NFkappaB-dependent gene expression. *J Virol* 80:10763–10771
147. Taylor RT, Bresnahan WA. 2006. Human cytomegalovirus immediate-early 2 protein IE86 blocks virus-induced chemokine expression. *J Virol* 80:920–928
148. DeFilippis VR, Sali T, Alvarado D, White L, Bresnahan W, Fruh k. 2010. Activation of the Interferon Response by Human Cytomegalovirus Occurs via Cytoplasmic Double-Stranded DNA but Not Glycoprotein B. *J Virol* 83: 8913–8925.

149. DeFilippis VR, Alvarado D, Sali T, Rothenburg S, Fruh K. 2010. Human cytomegalovirus induces the interferon response via the DNA sensor ZBP1. *J Virol* 84: 585–598.
150. Paijo J, Döring M, Spanier J, Grabski E, Nooruzzaman M, Schmidt T, et al. 2016. cGAS Senses Human Cytomegalovirus and Induces Type I Interferon Responses in Human MonocyteDerived Cells. *PLoS Pathog* 12(4): e1005546.
151. Li T, Chen J, Cristea IM. 2013. Human cytomegalovirus tegument protein pUL83 inhibits IFI16mediated DNA sensing for immune evasion. *Cell Host Microbe* 14: 591–599
152. Shuai K, Liu B. 2003. Regulation of JAK-STAT signalling in the immune system. *Nat Rev Immunol* 3:900–911.
153. Paulus C, Krauss S, Nevels M. 2006. A human cytomegalovirus antagonist of type I IFN-dependent signal transducer and activator of transcription signaling. *Proc Natl Acad Sci U S A* 103:3840–3845.
154. Child SJ, Hakki M, De Niro KL, Geballe AP. 2004. Evasion of cellular antiviral responses by human cytomegalovirus TRS1 and IRS1. *J Virol* 78:1.
155. Halenius A, Gerke CL, Hengel H. 2015. Classical and non-classical MHC I molecule manipulation by human cytomegalovirus: so many targets—but how many arrows in the quiver? *Cel. & Mol. Immunol.* 12,139–153.
156. Koch J, Guntrum R, Heintke S, Kyritsis C, Tampe, R. 2004. Functional dissection of the transmembrane domains of the transporter associated with antigen processing (TAP). *J Biol Chem* 279: 10142–10147.

157. Chang SC, Momburg F, Bhutani N, Goldberg AL. 2005. The ER aminopeptidase, ERAP1, trims precursors to lengths of MHC class I peptides by a “molecular ruler” mechanism. *Proc Natl Acad Sci USA* 102: 17107–17112.
158. Jones TR, Wiertz EJ, Sun L, Fish KN, Nelson JA, Ploegh HL. 1996. Human cytomegalovirus US3 impairs transport and maturation of major histocompatibility complex class I heavy chains. *Proc Natl Acad Sci USA* 93: 11327–11333..
159. Lee S, Park B, Ahn K. 2003. Determinant for endoplasmic reticulum retention in the luminal domain of the human cytomegalovirus US3 glycoprotein. *J Virol* 77: 2147–2156.
160. Lee S, Yoon J, Park B, Jun Y, Jin M, Sung HC et al. 2000. Structural and functional dissection of human cytomegalovirus US3 in binding major histocompatibility complex class I molecules. *J Virol* 74: 11262–11269.
161. Jones TR, Sun L. 1997. Human cytomegalovirus US2 destabilizes major histocompatibility complex class I heavy chains. *J Virol* 71: 2970–2979
162. Gewurz BE, Wang EW, Tortorella D, Schust DJ, Ploegh HL. 2001. Human cytomegalovirus US2 endoplasmic reticulum-lumenal domain dictates association with major histocompatibility complex class I in a locus-specific manner. *J Virol* 75: 5197–5204.
163. Wiertz EJ, Tortorella D, Bogyo M, Yu J, Mothes W, Jones TR et al. 1996. Sec61-mediated transfer of a membrane protein from the endoplasmic reticulum to the proteasome for destruction. *Nature* 384: 432–438.
164. Gewurz BE, Gaudet R, Tortorella D, Wang EW, Ploegh HL, Wiley DC et al. 2001. Antigen presentation subverted: structure of the human cytomegalovirus

protein US2 bound to the class I molecule HLAA2. *Proc Natl Acad Sci USA* 98: 6794–6799.

165. Van den Boomen, D. J. H., & Lehner, P. J. 2015. Identifying the ERAD ubiquitin E3 ligases for viral and cellular targeting of MHC class I. *Mol. Immunol*, 68(2),106–111.

166. Hassink GC, Barel MT, van Voorden SB, Kikkert M, Wiertz EJ. 2006. Ubiquitination of MHC class I heavy chains is essential for dislocation by human cytomegalovirus-encoded US2 but not US11. *J Biol Chem* 281: 30063–30071.

167. Stagg HR, Thomas M, van den Boomen D, Wiertz EJ, Drabkin HA, Gemmill RM et al. 2009. The TRC8 E3 ligase ubiquitinates MHC class I molecules before dislocation from the ER. *J Cell Biol* 186: 685–692S.

168. Barel MT, Ressing M, Pizzato N, van Leeuwen D, Le Bouteiller P, Lenfant F et al. 2003. Human cytomegalovirus-encoded US2 differentially affects surface expression of MHC class I locus products and targets membrane-bound, but not soluble HLA-G1 for degradation. *J Immunol* 171: 6757–6765.

169. Ben-Arieh SV, Zimmerman B, Smorodinsky NI, Yaacubovicz M, Schechter C, Bacik I et al. 2001. Human cytomegalovirus protein US2 interferes with the expression of human HFE, a nonclassical class I major histocompatibility complex molecule that regulates iron homeostasis. *J Virol* 75: 10557–10562.

170. Vahdati-Ben Arieh S, Laham N, Schechter C, Yewdell JW, Coligan JE, Ehrlich R. 2003. A single viral protein HCMV US2 affects antigen presentation and intracellular iron homeostasis by degradation of classical HLA class I and HFE molecules. *Blood* 101: 2858–2864.

171. Han J, Rho SB, Lee JY, Bae J, Park SH, Lee SJ et al. 2013. Human cytomegalovirus (HCMV) US2 protein interacts with human CD1d (hCD1d) and down-regulates invariant NKT (iNKT) cell activity. *Mol Cells* 36: 455–464.
172. Tomazin R, Boname J, Hegde NR, Lewinsohn DM, Altschuler Y, Jones TR et al. 1999. Cytomegalovirus US2 destroys two components of the MHC class II pathway, preventing recognition by CD41 T cells. *Nat Med.* 5: 1039–1043.
173. Hsu, J.L., van den Boomen, D.J., Tomasec, P., Weekes, M.P. et al. 2015. Plasma membrane profiling defines an expanded class of cell surface proteins selectively targeted for degradation by HCMV US2 in cooperation with UL141. *PLoS Pathog.* 11, e1004811.
174. Wiertz EJ, Jones TR, Sun L, Bogyo M, Geuze HJ, Ploegh HL. 1996. The human cytomegalovirus US11 gene product dislocates MHC class I heavy chains from the endoplasmic reticulum to the cytosol. *Cell* 84: 769–779.
175. Lee SO, Hwang S, Park J, Park B, Jin BS, Lee S et al. 2005. Functional dissection of HCMV US11 in mediating the degradation of MHC class I molecules. *Biochem Biophys Res Commun* 330: 1262–1267.
176. Barel MT, Pizzato N, van Leeuwen D, Bouteiller PL, Wiertz EJ, Lenfant F. 2003. Amino acid composition of alpha1/alpha2 domains and cytoplasmic tail of MHC class I molecules determine their susceptibility to human cytomegalovirus US11-mediated downregulation. *Eur J Immunol* 33: 1707–1716.
177. Lilley BN, Ploegh HL. 2004. A membrane protein required for dislocation of misfolded proteins from the ER. *Nature* 429: 834–840.

178. Lilley BN, Tortorella D, Ploegh HL. 2003. Dislocation of a type I membrane protein requires interactions between membrane-spanning segments within the lipid bilayer. *Mol Biol Cell* 14: 3690–3698.
179. Cho S, Kim BY, Ahn K, Jun Y. 2013. The C-terminal amino acid of the MHCI heavy chain is critical for binding to Derlin-1 in human cytomegalovirus US11-induced MHC-I degradation. *PLoS One* 8: e72356.
180. Hassink, G.C., Barel, M.T., Van Voorden, S.B., Kikkert, M., Wiertz, E.J., 2006. Ubiquitination of MHC class I heavy chains is essential for dislocation by human cytomegalovirus-encoded US2 but not US11. *J. Biol. Chem.* 281, 30063–30071
181. Kikkert, M., Hassink, G., Barel, M., Hirsch, C., van der Wal, F.J., Wiertz, E., 2001. Ubiquitination is essential for human cytomegalovirus US11-mediated dislocation of MHC class I molecules from the endoplasmic reticulum to the cytosol. *Biochem. J.* 358, 369–377.
182. Cadwell, K., Coscoy, L., 2005. Ubiquitination on nonlysine residues by a viral E3 ubiquitin ligase. *Science*, 127–130.
183. Van de Weijer, M.L., Bassik, M.C., Luteijn, R.D., Voorburg, C.M., Lohuis, M.A., Kremmer, E., Hoeben, R.C., LeProust, E.M., Chen, S., Hoelen, H., Rensing, M.E., Patena, W., Weissman, J.S., McManus, M.T., Wiertz, E.J., Lebbink, R.J., 2014. A high-coverage shRNA screen identifies TMEM129 as an E3 ligase involved in ER-associated protein degradation. *Nat. Commun.* 5, 3832.
184. Van den Boomen, D.J., Timms, R.T., Grice, G.L., Stagg, H.R., Skodt, K., Dougan, G., Nathan, J.A., Lehner, P.J., 2014. TMEM129 is a Derlin-1 associated

ERAD E3 ligase essential for virus-induced degradation of MHC-I. *Proc. Natl. Acad. Sci. U S A* 111, 11425–11430.

185. Ahn K, Gruhler A, Galocha B, Jones TR, Wiertz EJ, Ploegh HL et al. 1997. The ER-luminal domain of the HCMV glycoprotein US6 inhibits peptide translocation by TAP. *Immunity* 6: 613–621.

186. Lehner PJ, Karttunen JT, Wilkinson GW, Cresswell P. 1997. The human cytomegalovirus US6 glycoprotein inhibits transporter associated with antigen processing-dependent peptide translocation. *Proc Natl Acad Sci USA* 94: 6904–6909.

187. Dugan GE, Hewitt EW. 2008. Structural and functional dissection of the human cytomegalovirus immune evasion protein US6. *J Virol* 82: 3271–3282.

188. Hewitt EW, Gupta SS, Lehner PJ. 2001. The human cytomegalovirus gene product US6 inhibits ATP binding by TAP. *EMBO J* 20: 387–396.

189. Furman MH, Dey N, Tortorella D, Ploegh HL. 2002. The human cytomegalovirus US10 gene product delays trafficking of major histocompatibility complex class I molecules. *J Virol* 76: 11753–11756.

190. Park B, Spooner E, Houser BL, Strominger JL, Ploegh HL. 2010. The HCMV membrane glycoprotein US10 selectively targets HLA-G for degradation. *J Exp Med* 207: 2033–2041

191. Kuijpers TW, Baars PA, Dantin C, van den Burg M, van Lier RA, et al. 2008. Human NK cells can control CMV infection in the absence of T cells. *Blood* 112: 914–915.

192. Prod'homme V, Griffin C, Aicheler RJ, Wang EC, McSharry BP, et al. (2007) The human cytomegalovirus MHC class I homolog UL18 inhibits LIR-1+ but activates LIR-12 NK cells. *Journal of immunology* 178: 4473–4481
193. Eagle RA, Traherne JA, Ashiru O, Wills MR, Trowsdale J. 2006. Regulation of NKG2D ligand gene expression. *Hum Immunol* 67: 159–169
194. Venkataraman GM, Suciú D, Groh V, Boss JM, Spies T 2007. Promoter region architecture and transcriptional regulation of the genes for the MHC class I-related chain A and B ligands of NKG2D. *Journal of immunology* 178: 961– 969.
195. Yang Z, Bjorkman PJ. 2008. Structure of UL18, a peptide-binding viral MHC mimic, bound to a host inhibitory receptor. *Proc Natl Acad Sci USA*.105: 10095–10100.
196. Navarro F, Llano M, Bello n T, Colonna M, Geraghty DE, Lo pez-Botet M. 1999. The ILT2(LIR1) and CD94/NKG2A NK cell receptors respectively recognize HLA-G1 and HLA-E molecules co-expressed on target cells. *Eur J Immunol* 29: 277–283
197. Reyburn HT, Mandelboim O, Vale s-Go ímez M, Davis DM, Pazmany L, Strominger JL. 1997. The class I MHC homologue of human cytomegalovirus inhibits attack by natural killer cells. *Nature* 386: 514–517.
198. Leong CC, Chapman TL, Bjorkman PJ, Formankova D, Mocarski ES, Phillips JH et al. 1998. Modulation of natural killer cell cytotoxicity in human cytomegalovirus infection: the role of endogenous class I major histocompatibility complex and a viral class I homolog. *J Exp Med* 187: 1681–1687.

199. Park B, Oh H, Lee S, Song Y, Shin J, Sung YC et al. 2002. The MHC class I homolog of human cytomegalovirus is resistant to down-regulation mediated by the unique short region protein (US)2, US3, US6, and US11 gene products. *J Immunol* 168: 3464–3469.
200. Braud VM, Allan DS, O’Callaghan CA, Söderström K, D’Andrea A, Ogg GS et al. 1998. HLA-E binds to natural killer cell receptors CD94/ NKG2A, B and C. *Nature* 391: 795–799
201. Braud V, Jones EY, McMichael A. 1997. The human major histocompatibility complex class Ib molecule HLA-E binds signal sequence-derived peptides with primary anchor residues at positions 2 and 9. *Eur J Immunol* 27: 1164–1169.
202. Llano M, Guma M, Ortega M, Angulo A, Lopez-Botet M. 2003. Differential effects of US2, US6 and US11 human cytomegalovirus proteins on HLA class Ia and HLA-E expression: impact on target susceptibility to NK cell subsets. *Eur J Immunol* 20: 2744–2754.
- 203.. Tomasec P, Braud VM, Rickards C, Powell MB, McSharry BP, et al. 2000. Surface expression of HLA-E, an inhibitor of natural killer cells, enhanced by human cytomegalovirus gpUL40. *Science* 287: 1031.
204. Wang EC, McSharry B, Retiere C, Tomasec P, Williams S, et al. 2002. UL40-mediated NK evasion during productive infection with human cytomegalovirus. *Proceedings of the National Academy of Sciences of the United States of America* 99: 7570–7575.
205. Eagle RA, Trowsdale J 2007. Promiscuity and the single receptor: NKG2D. *Nature reviews Immunology* 7: 737–744.

- 206 .Chalupny NJ, Sutherland CL, Lawrence WA, Rein-Weston A, Cosman D. 2003. ULBP4 is a novel ligand for human NKG2D. *Biochem Biophys Res Commun* 305: 129–135.
207. Wu J, Chalupny NJ, Manley TJ, Riddell SR, Cosman D, et al. 2003. Intracellular retention of the MHC class I-related chain B ligand of NKG2D by the human cytomegalovirus UL16 glycoprotein. *Journal of immunology* 170: 4196–4200.
208. Kubin M, Cassiano L, Chalupny J, Chin W, Cosman D, et al. 2001. ULBP1, 2, 3: novel MHC class I-related molecules that bind to human cytomegalovirus glycoprotein UL16, activate NK cells. *European journal of immunology* 31: 1428–1437.
209. Eagle RA, Traherne JA, Hair JR, Jafferji I, Trowsdale J 2009. ULBP6/ RAET1L is an additional human NKG2D ligand. *European journal of immunology* 39: 3207–3216.
210. Rolle A, Mousavi-Jazi M, Eriksson M, Odeberg J, Soderberg-Naucler C, et al. 2003. Effects of human cytomegalovirus infection on ligands for the activating NKG2D receptor of NK cells: up-regulation of UL16-binding protein (ULBP)1 and ULBP2 is counteracted by the viral UL16 protein. *Journal of immunology* 171: 902–908.
211. Bennett NJ, Ashiru O, Morgan FJ, Pang Y, Okecha G, et al. 2010. Intracellular sequestration of the NKG2D ligand ULBP3 by human cytomegalovirus. *Journal of immunology* 185: 1093–1102.

212. Ashiru O, Bennett NJ, Boyle LH, Thomas M, Trowsdale J, et al. 2009. NKG2D ligand MICA is retained in the cis-Golgi apparatus by human cytomegalovirus protein UL142. *Journal of virology* 83: 12345–12354.
213. Stern-Ginossar N, Elefant N, Zimmermann A, Wolf DG, Saleh N, Biton M et al. 2007. Host immune system gene targeting by a viral miRNA. *Science* 317: 376–381.
214. Fielding CA, Aicheler R, Stanton RJ, Wang EC, Han S, Seirafian S et al. 2014. Two novel human cytomegalovirus NK cell evasion functions target MICA for lysosomal degradation. *PLoS Pathog* 10:e1004058
215. Aron T, Achdout H, Levi O, et. al. 2005. Inhibition of the NKp30 activating receptor by pp65 of human cytomegalovirus. *Nat. Immunol* 6, 515–523.
216. Prodhomme V, Sugrue DM, Stanton RJ, Nomoto A, Davies J, et al. 2010. Human cytomegalovirus UL141 promotes efficient downregulation of the natural killer cell activating ligand CD112. *The Journal of general virology* 91: 2034–2039.
217. Tomasec P, Wang EC, Davison AJ, Vojtesek B, Armstrong M, et al. 2005. Downregulation of natural killer cell-activating ligand CD155 by human cytomegalovirus UL141. *Nature immunology* 6: 181–188.
218. Smith W, Tomasec P, Aicheler R, Loewendorf A, Nemcovicova I, et al. 2013. Human Cytomegalovirus Glycoprotein UL141 Targets the TRAIL Death Receptors to Thwart Host Innate Antiviral Defenses. *Cell host & microbe* 13: 324–335.
219. Jonjić S, Pavić I, Polić B, Crnković I, Lucin P, et al. 1994. Antibodies are not essential for the resolution of primary cytomegalovirus infection but limit dissemination of recurrent virus. *J Exp Med.* 179:1713–1717

220. Schoppel K, Kropff B, Schmidt C, Vornhagen R, Mach M. 1997. The humoral immune response against human cytomegalovirus is characterized by a delayed synthesis of glycoprotein-specific antibodies. *J Infect Dis.* 175: 533–544.
221. Kropff B, Burkhardt C, Schott J, Nentwich J, Fisch T, Britt W, Mach M. 2012. Glycoprotein N of human cytomegalovirus protects the virus from neutralizing antibodies. *PLoS Pathog.* 8(10):e1002999.
222. Manley K, Anderson J, Yang F, Szustakowski J, Oakeley EJ, et al. 2011. Human cytomegalovirus escapes a naturally occurring neutralizing antibody by incorporating it into assembling virions. *Cell Host Microbe.* 10: 197–209.
223. Atalay R, Zimmermann A, Wagner M, Borst E, Benz C, et al. 2002. Identification and expression of human cytomegalovirus transcription units coding for two distinct Fcγ receptor homologs. *J Virol.* 76: 8596–8608
224. Lilley BN, Ploegh HL, Tirabassi RS. 2001. Human cytomegalovirus open reading frame TR11/IRL11 encodes an immunoglobulin G Fc-binding protein. *J Virol* 75: 11218–11221.
225. Sprague ER, Reinhard H, Cheung EJ, Farley AH, Trujillo RD, et al. 2008. The human cytomegalovirus Fc receptor gp68 binds the Fc CH2-CH3 interface of immunoglobulin G. *J Virol* 82: 3490–3499.
226. Corrales-Aguilar E, Trilling M, Hunold K, Fiedler M, Le VT, Reinhard H, Ehrhardt K, Merc é-Maldonado E, Aliyev E, Zimmermann A, Johnson DC, Hengel H. 2014. Human cytomegalovirus Fcγ binding proteins gp34 and gp68 antagonize Fcγ receptors I, II and III. *PLoS Pathog* 15;10(5):e1004131.

227. Cortese, M., Calò, S., D'Aurizio, R., Lilja, A., Pacchiani, N., & Merola, M. 2012. Recombinant Human Cytomegalovirus (HCMV) RL13 Binds Human Immunoglobulin G Fc. *PLoS ONE*, 7(11), e50166.
228. Vembar S S, Brodsky J L. 2008. One step at a time: endoplasmic reticulum-associated degradation, *Nat Rev Mol Cell Biol.* 9, 944–957.
229. Ellgaard, L. & Helenius, A. 2003. Quality control in the endoplasmic reticulum. *Nature Rev. Mol. Cell Biol.* 4, 181–191.
230. Olzmann A, Kopito R, Christianson J. 2013. The Mammalian Endoplasmic Reticulum-Associated Degradation System. *Cold Spring Harb Perspect Biol* 5:a013185
231. Morito, Daisuke et al. 2015. Pathogenic Hijacking of ER-Associated Degradation: Is ERAD Flexible? *Mol. Cell.*59 (3) : 335 - 344.
232. Helenius A, Aebi M. 2004. Roles of N-linked glycans in the endoplasmic reticulum. *Annu Rev Biochem* 73: 1019– 1049.
233. Aebi M, Bernasconi R, Clerc S, Molinari M. 2010. N-glycan structures: Recognition and processing in the ER. *Trends Biochem Sci* 35: 74–82.
234. Hebert DN, Bernasconi R, Molinari M. 2010. ERAD substrates: Which way out? *Semin Cell Dev Biol* 21: 526–532.
235. Hosokawa N, Tremblay LO, Sleno B, Kamiya Y, Wada I, Nagata K, Kato K, Herscovics A. 2010. EDEM1 accelerates the trimming of α 1,2-linked mannose on the C branch of N-glycans. *Glycobiology* 20: 567–575.

236. Hosokawa N, Wada I, Nagasawa K, Moriyama T, Okawa K, Nagata K. 2008. Human XTP3-B forms an endoplasmic reticulum quality control scaffold with the HRD1-SEL1L ubiquitin ligase complex and BiP. *J Biol Chem* 283: 20914–20924.
237. Hosokawa N, Kamiya Y, Kamiya D, Kato K, Nagata K. 2009. Human OS-9, a lectin required for glycoprotein endoplasmic reticulum-associated degradation, recognizes mannose-trimmed N-glycans. *J Biol Chem* 284: 17061–17068.
238. Bernasconi R, Pertel T, Luban J, Molinari M. 2008. A dual task for the Xbp1-responsive OS-9 variants in the mammalian endoplasmic reticulum: Inhibiting secretion of misfolded protein conformers and enhancing their disposal. *J Biol Chem* 283: 16446–16454.
239. Mueller B, Klemm EJ, Spooner E, Claessen JH, Ploegh HL. 2008. SEL1L nucleates a protein complex required for dislocation of misfolded glycoproteins. *Proc Natl Acad Sci* 105: 12325–12330.
240. Greenblatt EJ, Olzmann JA, Kopito RR. 2011. Derlin-1 is a rhomboid pseudoprotease required for the dislocation of mutant α -1 antitrypsin from the endoplasmic reticulum. *Nat Struct Mol Biol* 18: 1147–1152.
241. Bondar AN, del Val C, White SH. 2009. Rhomboid protease dynamics and lipid interactions. *Structure* 17:395–405.
242. Rabinovich E, Kerem A, Frohlich KU, Diamant N, BarNun S. 2002. AAA-ATPase p97/Cdc48p, a cytosolic chaperone required for endoplasmic reticulum-associated protein degradation. *Mol Cell Biol* 22: 626–634.
243. Delabarre B, Christianson J, Kopito R, Brunger A. 2006. Central pore residues mediate the p97/VCP activity required for ERAD. *Mol Cell* 22: 451–462.

244. Wang Q, Li L, Ye Y. 2008b. Inhibition of p97-dependent protein degradation by Eeyarestatin I. *J Biol Chem* 283: 7445–7454.
245. Burr ML, Cano F, Svobodova S, Boyle LH, Boname JM, Lehner PJ. 2011. HRD1 and UBE2J1 target misfolded MHC class I heavy chains for endoplasmic reticulum-associated degradation. *Proc Natl Acad Sci* 108: 2034–2039.
246. Song B-L, Sever N, DeBose-Boyd RA. 2005. Gp78, a membrane-anchored ubiquitin ligase, associates with Insig-1 and couples sterol-regulated ubiquitination to degradation of HMG CoA reductase. *Mol Cell* 19: 829–840.
247. Lenk U, et al. 2002. A role for mammalian Ubc6 homologues in ER-associated protein degradation. *J Cell Sci* 115:3007–3014
248. Chen B, et al. 2006. The activity of a human endoplasmic reticulum-associated degradation E3, gp78, requires its Cue domain, RING finger, and an E2-binding site. *Proc Natl Acad Sci USA* 103:341–346.
249. Hassink G, Kikkert M, van Voorden S, Lee SJ, Spaapen R, van Laar T, Coleman CS, Bartee E, Fruh K, Chau V, et al. 2005. TEB4 is a C4HC3 RING finger-containing ubiquitin ligase of the endoplasmic reticulum. *Biochem J* 388: 647–655.
250. Morito D, Hirao K, Oda Y, Hosokawa N, Tokunaga F, Cyr DM, Tanaka K, Iwai K, Nagata K. 2008. Gp78 cooperates with RMA1 in endoplasmic reticulum-associated degradation of CFTRDF508. *Mol Biol Cell* 19: 1328–1336.
251. Lu JP, Wang Y, Sliter DA, Pearce MM, Wojcikiewicz RJ. 2011. RNF170 protein, an endoplasmic reticulum membrane ubiquitin ligase, mediates inositol 1,4,5-trisphosphate receptor ubiquitination and degradation. *J Biol Chem* 286: 24426–24433.

252. Burr, M.L., van den Boomen, D.J., Bye, H., Antrobus, R., Wiertz, E.J., Lehner, P.J., 2013. MHC class I molecules are preferentially ubiquitinated on endoplasmic reticulum luminal residues during HRD1 ubiquitin E3 ligase-mediated dislocation. *Proc. Natl. Acad. Sci.* 110, 14290–14295, U S A.
253. Meyer H, Bug M, Bremer S. 2012. Emerging functions of the VCP/p97 AAA-ATPase in the ubiquitin system. *Nat Cell Biol* 14: 117 –123.
254. Ye, Y., Meyer, H. H., and Rapoport, T. A. 2003. Function of the p97-Ufd1-Npl4 complex in retrotranslocation from the ER to the cytosol: dual recognition of non-ubiquitinated polypeptide segments and polyubiquitin chains. *J. Cell Biol.* 162, 71–84. doi: 10.1083/jcb.200302169
255. Li G, Zhao G, Zhou X, Schindelin H, Lennarz WJ. 2006. The AAA ATPase p97 links peptide N-glycanase to the endoplasmic reticulum-associated E3 ligase autocrine motility factor receptor. *Proc Natl Acad Sci* 103: 8348–8353.
256. Husnjak, K. et al. 2008. Proteasome subunit Rpn13 is a novel ubiquitin receptor. *Nature* 453, 481–488.
257. Soetandyo, N., and Ye, Y. 2010. The p97 ATPase dislocates MHC class I heavy chain in US2-expressing cells via a Ufd1-Npl4-independent mechanism. *J. Biol. Chem.* 285, 32352–32359.
258. Mueller, B., Lilley, B.N., and Ploegh, H.L. 2006. SEL1L, the homologue of yeast Hrd3p, is involved in protein dislocation from the mammalian ER. *J. Cell Biol.* 175, 261–270.

259. Furman, M.H., Loureiro, J., Ploegh, H.L., Tortorella, D. 2003. Ubiquitinylation of the cytosolic domain of a type I membrane protein is not required to initiate its dislocation from the endoplasmic reticulum. *J. Biol. Chem.* 278, 34804–34811.
260. Lindwasser, O.W., Chaudhuri, R., and Bonifacino, J.S. 2007. Mechanisms of CD4 downregulation by the Nef and Vpu proteins of primate immunodeficiency viruses. *Curr. Mol. Med.* 7, 171–184.
261. Margottin, F., Bour, S.P., Durand, H., Selig, L., Benichou, S., Richard, V., Thomas, D., Strebel, K., and Benarous, R. 1998. A novel human WD protein, h-beta TrCp, that interacts with HIV-1 Vpu connects CD4 to the ER degradation pathway through an F-box motif. *Mol. Cell* 1, 565–574.
262. Magada ´n, J.G., Pe ´rez-Victoria, F.J., Sougrat, R., Ye, Y., Strebel, K., and Bonifacino, J.S. 2010. Multilayered mechanism of CD4 downregulation by HIV-1Vpu involving distinct ER retention and ERAD targeting steps. *PLoS Pathog.* 6, e1000869.
263. Magada ´n, J.G., and Bonifacino, J.S. 2012. Transmembrane domain determinants of CD4 Downregulation by HIV-1 Vpu. *J. Virol.* 86, 757–772.
264. Inoue, T., Moore, P., and Tsai, B. 2011. How viruses and toxins disassemble to enter host cells. *Annu. Rev. Microbiol.* 65, 287–305.
265. Wernick, N.L., Chinnapen, D.J., Cho, J.A., and Lencer, W.I. 2010. Cholera toxin: an intracellular journey into the cytosol by way of the endoplasmic reticulum. *Toxins (Basel)* 2, 310-325.
266. Williams, J.M., Inoue, T., Banks, L., and Tsai, B. 2013. The ERdj5-Sel1L complex facilitates cholera toxin retrotranslocation. *Mol. Biol. Cell* 24, 785–795.

267. Bernardi, K.M., Williams, J.M., Kikkert, M., van Voorden, S., Wiertz, E.J., Ye, Y., and Tsai, B. 2010. The E3 ubiquitin ligases Hrd1 and gp78 bind to and promote cholera toxin retro-translocation. *Mol. Biol. Cell* 21, 140–151.
268. Abujarour, R.J., Dalal, S., Hanson, P.I., and Draper, R.K. 2005. p97 Is in a complex with cholera toxin and influences the transport of cholera toxin and related toxins to the cytoplasm. *J. Biol. Chem.* 280, 15865–15871.
269. Kothe, M., Ye, Y., Wagner, J.S., De Luca, H.E., Kern, E., Rapoport, T.A., and Lencer, W.I. 2005. Role of p97 AAA-ATPase in the retrotranslocation of the cholera toxin A1 chain, a non-ubiquitinated substrate. *J. Biol. Chem.* 280, 28127–28132
270. Ahn K, Angulo A, Ghazal P, Peterson PA, Yang Y, Früh K. 1996. Human cytomegalovirus inhibits antigen presentation by a sequential multistep process. *Proc Natl Acad Sci U S A*;93(20):10990-5.
271. Zhu, X., Peng, J., Raychowdhury, R., Nakajima, A., Lencer, W. I., & Blumberg, R. S. (2002). The heavy chain of neonatal Fc receptor for IgG is sequestered in endoplasmic reticulum by forming oligomers in the absence of beta2-microglobulin association. *J. Biol. Chem.* 277, 703–714.
272. Dickinson, B.L., Badizadegan, K., Wu, Z., Ahouse, J.C., Zhu, X., Simister, N.E., Blumberg, R.S., and Lencer, W.I. 1999. Bidirectional FcRn-dependent IgG transport in a polarized human intestinal epithelial cell line. *J. Clin. Invest.* 104, 903–91.
273. Kostova Z, Tsai YC, Weissman AM. 2007. Ubiquitin ligases, critical mediators of endoplasmic reticulum-associated degradation. *Semin Cell Dev Biol* 18: 770–779.
274. Deshaies, R.J., and Joazeiro, C.A. 2009. RING domain E3 ubiquitin ligases. *Annu. Rev. Biochem.* 78, 399–434.

275. Ross SA, Arora N, Novak Z, Fowler KB, Britt WJ, Boppana SB. 2010. Cytomegalovirus reinfections in healthy seroimmune women. *J Infect Dis.* 201;386–9.
276. Hansen, S. G., Powers, C. J., Richards, R., Ventura, A. B., Ford, J. C., Siess, D. Fröh, K. 2010. Evasion of CD8+ T cells is critical for super-infection by cytomegalovirus. *Science* 328:(5974)102–106.
277. Ndjamen, B., Joshi, D. S., Fraser, S. E., & Bjorkman, P. J. 2016. Characterization of Antibody Bipolar Bridging Mediated by the Human Cytomegalovirus Fc Receptor gp68. *Journal of Virology*, 90(6), 3262–3267.
278. Meshesha, M. K., Veksler-Lublinsky, I., Isakov, O., Reichenstein, I., Shomron, N., Kedem, KAvni, Y. S. 2012. The microRNA Transcriptome of Human Cytomegalovirus (HCMV). *The Open Virology Journal*, 6, 38–48.
279. Vivier, E., & Ugolini, S. (2011). Natural Killer Cells: From Basic Research to Treatments. *Frontiers in Immunology*, 2, 18.
280. Kulinski, J. M., Tarakanova, V. L., & Verbsky, J. (2013). Regulation of Antiviral CD8 T-Cell Responses. *Critical Reviews in Immunology*, 33(6), 477–488.
281. Kuijpers TW, Baars PA, Dantin C, van den Burg M, van Lier RA, Roosnek E. 2008. Human NK cells can control CMV infection in the absence of T cells. *Blood*. 2008 Aug 1;112(3):914-5.
282. Nimmerjahn F1, Ravetch JV. 2007. Fc-receptors as regulators of immunity. *Adv Immunol.* 96:179-204.

283. Snyderman DR, et al. 1987. Use of cytomegalovirus immune globulin to prevent cytomegalovirus disease in renal-transplant recipients. *N. Engl. J. Med.* 317:1049 – 1054
284. Schoppel K1, Kropff B, Schmidt C, Vornhagen R, Mach M. 1997. The humoral immune response against human cytomegalovirus is characterized by a delayed synthesis of glycoprotein-specific antibodies. *J Infect Dis.* 175(3):533-44.
285. Tirosh B, Iwakoshi NN, Lilley BN, Lee AH, Glimcher LH, Ploegh HL. 2005. Human cytomegalovirus protein US11 provokes an unfolded protein response that may facilitate the degradation of class I major histocompatibility complex products. *J Virol.* 79(5):2768-79.
286. Machold RP, Wiertz EJ, Jones TR, Ploegh HL. 1997. The HCMV gene products US11 and US2 differ in their ability to attack allelic forms of murine major histocompatibility complex (MHC) class I heavy chains. *J Exp Med.* 20;185(2):363-6.
287. Loureiro J, Lilley BN, Spooner E, Noriega V, Tortorella D, Ploegh HL. 2006. Signal peptide peptidase is required for dislocation from the endoplasmic reticulum. *Nature.* 15;441(7095):894-7
289. Chevalier MS, Daniels GM, Johnson DC. 2002. Binding of human cytomegalovirus US2 to major histocompatibility complex class I and II proteins is not sufficient for their degradation. *J Virol.* 76(16):8265-75.
290. Hansen SG, Sacha JB, Hughes CM, Ford JC, Burwitz BJ, Scholz I, Gilbride RM, Lewis MS, Gilliam AN, Ventura AB, Malouli D, Xu G, Richards R, Whizin N, Reed JS, Hammond KB, Fischer M, Turner JM, Legasse AW, Axthelm MK, Edlefsen PT,

- Nelson JA, Lifson JD, Fröh K, Picker LJ. 2013. Cytomegalovirus vectors violate CD8+ T cell epitope recognition paradigms. *Science*. 340(6135):1237874.
291. Guerriero, C. J., & Brodsky, J. L. 2012. The delicate balance between secreted protein folding and endoplasmic reticulum-associated degradation in human physiology. *Physiological Reviews*, 92(2), 537–576.
292. Hegde, R. S. & Ploegh, H. L. 2010. Quality and quantity control at the endoplasmic reticulum. *Curr. Opin. Cell Biol.* 22, 437–446.
293. Isaacson MK1, Ploegh HL. 2009. Ubiquitination, ubiquitin-like modifiers, and deubiquitination in viral infection. *Cell Host Microbe*. 18;5(6):559-70.
294. Zhu X, Peng J, Chen D, Liu X, Ye L, Iijima H, Kadavil K, Lencer WI, Blumberg RS. 2005. Calnexin and ERp57 facilitate the assembly of the neonatal Fc receptor for IgG with beta 2-microglobulin in the endoplasmic reticulum. *J Immunol*. 15;175(2):967-76.
295. Randow F1, Lehner PJ. 2009. Viral avoidance and exploitation of the ubiquitin system. *Nat Cell Biol.* 11(5):527-34.
296. Hamprecht, Klaus et al. 2008. Cytomegalovirus transmission to preterm infants during lactation. *J Clin Virol.* 41(3):198-205.